The Effects of Polymer Structures on their Protective Properties.

by

Jane. P. Lomas B.Sc., M.Sc.

A thesis submitted to the University of Manchester for the degree of Doctor of Philosophy in the Faculty of Technology.

Corrosion and Protection Centre
U.M.I.S.T.

Feburary 1983

Declaration

The author declares that no portion of the work referred to in this thesis has been submitted to any other University or other institute of learning in support of another degree or qualification.

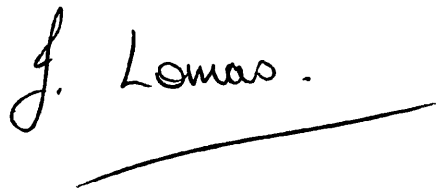

To my family

Acknowledgements.

The author wishes to extend her thanks to the following;
to her supervisors, Dr. J.L. Dawson and Dr. J.D. Scantlebury, for their continuous help, advice and interest throughout the duration of this work,
to the industrial collaboraters, I.C.I. Ltd. Paints Division, Slough and in particular to Mr T. Strivens, for supplying the polymer samples and providing technical information,
to Mr H.A. Powell (I.C.I.) and Mr A. Jackson (U.M.I.S.T.) for the Tg information,
to Dr L.M. Callow, for his encouragement and guidance in many matters,
to Drs. K. Hladky, G.Sussex, D. Eden and other friends and colleagues for varied and helpful discussions,
to the S.E.R.C. for financial support.

Special thanks are due to my husband Pete, for drawing the diagrams. Without his patience, support and culinary skills.....

Abstract.

The behaviour of acrylic and vinyl based polymers in 3% sodium chloride solution, was studied under a number of experimental conditions. The infra-red spectra and glass transition temperatures of the polymers, were determined experimentally.

The a.c. impedance response of both free and attached films, to changes in the solution temperature and to the creation of a pinhole in the films, was monitored. It was found that there was little change in the impedance data with temperature, but the presence of a pinhole in a film, can be detected with this technique.

Vinyl films were immersed in both aerated and deaerated salt solution and it was observed that a faster corrosion rate occurred in the deaerated solution. A possible explanation for this phenomenon, is suggested.

The impedance response of coatings of different thicknesses and the effects of different substrate preparations, were also examined. With a thick, intact coating, there is little correlation between the impedance data and the underfilm corrosion processes. Only the impedance response of the film itself is monitored. For thinner or more defective coatings, the impedance data shows some correlation with the observed corrosion events.

The rest potential of the specimens was also monitored with time. It was noted that for an intact film, it was difficult to measure the rest potential. For more defective films, the rest potential appeared to decrease as corrosion processes occurred on the specimen.

Chapter 1. Paint and Corrosion Protection.

Chapter 2. Experimental.

Chapter 3. Results.

Chapter 4. Discussion.

Chapter 5. Conclusions and recommendations.

Chapter 1.Paint and Corrosion Protection.

1.1 Introduction.

The problems involved in protecting a structure made from a corrodible material such as mild steel, have been known for many years and there are a number of technological methods used to control the corrosion of such materials and structures. Protection can be achieved sucessfully under certain conditions, for example, the use of Cathodic Protection can completely prevent corrosion of a substrate, providing that both structure and Cathodic Protection system are in an aqueous environment. Special protection problems are present for structures requiring protection against aggressive corrodants such as salt spray or acid attack. In these situations, the application of a coating to the metal may be the only viable or the most economic means of its protection and it is therefore important that the choice and application of the coating is suitable for the particular situation. Much effort has been devoted to the study of paint film behaviour and to the development of specific paints for particular environments. and the rest of this chapter describes some of the experimental work carried out on paints The test methods often used in paint performance assessment.

1.2 Composition of paints.

The function of any paint, apart from any decorative aspects, is to prevent the corrosion of the underlying substrate <1> and it is important that the coating is chosen to be able to withstand the particular environment in which it is placed <2>. Whilst there are many suitable compounds which may be incorporated into a paint, the required performance of the dry coating will govern the choice of constituents. Paints are made up from several compounds <3> and may contain a wide variety of ingredients. The most important of which is the vehicule or resin; this is the base material for the paint, and the structure and composition of the resin or polymer used will determine many of the physical characteristics of the dry film <4>.

The polymer also determines the flexibility of the coating under conditions of movement or stress, the resistance of the coating to abraision and wear, as well as its resistance to chemical attack and other harmful agents such as ultra-violet light, water and oxygen, the latter two being the major causes of corrosion of steel.

Type of Paint	Resins or Binders	Solvents	Typical Uses
Non-convertible Coatings			
Cellulose Laquer	Cellulose Nitrate	Ketones, White Spirit, Alcohols	Car Paints
Chlorinated Rubber	Chlorinated Rubber	Xylene	Marine Paints
Varnish	Shellac, Copal, Novolac	Ethanol	Decorative Wood Coatings
Vinylite	Vinyl Co-polymers	Ketones, Xylene	Bridge Paints
Convertible Coatings			
Alkyd Paints	Linseed Oil, Alkyd	White Spirit Turpentine	Artists Oil Paints, Gloss Paint
Acrylic	Acrylic Acids, Acrylic Esters	Xylene, Ketones, White Spirit	Car Paint
Epoxy Paint	Expoxide Resin (Amino cured)	Esters	Scaffolding, Steel Tube, Products

Table 1.1 Composition and use of some paints.

Once a polymer base has been chosen, other materials may be added to it, such as pigments, which can play a dual role in a paint film. Firstly they may act as colouring agents, providing a decorative as well as protective film and secondly, pigments may actively help to prevent substrate corrosion <5> although the mechanisms by which this protection is achieved is not well understood, since they are normally inert. Other

inert compounds known as fillers may also be added to paints to increase the opacity (or covering power) of the paint thus reducing the required amount of the more expensive pigments. Another series of compounds which may be incorporated into paints are plasticising agents, which help to maintain the dry paint film in a flexible or "rubbery" state. These are added to paints designed for the protection of structures which are liable to movement or changes in temperature <6>, or impact, where another coating may be liable to cracking or chipping.

The final main constituent of paints is the solvent, whose function is to bind together homogeneously all the solid constituents of the paint and to aid in the application of the coating, by providing an appropriate viscosity for the painting technique chosen. The choice of the solvent for a paint is very important since the incorrect matching of solvents in paints which are to be overlaid on each other, may lead to internal strain in the coatings <7> which in turn may cause cracking of the paint and, obviously, impaired corrosion resistance. It has also been suggested, that the solvent may be partly responsible for the orientation of any side groups on the polymer chains and that this in turn may influence the protective abilities of the paint <8>.

Whilst the constituents of a paint must be carefully chosen for their combined protective ability in a particular environment, the method of curing of the film is also important as it affects the properties of the coating. There are many methods used for curing paints, but perhaps the most simple is that of solvent evaporation and non-convertible coatings utilise this curing method.Paint is applied to the substrate and left whilst the solvent evaporates leaving the finished coating, the polymer

remains chemically unchanged and may be re-dissolved in a suitable solvent. Paints such as chlorinated rubbers <9> are often applied in this way because this curing method leaves polymer chains free to move giving some flexibility to the coating. In contrast, a convertible coating is chemically changed from its constituents and cannot be re-dissolved in the solvent. This change is brought about by cross linking suitable side chains on the polymer (or backbone) and this may be achieved by heating (or stoving) the paint after application. As stoving is obviously an unsuitable method for large painted structures, cross linking agents may be mixed into the paint instead. As these agents often act quickly it is necessary to mix the paint just prior to application, and many such paint systems are sold in a "two pack" form, the cross linking agent being mixed into one part. Many epoxy paints are available in this form and cross linked paints have the advantage of being more resistant to chemical attack than many non-convertible coatings, although they may not be as flexible.

The design of a paint for a particular environment is very important and in order to improve the corrosion resistance of paints, it is necessary to understand the processes which can lead to the deterioration and eventual breakdown of a coating and in particular, the mechanisms by which agressive species permeate through the coating to the underlying substrate, as well as their effects on the paint itself. The next sections review some of the work carried out into the processes of corrosion by aqueous species.

1.3 Paint as a physical barrier.

It is generally accepted that a coating protects the substrate by acting as a barrier between the metal and the environment <10,11,12>. This barrier must therefore be tough, chemical resistant and have a low permeation to aggressive species such as water molecules, oxygen, ions, etc. It is the penetration and permeation of these species through the paint to the metal substrate, which are the major causes of the breakdown of the protective function of the coating <13>. However, the action of a paint as a barrier only, was challenged by Mayne <14>, who observed that polymer films are porous enough to allow the permeation of sufficient water and oxygen to cause as much corrosion to occur on a painted specimen as on an unpainted one. He suggests that the barrier function is not the only method by which a coating protects the underlying substrate against corrosion. Cherry <15> considered the anodic and cathodic processes which occur on both coated and uncoated systems and suggested that the vehicule itself may affect the anodic reaction which occurs, since the potential of a painted specimen is more noble than that of an uncoated one and the critical current density to cause polarization is less for a coated electrode. Michaels <16> considered the chemistry and structure of the polymer itself, as well as the composition and distribution of pigments and fillers in the paint. He also examined the methods by which coatings are applied and concluded that all these factors govern the protective ability of the paint, as does the electrochemical nature of the substrate <13> and the combined effects of substrate and polymer interactions <10>. Mayne <17> also considered the

way in which paints protect metal. For example, Zinc rich paints can be applied as a cathodic protection coating for steel substrates and anodic passivation, utilising the degradation products of metal soaps, usually those of lead. Perhaps his most generally applicable proposal and the one which is in agreement with the findings of other workers, <11,12,18> is the theory of resistance inhibition. He suggests that the paint (whether pigmented or not) acts as a protective coating by placing a barrier with a high ionic resistance between the anodic and cathodic areas on the metal surface, causing a reduction in the corrosion current which flows between these sites. The degree to which a particular coating is successful in this function, depends upon the structure of the cured film, which will determine the rate at which penetration of the coating by corrosive species will take place, since it is the presence of water and ions in the film which causes a short circuit of the high resistance path either through the paint itself, or at the paint-metal interface <19>. Bacon, Smith and Rugg <18> observed the electrolytic resistance of paint films and proposed that it is a useful method of assessing the protective ability of a coating, since the electrolytic resistance is determined by the ease of diffusion of aggressive species through the coating to the substrate. They noted that if the electrolytic resistance was greater than log R^{8} Ohms cm^{2}, then the paint was protective, but if this value fell to log R^{6} Ohms cm^{2} or lower, the coating was not protective. Using this method of assessment, it was possible, they suggested, to observe the deterioration and breakdown of a paint by following the changes in its electrolytic resistance with time.

1.4 Water transport in coatings.

Much work has been performed which shows that water permeates into a coating then through to the substrate, where, in combination with oxygen which has also traversed the film, corrosion can occur. However, the mechanisms of these processes are less well understood and there are a wide variety of experimental techniques used to determine how water enters and passes through a film and how much water is retained in the film. The most popular methods of assessing the absorption of water by a coating are gravimetric; where samples of paint are soaked in water for varying periods of time and then re-weighed, the change in weight being due to water uptake by the film; and the capacitance method, which measures the the change in the dielectric of the paint and relates it to water absorption by the film. Although both these methods are useful <20,21,22>, the results obtained by each method vary between paint types and these variations have been attributed to differences in the distribution of water within paint films <20>. It is suggested that water first penetrates into a coating via pores or fissures in the film <23> or enters at a "holiday" or imperfection <24>. Further penetration into the coating may be achieved by the water dissolving in the coating forming a solution in the polymer matrix <21> which reduces the resistance of the polymer in that area, by forming a "conducting phase", the remainder of the paint continues to act as a dielectric, as shown overleaf <25>;

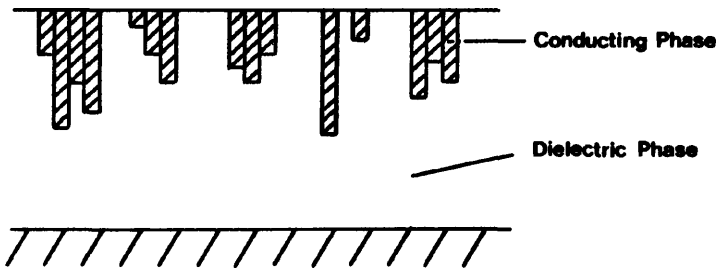

Figure 1.1 Phases in a paint film.

This process of water permeation and absorption into a film may be monitored by following the changes in the capacitance of the film <26> and there is some evidence that the distribution of the water within the paint may be elucidated from capacitance changes <20,22,27>. Perera and Heertjes <28> suggested that the concentration of water already present in a film could have an effect on the rate of entry of more water into the coating. This observation supports the "clustering theory" of Zimm and Lundberg <29> who proposed the idea that when one water molecule enters the film, other water molecules follow its path, rather than entering the coating elsewhere on its surface. In this way, water molecules enter the film as a wedge shape rather than in narrow pores. Where there are ionisable or hydrophillic groups, such as carboxyl groups, present in the paint, either as part of the polymer backbone or present as pigments etc. in the film, water molecules may tend to cluster around these groups, rather than being dispersed evenly throughout the coating <30> and therefore the structure of the film will help to determine the distribution of groups of water molecules within itself.

The problem of determining the method by which water permeates into a film, whether the film contains pores or not <31>, has been examined using a number of different techniques, such as permeation <32,33>, sorption <34,35> and conduction <36> of water through the paint film, as well as diffusion of water vapour <37,38,39,40> through both free and attached films <41> and coatings containing pigments <42>. The results of all these experimental techniques and conditions seem to indicate that water enters a film initially as a result of a pressure difference of water across the film and that this process may be considered in three parts <35>. Firstly, the sorption of water molecules onto the coating at the paint-solution interface. Secondly, the diffusion of the absorbed water through the film under a concentration gradient across the film, and lastly, the de-sorption from the polymer at the paint-metal interface. In this process, it is generally considered that the diffusion of water through the film, is the rate determining step and the mechanisms by which this transport occurs has been examined. Kittelberger and Elm <43> suggested that the diffusion of water occurs under osmotic control since a greater quantity of water was absorbed by films placed in dilute solutions, than in solutions of concentrated electrolyte. The findings of Brasher and Nurse <44> agreed with this theory and they noted that in the early stages of immersion in an electrolyte, the concentration of the water is the most important factor, whilst in later stages of immersion, the ionic concentration of the solution becomes the more important parameter as the film may act as a semi-permeable membrane <45> allowing the diffusion of water and certain ions; the structure of the film and the degree of cross linking of the polymer, governing the size of ions which can penetrate the film <46,47>.

Electroendosmosis, the movement of water through a film under the influence of an electrical potential gradient, has also been examined by several workers <48,49> as a means of explaining the causes of blister formation by certain paint films and it was observed <48> that water migrates to the cathode site under the paints which are composed of negatively charged side groups, for example, carboxyl groups, on the polymer chains. Conversely, water migrates to the anodic sites of paints with positively charged groups, such as ammonium groups, on the polymer backbone.

The effect of the temperature of the experimental solution on the absorption of water into coatings has also been considered <30,46,50> and the results indicate that a greater quantity of water is absorbed by paints at higher solution temperatures, although the increase may be only slight for some coatings and for some films there is actually a decrease in the water absorption as the paint passes through its glass transition temperature <51,52>. That is, the temperature at which a polymer changes from a "glassy" state, in which it may be brittle, to a "rubbery" state, in which it is more flexible. The exact temperature at which this transition occurs depends on the structure and composition of the paint and may be determined experimentally, as described in this work.

In practice however, few paint systems are exposed solely to the influence of water as the only aggressive species and the permeability of both water and ionic species through paint films and their combined effect on the substrate should be considered, when examining the protective abilities of a paint film.

1.5 Effects of ions on paints.

The ability of a paint coating to withstand the corrosive action of water and ions, was thought to be dependant upon the electrolytic resistance of the film and that whilst this resistance differed between good (protective) and bad (non-protective) paint films, it was uniformly distributed over the particular film <18>. However, work by Kinsella and Mayne <36> showed that the resistance of a paint film does vary over the surface of the coating and that these differences fell into two categories which they termed D and I type areas. For areas of the film where the resistance is high, the resistance of the film did not follow that of the external solution and this was termed an I or "Indirect" area. "Direct" or D areas, do follow the resistance of the external solution and their electrical resistance is low in comparison to the I areas. Mayne and Mills <53>, reported that where corrosion is occuring, the film at that site is of the D type, whereas areas which show no corrosion have films above them of the I type. They suggest that films with a high electrolytic resistance will be more protective than ones of a low electrolytic resistance. Further work in this area revealed that D and I areas could be detected by microhardness measurements, D areas being softer than I areas and it was suggested that this could be related to the structure of the paints. The I areas being perhaps more cross linked than the D areas, which may be more plasticised than the I areas <54>.

When a paint film is initially immersed in an electrolytic solution, the coating absorbs water first and ionic species later, by an ion exchange mechanism <55,56>. Hydrogen ions, which were originally present

in the film as counter ions on the side groups of the polymer chains, become "ionised" when the film absorbs water. The now "free" hydrogen ions can ion exchange for other cations present in the external solution which will enter the film under a concentration gradient. The ingressing and exchanging cations may be monovalent (for example Na^{+} ,K^{+} ,) or divalent ions (such as Ca^{2+},Mg^{2+},), the latter, ion exchanging for two hydrogen ions <57>. These two processes, namely water absorption and ion exchange have been termed the "fast" and "slow" changes respectively <58>. The fast change (water uptake) occurs within minutes or hours of immersion, whilst the slow change (ion exchange) may take place over a period of days or weeks depending upon the film itself and the external solution. Radiotracer studies, using labelled water molecules and Na^{+} and Cl^{-} ions, have confirmed the theories of water permeation into a film by diffusion processes and the ion exchange processes of ions in the electrolyte becoming associated with fixed groups on the polymer chains, whilst the hydrogen ions can diffuse into the external solution <59,60>. Glass and Smith <60> also concluded from their tracer work, that the diffusion processes follow Fick's laws and that the diffusion is inversely proportional to the thickness of the film, but directly proportional with time of immersion. Other studies involving diffusion rates have reported that there is a linear relationship between the resistance of the membrane and the rate of ion diffusion, a high resistance film having a low ion diffusion rate <61> and that ions entering a film may not interact directly with polymeric side groups, but may be shielded from interactions by a large number of water molecules clustering around the ion <62>.

Since studies of ion exchange processes and water absorption mechanisms have been carried out using both free and attached films and although objections have been raised as to the validity of performing absorption experiments on free films since the free film may not have the same stresses or distortions as an attached film <63>, it is generally accepted that the lack of a substrate removes the complications of paint-substrate interactions. Although water diffusion and ion exchange can take place from both sides of a detached film, this increased absorption can be taken into account when analyzing the results. When such data is compared with results from attached film experiments, information concerned with the adhesion of the paint film may be obtained <53>.

1.6 Non-electrical methods of paint testing.

There are many problems associated with paint testing and the assessment of a paints performance in a particular environment and a large number of different tests are available <64>, ranging from long term testing <65>, which may be costly in terms of the amount of work involved, as well as the time taken to make measurements of certain paint parameters, such as the hardness of the dry film <66>. As with all areas of paint testing, the experimental techniques, exposure conditions and methods of assessment vary considerably between both tests and workers. Painted panels are often exposed to an "accelerated weathering test", based on the use of a salt spray chamber. Specimens may be scribed with a single scoring mark, or a cross, or left undamaged, prior to exposure.

After completion of the test, specimens are removed from the cabinet and examined for corrosion. This is usually a visual examination, but simple "peel-off" tests may also be used. Sticky tape is pressed down over the scored area and pulled off, any paint adhering to the tape is assessed for area and condition. Unfortunately, the amount of paint which may be pulled off the sample can vary considerably between workers and from one panel to the next, depending on the firmness of application of the tape and the angle and speed with which it is pulled off.

It is important, when assessing the protective abilities of a paint, to test it in several environments, as a paint may be protective against some corrosive species or in certain environmental conditions and much less protective in other situations <67>.

These types of tests, using simulated environments have several problems. Firstly, they require a large number of test specimens if the results are to be statistically significant and if the result of testing with time of exposure is to be considered. Secondly, it is difficult to simulate "real" exposure conditions in an accelerated test and thirdly, the assessment of the performance of a paint presents many difficulties. Consequently, much research has been aimed at finding quicker, easier and more accurate methods of paint testing. The adhesive properties and abilities of a paint in a given environment was considered as one possible alternative technique. It was suggested that loss of adhesion to a substrate is caused by permeation of water through the film <30> and its subsequent collection at the interface between the substrate and the coating <19,68>. A number of adhesion test methods based on different techniques, such as "direct pull-off" <69>, "sandwich pull-off" <70> and

"torque wrench" <71> methods been used, but all suffer from disadvantages. These are usually problems involving the adhesive and cohesive strength of the paints. If the adhesive strength between the paint and the substrate is greater than the adhesive strength between the paint and the test apparatus, the paint is not pulled off the substrate. Where a cohesive failure occurs, paint remains adhered to both substrate and apparatus. The quantity of paint adhering to the substrate may be small and may not completely cover the test area, in such cases, it is difficult to assess the mode of failure of the specimen. These problems have recently been reviewed and a new, more accurate adhesion testing technique has been developed <72>. However, using adhesion test methods, it is difficult to obtain "in-situ" results and it is the adhesion of a paint whilst undergoing exposure to solutions or sprays, that may be of interest in the testing of a particular paint. Alternatively, a non-destructive test method may be required. Many electrical techniques have been developed for examining the behaviour of bare metals in a chosen test environment and some of these tests have been applied to painted specimens, as described in the next sections.

1.7 Test methods based on direct current.

Paint testing methods based on direct current measurements enable experiments to be performed on a test specimen, whilst it is undergoing exposure to the test environment. Because of the "non-destructive" nature of electrical tests, measurements can be carried out on the same panels over a period of time, thereby avoiding the necessity of preparing and testing a large number of panels. One popular technique, originally developed for examining the corrosion of bare metal specimens, which has

been utilised in the testing of paints, is that of polarising the specimen to produce polarisation curves. A known current is applied to the test system in small increments and the resulting change in the voltage is measured. The experiment is usually performed at potentials above and below the measured rest potential (Ecorr) of the specimen and a graph of potential against log current plotted. From this plot, the Tafel slopes (β) of the anodic and cathodic processes can be obtained. Under ideal conditions, these plots may be extrapolated back to Ecorr, to give icorr directly. Where such extrapolation is not possible, the values of the Tafel slopes, together with the polarisation resistance (Rp) of the system (the ratio of the applied current to potential, measured at steady state), may be substituted into the Stern-Geary equation <73> to obtain icorr;

$$i_{CORR} = \frac{\beta_a \beta_c}{2.3(\beta_a+\beta_c) R_P}$$

where: i_{CORR} = corrosion current
β_a = anodic Tafel slope
β_c = cathodic Tafel slope
R_P = polarisation resistance

However, the validity of using the results from polarisation curves obtained from coated specimens, has been questioned, since it may be difficult to obtain the true rest potential of a specimen before an experiment is performed <74>. The polarisation of a specimen away from its rest potential, may affect the future corrosion behaviour of that test sample <75>, or it may alter the rest potential of the panel. Stern and Geary themselves noted that their relationship holds only for a freely corroding specimen in the absence of resistance and concentration polarisation effects and when the specimen is under activation control. These conditions are not necessarily present under a paint coating and

therefore, whilst theoretically, polarisation of the specimen is a useful technique for obtaining data pertaining to the corrosion rate of the specimen, it must be applied with care to coated samples.

Polarisation resistance is another commonly used technique for examining the corrosion behaviour of painted metal. In this method, a small perturbing voltage (say 10mV) is applied to an electrode and the response of the specimen is monitored. The resistance value obtained from the electrode, is known as the polarisation resistance (Rp) and is used to calculate the corrosion rate of the specimen. The polarisation resistance is a combination of the charge transfer resistance of the metal, the film and solution resistances. This technique cannot always be sucessfully applied to coated electrodes, since it requires steady state conditions during the experiment and a constant rest potential. It is affected by such factors as the resistance of the paint and the ohmic drop and these must be taken into consideration when the results are examined <74>. The uses and problems associated with this technique in the context of coated specimens, has been recently reviewed <76>.

Other polarisation techniques, have involved the application of a coating, exposure of the specimen to the chosen test conditions and the subsequent removal of the coating prior to the polarisation experiments. This method is designed to show whether certain paints chemically affect the substrate <77>. Some workers have detected and measured electrolysis currents present under paint films <78> and compared the corrosion rates calculated from this data, with data from weight loss experiments. Others have examined the resistance of the paint film itself and related these values to the ionic permeability of the paint <79,80,81>.

Reviews of the various d.c. techniques used to examine the corrosion protection of steel by paint films <74,75>, agree that whilst in theory, polarisation experiments provide valuable information as to the corrosion rate of the substrate under a coating whether it is an organic coating such as paints, or whether it is an inorganic coating such as concrete <82>, it is generally advisable to perform only one experiment on each specimen, since during the polarisation run, the potential of the metal is polarised significantly away from the rest potential of the specimen and this may affect the initiation of corrosion sites on the metal surface, or, in extreme cases, may cause blistering of the paint <83>. Because of these problems and the added complication that polarisation methods give best results when the system is at a steady state, which rarely happens, as corrosion is an active process, alternative techniques of examining the corrosion behaviour of an actively corroding specimen without altering the processes involved, have been sought. One method which has proved to be useful in this respect, is that of a.c. impedance.

1.8 Test methods based on alternating current (a.c.).

1.8.1 Introduction to a.c. impedance.

When an a.c. signal is applied to a painted electrode, the perturbing voltage is low (often less than 50 mV r.m.s.) and therefore the system is not significantly disturbed from its rest potential. Experimentally, this is very important, since it allows measurements to be made on an actively corroding specimen as the corrosion process occurs, without waiting for steady-state conditions and without affecting the physical condition or electrochemical behaviour of the specimen.

A number of different experimental apparatus and methods based on a.c. impedance are available, but they have one problem in common, that of understanding and interpreting the resulting data. It is often useful to consider the data in terms of equivalent circuits, rather than treating it mathematically. An equivalent circuit is built up from a number of electrical components, such as resistors, capacitors and inductors, combined in an appropriate sequence. If an alternating current is applied to such a circuit, the resultant current will follow Ohm's law (V=IR), providing that the term for the resistance (R) is replaced by one for the reactance (X). The reactance of the components of an equivalent circuit can be expressed as follows;

$$X_R = R$$

$$X_L = j\omega L$$

$$X_C = \frac{1}{j\omega C}$$

where: X = reactance
R = resistance
C = capacitance
L = inductance
ω = angular frequency
$j = \sqrt{-1}$

When the various components are combined in series or parallel or both, the total impedance (Z) of the system may be calculated and represented graphically in two ways. Firstly, in terms of its "real" or resistive components (Z') and the "imaginary" or capacitive components (Z"). Secondly, in terms of $|Z|$, the vectorial sum of the real and imaginary parts of the impedance and θ, the phase angle, which is formed between $|Z|$ and the real axis, Z' (Polar format). Both these forms may be represented on a Nyquist plot, on which the variation of the impedance with frequency can be represented, each point on the plot being the impedance of the experimental system at a particular frequency. An example of each type of plot is shown overleaf.

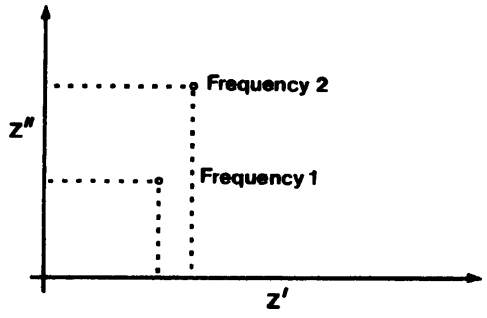

Figure 1.2 Real and Imaginary format.

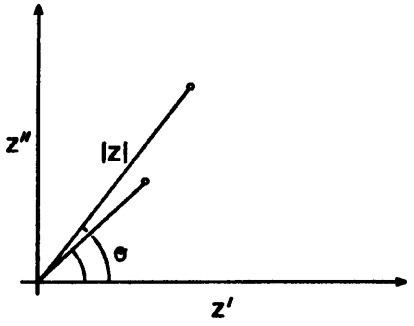

Figure 1.3 Polar format.

The impedance response of a corroding system can vary considerably with experimental conditions and time and it is convenient to consider changes which are taking place on the specimen, in terms of variations in the equivalent circuits elements, values and combinations. In order to design an equivalent circuit which behaves as an electrode, it is important to understand the response of the circuit components, both individually and in simple combinations, to an a.c. signal. Some examples of circuits their Nyquist plots are shown overleaf;

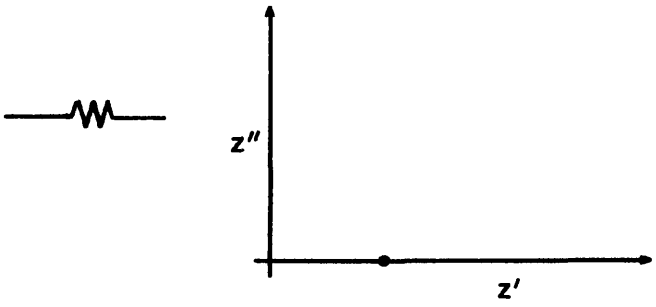

Figure 1.4 Nyquist plot of a resistor.

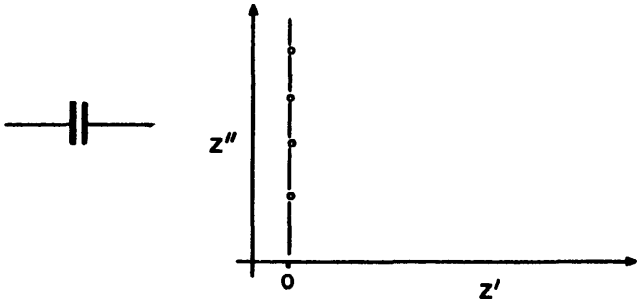

Figure 1.5 Nyquist plot of a capacitor.

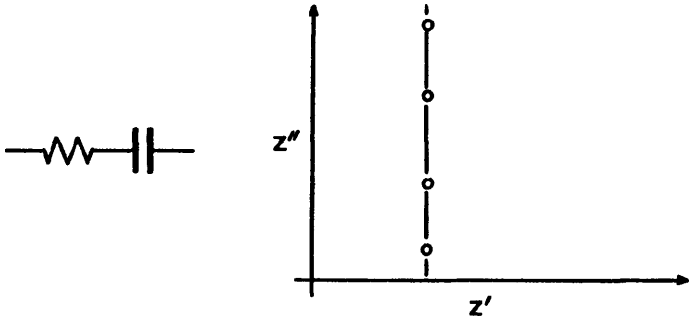

Figure 1.6 Nyquist plot of a resistor and capacitor in series.

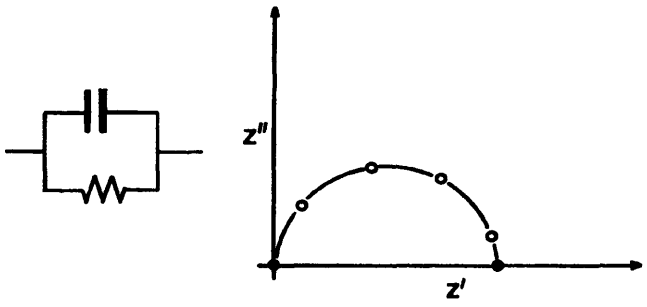

Figure 1.7 Nyquist plot of a resistor and capacitor in parallel.

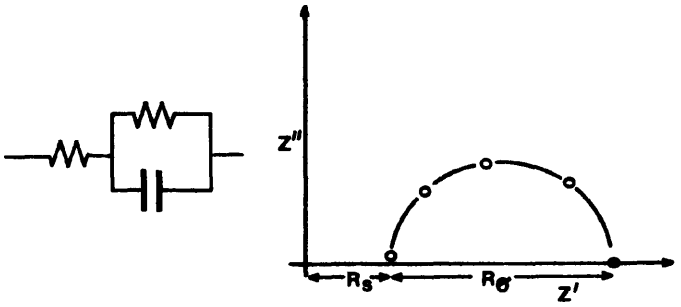

Figure 1.8 Nyquist plot of a resistor and capacitor network.

The latter circuit is known as Randles equivalent circuit, after Randles, who first proposed the idea of examining impedance data in this way <84>. From this equivalent circuit, several useful pieces of information may be obtained.

Rs is the ohmic resistance of the system. It includes the resistance of the leads, the solution and any high impedance paths such as paint films.

C is the capacitance of the system, often that of the electrochemical double layer on the metal surface, resulting from adsorbed ions and water molecules. In some cases, this capacitance may be masked by the capacitance of paint coatings on the electrode.

Rθ is the charge transfer resistance across the electrochemical double layer of the electrode. It can be related to the corrosion rate of the metal for an activation controlled system. In such cases, Rθ is equivalent to Rp (the resistance which is measured using linear polarisation techniques). By substituting Rθ for Rp in the Stern-Geary equation, the corrosion rate of the system may be determined <85,86>.

In practice, few experimental systems behave in the simple manner described by the Randles equivalent circuit and the effects of diffusion must also be taken into consideration. The Warburg diffusion effects, have been described mathematically <87,88> and may also be represented in terms of an equivalent circuit, as shown below;

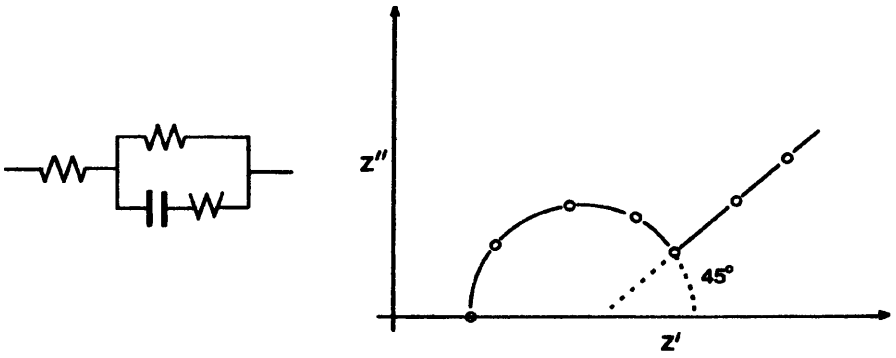

Figure 1.9 Equivalent circuit and Nyquist plot showing Warburg diffusion.

Coated electrodes often show great variation in the shape and size of the Nyquist plots obtained and rarely conform to the idealised equivalent circuits shown here, since there are many factors to consider when examining underfilm corrosion. This can make the interpretation of the impedance data very difficult in some instances and it is often impossible to calculate all the different parameters from the plot (such as Rθ, Capacitance etc.) with any degree of accuracy. In the cases shown below, it is difficult to determine which are the true values of Rs and Rθ, making an accurate calculation of the corrosion rate virtually impossible.

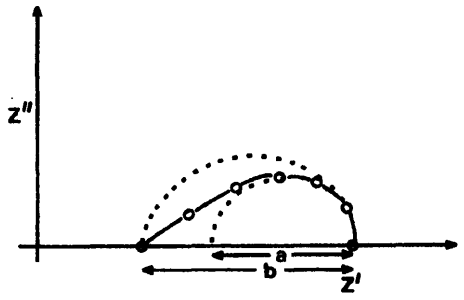

Figure 1.10 Asymmetrical impedance plot.

When this situation arises, it may be more meaningful to study general trends in terms of the shape and size of the plot, in relation to the observed corrosion behaviour of the specimen, rather than try to extract numerical data from the impedance plots.

1.8.2 Experimental use of the a.c. impedance technique.

The impedance technique is often applied to an experimental system in the hope of obtaining new information which cannot be obtained using any other experimental method. Whilst information and a great quantity of data are easily obtained using modern digital electronics, the interpretation and understanding of the data, as well as its processing into a useful format, are often difficult <89>. To overcome these problems, much theoretical work into the relationships and derivations of the various parameters measured by a.c. impedance has been carried out and different graphical representations of such parameters have been proposed <90,91>. Many experimental systems have been analysed <92> and eqivalent circuits designed to match the impedance data obtained <93,94>, as well as reports of the factors which can affect the analysis of impedance measurements <95> and may contribute to inaccuracies and errors in the results <96>. Early impedance experiments were carried out using bridge balancing techniques, which had the advantage of giving accurate data, but the disadvantages of being slow and difficult to operate and having a limited frequency range. Nevertheless, the viability, usefulness and promise of the impedance technique was demonstrated by Sluyters and his co-workers both theoretically <97> and practically <98> as a means of determining many useful parameters and obtaining much useful information about an electrochemical system, from one experimental technique <99,100,101>.

The inherent flexibility of the impedance technique due to its ability

to measure both high, low and changing impedances in experimental systems, coupled with the speed of modern digital equipment, has made it a useful research tool for many diverse areas of corrosion assessment and investigation. These areas include studies of different inhibitors and their actions <102>, corrosion of reinforcing bars in concrete <103>, galvanic effects <104>, molten salts <105,106> and the behaviour of copper alloys in a number of environments <107>. The impedance technique has also been sucessfully applied to experiments utilising rotating disk electrodes, in which measurements can be made of diffusion rates across the electrochemical double layer <108,109>, to various aspects of corrosion monitoring <110> and, of course, to painted electrodes. Much of the reported work involving impedance studies of paint films, has been concerned with the measurement of the specimens with time <111,112>, surface pre-treatment <113>, the design of new electrode systems <114> and the response of painted specimens to a variety of experimental conditions <115,116,117,118>.

1.9 Rationale for present work.

In all the impedance experiments performed, it has been assumed that the processes monitored by this technique, mirror the corrosion behaviour occurring under the film and it was decided to investigate this postulate. Several different experimental systems were considered. The effects of temperature and a pinholes were examined for both attached and detached films. The glass transition temperatures were located and the impedance behaviour with time, coating thickness, substrate preparation and the presence and absence of oxygen, were also investigated.

Although much of the reported experimental work described earlier relates the processes involved in corrosion, to the structure of the paint films, little work has been carried out relating the data obtained from impedance studies under polymer films, to the visual observations of the corrosion of the specimens.

To this end, it was decided therefore, to study three coating types. A non-convertible coating, a cross linked coating and a gel with a very open structure and it was anticipated that these different coating types would provide contrasting results. In order to study the effects of film structure in more detail, two different acrylic type (convertible) polymers and four different vinylite coatings (non-convertible) were chosen for their differences in structure and composition from each other. Again it was anticipated that any variations in the corrosion behaviour of these polymers and in the impedance plots and other experimental data obtained, could be related to the differences between the polymers. Pigments and fillers were not included in any of the films, in order to allow easier visual observations of the corrosion phenomena which occurred under the films. It was also anticipated that any differences in electrochemical data could be related to differences in the structure of the films.

Chapter 2. Experimental.

2.1 Substrate preparation.

The majority of the experiments reported here, were performed on polymers cast onto mild steel panels, supplied by "Pyrene Chemical Services Ltd.", to B.S. 1449 <119>. The panels, (15x10x0.12cm) were supplied polished on one side and oiled. The oil was removed by immersing and wiping each panel in trichloroetheylene (Analar) followed by rinsing in fresh trichloroethylene and dried in a stream of hot air. After preparation, panels were stored in a desiccator over silica gel, prior to coating.

For long term immersion experiments, two different methods of substrate preparation were used. Firstly, "Pyrene" panels, prepared as described previously and secondly, mild steel of the composition given below. This steel was supplied with an adherent rust layer, which was removed by pickling.

Element	% Weight
C	0.18
Cr	0.03
Ni	0.05
Cu	0.02
Si	0.01

Table 2.1 Composition of the steel substrate.

Test panels (7.7x7.7x0.3 cm) were cut from the steel sheet, scrubbed in acetone and immersed in a beaker containing 1% Citric acid (Analar) in de-ionised water. The beaker was placed in an ultrasonic bath for 15 minutes, until the steel was clean and shiny. The panels were rinsed in running tap water and in de-ionised water, then rinsed in acetone and dried in a stream of hot air. Prepared panels were stored in a desiccator before coating. Citric acid was chosen for the pickling agent because it would not leave aggressive chloride ions on the freshly exposed steel surface. Such ions would act as contaminants under a paint coating. Polymers were cast onto both substrates in the hope that any differences in the long term corrosion behaviour between the two sets of panels, could be at least partly attributed to the preparation of the substrate.

2.2 Choice of polymers.

The polymers chosen for experimentation are of the convertible and non-convertible types. The convertible coating was supplied by the industrial collaboraters, I.C.I. Ltd., Paints Division, Slough, and was based upon acrylic type compounds. Initially, three different polymer formulations were mixed and sprayed onto pickled "Pyrene" panels at Paints Division and posted to Manchester after curing. After this initial batch, it was decided that this method of specimen preparation was unsatisfactory for several reasons. Firstly, panel preparation and polymer application would not necessarily be carried out by the same person each time, which could result in differences in specimens. Secondly, there was always a delay between panels curing and their arrival in Manchester, which may affect the future corrosion behaviour of the specimens. Thirdly, specimens were exposed to totally unknown

conditions during the journey and extremes of temperature or rough handling of the panels, could cause cracking or loss of adhesion of the polymer. Consequently, new samples of the polymer itself were supplied by Paints Division, ready for application, but with a new problem.The polymer solvent also acted as a solvent for the laquer lining of the paint cans, causing contamination of the polymer. This problem was quickly overcome by supplying the polymer mixtures in glass bottles. No further problems were encountered, until the freshly stoved panels were removed from the oven and a fine "rust haze" was visible over the surface of each one. This was probably due to the inclusion of an acid catalyst in the polymer mixture, since its removal resulted in the production of two acrylic formulations, both of which produced a good coating without underfilm corrosion occuring during stoving.

The two acrylic polymers are quite different in composition and have only two of their constituent compounds in common. The variation in these constituents gives rise to differences in the structure of the polymer coatings. Acrylic A was designed to have a more flexible backbone than acrylic B. This is due to the nature of the compounds which are co-polymerised together to form long chain molecules (the backbone). Constituent groups may either be incorporated completely into these chains, or only a part of the molecule may be linked directly into the backbone, the rest of the molecule acting as a "side group". These side groups and certain parts of the polymer chains (for example -C=O groups) may hydrogen bond to each other, or the chains may be chemically cross linked together, as with acrylics A and B. Overleaf, is a schematic diagram of two theoretical backbones, showing large and small side groups.

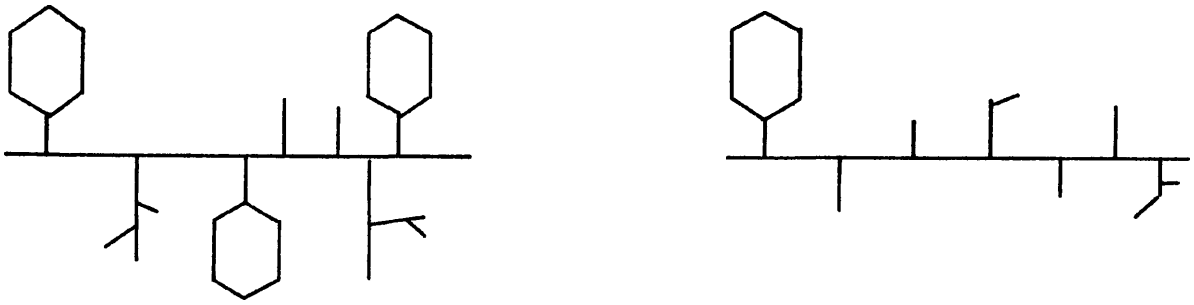

X Y

Figure 2.1 Two theoretical polymer chains.

Chain X contains many large ring structures and has longer side groups than chain Y. When several X chains are linked together, the bulky nature of the side groups will restrict many movements of the backbone, thereby producing a rigid structure. Molecule Y however, contains fewer rings and has shorter side chains than molecule X. When several Y chains are cross linked together, more chain twisting and flexing is possible, therefore polymer Y should have an inherently more flexible structure than polymer X. In the case of acrylics A and B, there are more styrene molecules incorporated into polymer B and B also contains many more longer chain side groups than polymer A. Acrylic B contains several butyl compounds which are based on four carbon atom chains (e.g. -C-C-C-C-), whilst in acrylic A, the constituent compounds are partly ethyl based (e.g. -C-C-). The longer chain side groups and the presence of a greater number of bulky styrene molecules in acrylic B, suggest that B is a less flexible polymer than acrylic A, since the side groups on B will restrict the degree of movement of the backbone. If the movement of the polymer backbone plays some part in the corrosion process, then acrylics A and B

should show different corrosion behaviour.

Both the acrylic polymers were cross linked by the same cross linking agent, Cymel 301, share the same solvent, xylene and the same stoving temperature, 152°C, leaving the only difference between A and B, that of their composition and structure.

The convertible coatings were of the vinylite type and the dry resin (manufactured by Union Carbide Ltd.), was supplied by W. and J. Leigh Ltd. Bolton. Union Carbide, claim <120> that the vinylites have good chemical resistance, low water vapour permeation and absorption, good toughness, flexibility and adhesion to clean metal substrates. Four vinylite compounds were used, each of a different composition, based on two or more of the following vinyl monomers. Unlike the acrylic polymers, the vinylite constituents are very similar and are all based on the vinyl linkage -C=C-.

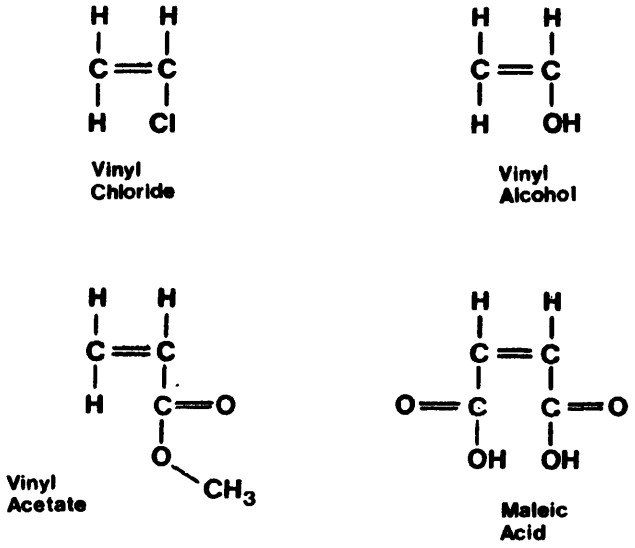

Figure 2.2 Four vinyl monomers.

It was expected that the structure of these polymers would be very similar in terms of the flexibility of the backbone, the major differences being the side groups attached to the backbone. Where the side groups are capable of hydrogen bonding, a "cross linked" type structure may result due to the interaction of side groups with each other and with the backbone itself. The degree of this association, will be related to the distribution of groups capable of hydrogen bonding, along the polymer chains. If the degree of inter and intra chain bonding is different for the different polymers, variations in their corrosion behaviour may occur. The vinylite and acrylic polymers produced transparent films when cured and no pigments were added to the polymers, so that the corrosion behaviour on the panels could be easily observed and related to electrochemical data obtained during testing.

2.3 Polymer preparation.

Acrylic polymers of the compositions given in the table overleaf, were supplied by I.C.I. ready for use. Where necessary, the polymers were thinned to a suitable viscosity with the recommended solvent, xylene, prior to casting.

Compound	% A	% B
Styrene	30	42.5
Methyl methacrylate	15	-
Butyl methacrylate	17	21.25
Hydroxy ethyl methacrylate	-	14
Hydroxy ethyl acrylate	15	-
2 Ethyl hexyl acrylate	20	-
Butyl acrylate	-	21.25
Methacrylic acid	3	-
Acrylic acid	-	1

Table 2.2 Acrylic polymer composition.

Vinylite polymers of the composition given below were made up using two different solvent mixes.

	% V_{Cl}	% V_{Ac}	% maleic acid	% V_{OH}
VYHH	86	14	-	-
VMCH	86	13	1	-
VAGH	91	3	-	6
VROH	80	-	-	20

Table 2.3 Vinylite polymer composition.

The initial solvent mixture (1) was as found in the literature <37>. However, it was noted that as the coating dried, the polymer surface often formed a six sided cell like structure, known as Bénard cells <121>. This structure is thought to be caused by solvent evaporation from film surfaces, leaving a differential viscosity between upper and lower

layers of the film. This leads to convection occuring within the film and the production of the "cell like" appearance of the dry film.This problem was overcome by omitting the methyl ethyl ketone (the highest boiling point solvent) from the mixture and using solvent mix (2).

Solvent	% vol (1)	% vol (2)
Methyl ethyl ketone	40	-
Methyl isobutyl ketone	40	50
Xylene	20	50

Table 2.4 Vinylite solvent mixtures.

Vinylite resin was stirred into the solvent slowly, to make a 40% w/v solution. Stirring was continued until a homogeneous polymer solution was obtained. It was then stored in dark glass bottles in a cupboard, to allow air bubbles to be released from the mixture, as their incorporation into a cast film would result in a defective dry film.

2.4 Polymer application and curing.

The acrylic and vinylite polymers were applied to prepared panels by spinning. This method produces a good coating of even thickness over the panel, which may be varied by altering the spinning time, a longer spin producing a thinner coating. The panel was mounted in the spinner (Sheen spinner, Sheen Instruments Ltd.), polymer solution poured onto the panel and spun for an appropriate length of time. Vinylite coatings were placed in a ventilated dust free drying chamber at 50C for fourteen days, or until the smell of solvent had disappeared from the panel. Acrylic panels

were stoved at 152°C for two hours. After curing, all panels were placed in a desiccator.

Polymers were also applied to glass panels and microscope slides, which had been washed in detergent and water and rinsed in running tap water and de-ionised water and then in acetone, before being dried in a stream of hot air. After appropriate curing, the plates and slides were soaked in de-ionised water to allow the easy removal of the films, which were used in detached film experiments, infra-red spectroscopy and for glass transition temperature analysis.

2.5 Dry film thickness measurement.

The thickness of the dry, cured films was measured to 2% accuracy using an Elcometer. Zero film thickness is set by placing the probe on an uncoated substrate. The change in the magnetic flux of the circuit caused by the inclusion of the paint film, is related to the film thickness, which is read off a gauge. A number of measurements were taken over each panel and an average value calculated.

2.6 Masking of specimens.

Cured coatings on "Pyrene" panels, were guillotined in half and a plastic coated multistranded copper wire soldered onto one end of each half panel. A steel block of known size and wrapped in "Teflon" tape, was placed in the centre of the coated side of a panel.The block was held in place by two wires wrapped around the panel and the panel was dipped into the masking medium; a 3:1 mixture of beeswax and colophony resin. This

mixture has excellent adhesion to both polymer and steel and good resistance to the salt test solution. When the masking had set, the "holding" wires and the steel block were removed from the panel, leaving an exposed area of coating surrounded by a wax trough, as shown below.

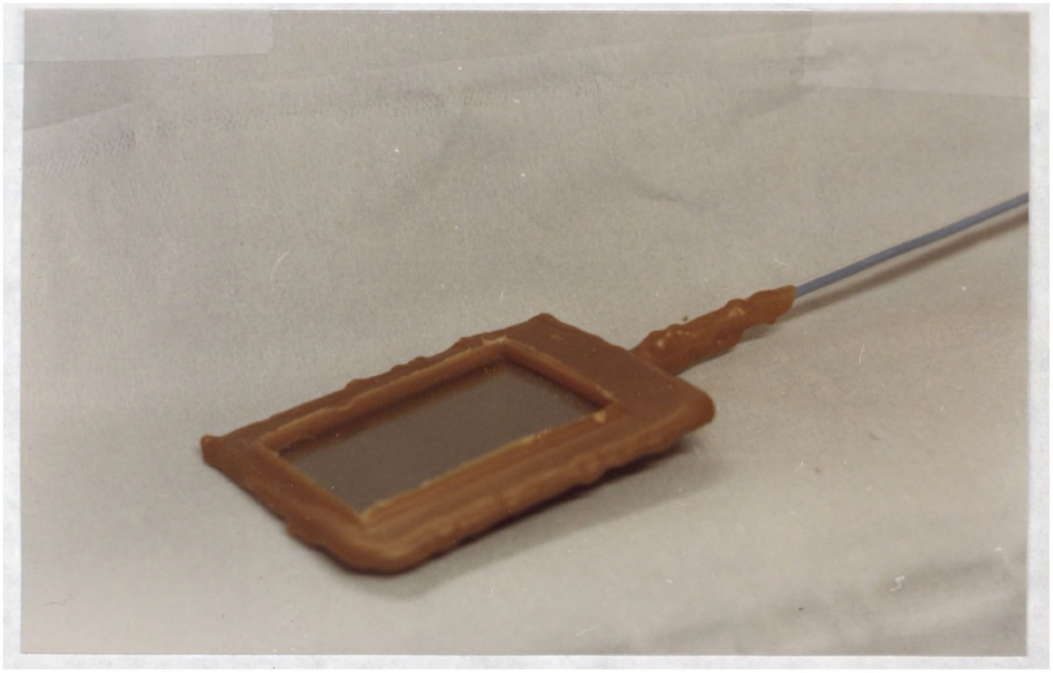

Plate 2.1 Wax masked specimen.

A length of glass tubing was slipped over the flexible wire and fixed to the panel with more of the masking mixture. The glass tube provides support for the panel during immersion, whilst the flexible wire allows easy electrical contact to be made with the specimen during experimentation. After a long period of immersion, the wax masking was melted off several specimens. Only the area exposed to the salt solution,

showed any evidence of corrosion.

2.7 Experimental solution.

The solution chosen for all the experiments was 3% sodiun chloride in de-ionised water, which is a common test solution. Since it contains only Na^+ and Cl^- ions, it represents a simple though aggressive test solution. The solution was aerated and filtered to restrict the build up of iron compounds during long term testing. The temperature of the solution during the experiments was thermostatically held at 25°C unless otherwise stated.

2.8 Choice of reference electrodes.

Two types of reference electrode were employed. Silver-silver chloride (Ag/AgCl) reference electrodes require no maintainance and have a potential about the same as a saturated calomel electrode (S.C.E.) The Ag/AgCl electrode remained immersed in the test solution during timed immersion tests. An S.C.E. was used during short term experiments.

2.9 Film characterisation techniques.

Introduction.

Polymer films were characterised in terms of both the groups present in the cured films, their glass transition temperatures and the behaviour of detached films, in order to provide a basis for comparison of the different polymers, when each was exposed to a variety of experimental

conditions. By comparing the responses of the polymers to the different environments, it may be possible to relate differences in corrosion behaviour of the polymers, to differences in the structures of the films.

2.9.1 Infra-red spectroscopy.

Thin films of each of the polymers were cast onto clean microscope slides, cured and soaked off in de-ionised water as previously described. Films were dried in a desiccator prior to testing, since initial experiments showed that water absorbed infra-red strongly over a wide band, masking any absorbtion by the polymer. Dry films were mounted in holders and placed in the spectrophotometer (Pye Unicam 1100 Infra-red spectraphotometer). The machine automatically scans over all the wavenumbers between 400 and 4000cm^{-1} and traces the results onto pre-calibrated chart paper. The wavenumbers at which absorbtion peaks are visible, can be compared with published data <122,123> and from these, the group or bond responsible for the peak may be elucidated. Infra-red spectroscopy operates on the principle that certain bonds and groups on polymer chains absorb infra-red light at a particular wavelength and it was hoped that this technique would provide information on constituent groups, cross linkages and bond formation and types, within each polymer.

As mentioned earlier, infra-red spectroscopy provided useful information as to the dryness of a film, but other problems became apparent. The cast films which produced the traces with the greatest peak definition were very thin (10-15μm). Thicker films absorbed infra-red light over a wider waveband and, as with the inclusion of water in the film, this led to a broadening of the absorbtion peaks and a loss of

definition. The presence of some solvents, where retained in the film, could also be detected using this technique. When the solvent contained infra-red absorbing groups different fron those in the polymer, these too would be visible on the trace, with the group or bond identifiable from published data. Thus by comparison with the structure of the solvent molecules, the trapped solvent may be identified. However, when the solvent's constituent groups are identical with those on the polymer, the presence of the retained solvent cannot be observed, as it will be masked by absorbtion of the polymer.

Whilst infra-red spectroscopy does provide useful information on the types of groups and bonds present in a polymer, there is no indication as to their order on the polymer backbone, or the relationship of one group to another.

2.9.2 Glass transition temperature measurements.

The glass transition temperature (Tg) of a polymer, is the temperature at which the polymer undergoes a change from the "glassy" to the "rubbery" state and this temperature may be measured using many methods. The Tg of the polymers used in these experiments, were measured using two different techniques. Firstly, by a microindentation method, carried out at I.C.I. (Slough), on the polymers cast onto aluminium and secondly, using a Differential Thermal Analysis (D.T.A.) method, in the Department of Polymers and Fibres, U.M.I.S.T. The D.T.A. technique was performed on both dry, as received, vinylite resins and on dry, detached vinyl and acrylic films.

The microindentation apparatus operates on the principle of penetration of a ball ended needle, which is under a constant load, into the polymer film, as a function of time and temperature. A specimen of the polymer, on an aluminium substrate, was fixed into the machine and allowed to equilibrate at the temperature chosen. The ball ended needle was mounted on the end of a beam and was allowed to rest lightly on the specimen surface. A recorder was switched on and a suitable weight lowered onto the beam, which pushes the needle into the polymer. When equilibrium was reached, the load was removed from the beam and the specimen allowed to "recover". The shape of the curve (as plotted on a "penetration depth" against "time" curve), is an indication of the rheological state of the film. By repeating this proceedure over a range of temperatures, the transition temperature between the "glassy" and the "rubbery" states of the polymer can be determined <124>.

Differential thermal analysis, (D.T.A.) was carried out using both dry resins and cured, detached films , on a Du Pont 900 Differential Thermal Analyzer. This technique is used in the study of the thermal behaviour of polymers as they undergo physical and chemical changes with temperature. The response of the polymer is monitored against an inert reference material, which does not undergo any changes over the temperature range studied.

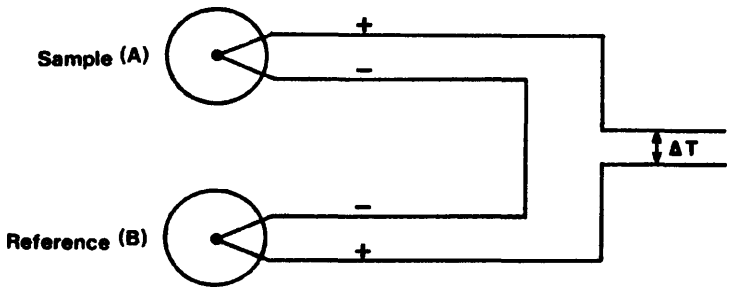

Figure 2.3 D.T.A. thermocouple arrangement.

Thermocouple A is placed in the sample to be analyzed and thermocouple B in the reference material, in this case, glass beads. Both sample and reference are exposed to the same conditions in the test chamber. When the temperature of both sample and reference is the same, the thermocouples produce identical voltages and the net voltage output is zero. When the temperatures of A and B differ, the difference in the net voltage reflects the difference in temperature between the sample and reference materials. This ΔT may be positive or negative, depending upon the processes occurring in the sample and by plotting ΔT against time, the shape of the resulting thermogram will provide information on the behaviour of the sample, such as, solvent loss, glass transition, melting, etc. <125>. The D.T.A. technique suffers from two problems. Firstly, if the thermal capacity of the reference and sample materials are markedly different, erroneous differences will be recorded between them. Secondly, polymer films are poor heat conductors and if several layers of cured film are used to produce the sample, there may be a delay between, for example, the glass transition of the outer pieces and that

of inner pieces of film, again causing confusing thermograms to be produced.

The indentation technique avoids both these problems, but suffers drawbacks of its own. The substrate used is aluminium and it is possible that the bonding of the polymer to aluminium may not be the same as to mild steel, giving a difference in response. Secondly, the thickness of the film may affect the depth of penetration of the needle and, therefore, the time to recovery of the deformed film.

None of these problems with either technique is of a serious nature, providing care is taken during sample preparation, to ensure that each film is of the same thickness and that only one thick piece of film is used in D.T.A. analysis. However, one major problem, common to both methods, is that of the effect of retained solvent. When a film cures, especially if by solvent evaporation, some of the solvent may not be able to escape from the bulk film before the surface layers become cured, thus trapping solvent in the film. This retained solvent, has the effect of plasticising the polymer, which causes a decrease in the measured glass transition temperature, as the film appears to be in the "rubbery" state. Trapped solvent may be released from the film by heating to a temperature greater than that of the boiling point of the solvent and the glass transition temperature of the film. This will provide a more accurate measurement of the Tg of the film, although care must be taken not to heat the sample to a temperature where decomposition of the polymer can occur.

2.9.3 Detached films.

The thickness of the dry detached film was measured prior to mounting. Only the vinylite type films were used in these experiments, as the acrylic films were very brittle when cast onto glass plates and cracked easily upon their removal from the plate, or during mounting. This is probably due to their being in the "glassy" state, that is, below their Tg at room temperature. Whilst the vinylites are also in their "glassy" state at ambient temperatures, they are inherently less brittle than the acrylic films and can be mounted without cracking.

The film was placed between two neoprene gaskets and bolted into position between glass arms, using Q.V.F. fittings. 3% sodium chloride solution was poured into each arm and a mild steel rod, coated in wax to within 2.5cm of each end, was introduced into one arm, as shown below.

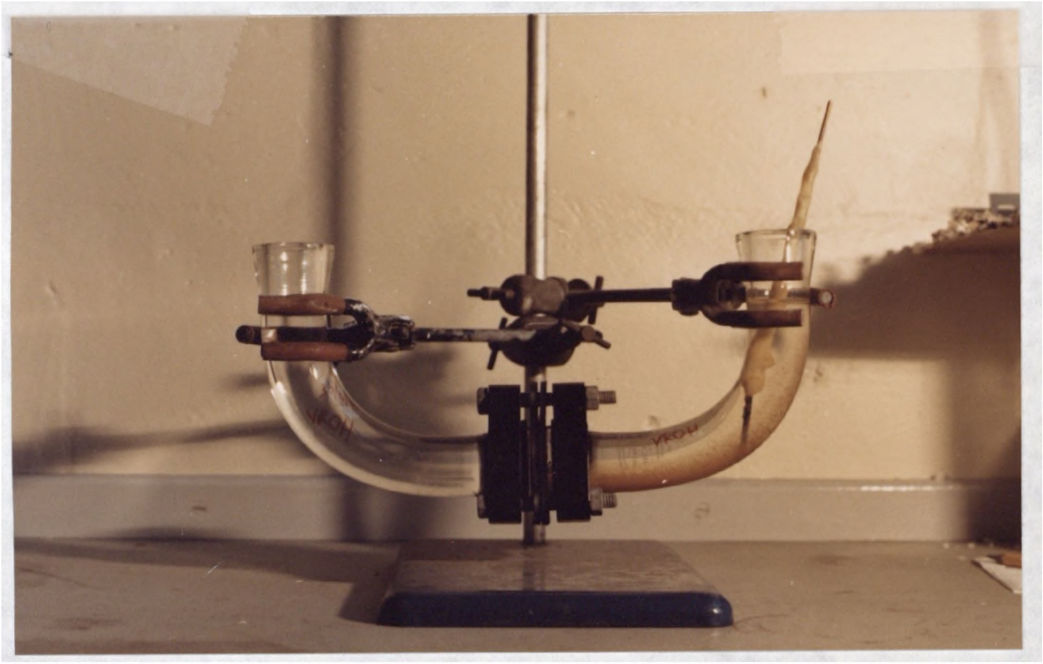

Plate 2.2 Detached film apparatus.

Calomel reference and platinum auxiliary electrodes were introduced, prior to impedance measurements being carried out. The potential of the working electrode was measured against a Calomel reference electrode using a Keighly 610C Electrometer and was potentiostatically held at the measured potential during the impedance run. The following three electrode arrangement was used, the potential being controlled using a potentiostat (Thompson ministat 251). Where several impedance measurements were made in succession, the potential of the panel was re-measured between each run.

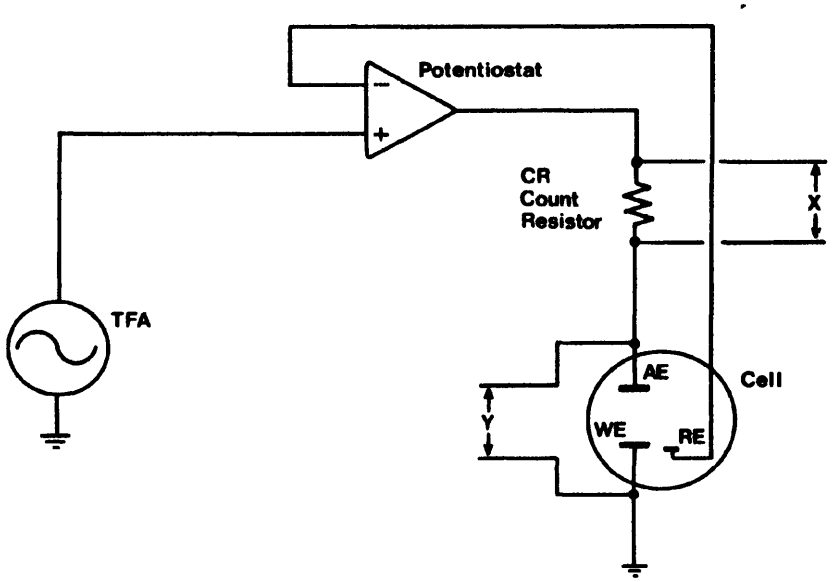

Figure 2.4 Three electrode wiring arrangement.

The Frequency Response Analyzer (Schlumberger, Solartron 1172 Frequency Response Analyzer) produces a sinusoidal wave of known frequency and amplitude, which is imposed on the experimental system. The resulting response is measured by the F.R.A. as Y/X and transferred via a

Data Transfer Unit (Schlumberger, Solartron DTU 3217), in "real" and "imaginary" format, to paper tape. The tape is fed into a microcomputer (Hewlett Packard HP85) for subsequent analysis.

Impedance measurements were performed on detached films over a period of time from immersion. After some time, a pinhole was deliberately created in each film by pushing the point of a large pin through the film, leaving a hole approximately 1mm. Impedance measurements were carried out over a period of time after the pinhole was created. The effect of the solution temperature on intact films was also considered. The apparatus was placed in a water bath containing de-ionised water and the temperature of the bath was raised in small increments, until the chosen temperature was reached in the glass arms. An impedance run was then performed and the cycle repeated, from ambient temperature to 65°C, just above the upper glass transition temperatures of the vinylites.

2.9.4 Agar.

After some time, it was noticed that the pinholes in the films contained a red/orange gel-like structure (presumably composed of iron compounds) and that several of the impedance parameters were also different from the earlier results. In order to study these changes further, an agar gel was used to create a giant "pinhole equivalent" over the surface of a specimen, in an attempt to simulate the conditions observed within the pinhole.

Agar agar (DIFCO), was mixed up in the ratio 1:10 with boiling de-ionised water and "cooked" for fifteen minutes to produce a gel. The

mixture was allowed to cool for a few minutes, to allow the release of air bubbles, before being poured into the wax trough of pre-masked "Pyrene" panels. When set, the panels were immersed in 3% sodium chloride solution and impedance runs carried out at regular intervals.

Agar is a colloid, obtained from the cell walls of the seaweed Gelidium and is an ester of the polysaccharide D-galactopyranose, whose structure is shown below <126>.

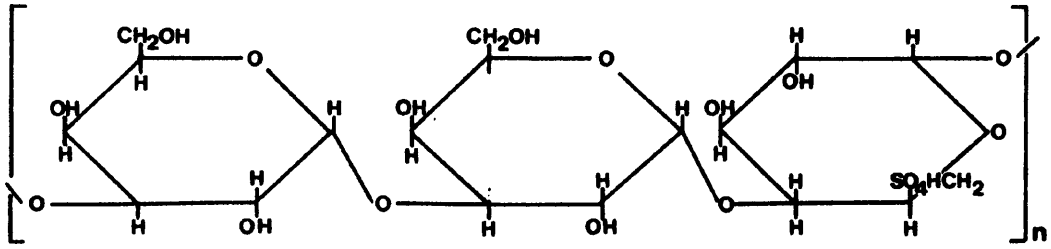

Figure 2.5 Structure of agar.

It is capable of absorbing up to twenty times its own weight of water <126> and in simple experiments, where agar was poured onto steel panels, left to set and then immersed in salt solution, it was found that the gel was also capable of absorbing orange iron compounds into itself. This is likely to be due to the "open" un-crosslinked, but probably hydrogen bonded nature of the polysaccharide chains.

2.10 Impedance behaviour of attached films.

2.10.1 Measurement of dry film capacitance.

The capacitance of several dry, prepared specimens, prior to immersion, was measured using the following technique. Mercury was poured into the wax trough created during the masking of the specimen. A Platinum counter electrode was dipped into the mercury and an impedance run carried out. A "two electrode" wiring circuit was used, as shown;

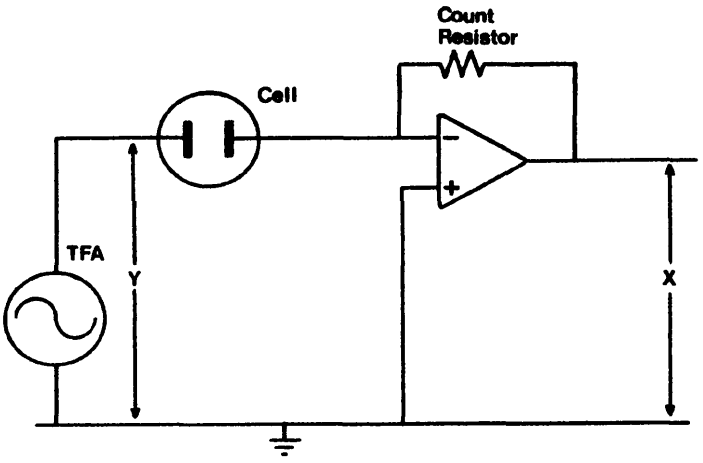

Figure 2.6 Two electrode wiring arrangement.

As with the three electrode measurements, the count resistor was chosen to have a value similar to that of the experimental cell. After measurements had been made, the mercury was carefully returned to its

container and the panel inverted and tapped gently, to ensure that all the mercury was removed, thus avoiding solution contamination. Specimens were then immersed in the 3% sodium chloride test solution.

2.10.2 Presence and absence of oxygen.

The test solution, 3% sodium chloride, was poured into reaction vessels and oxygen-free nitrogen (B.O.C.) was bubbled into the solution for forty-eight hours, to purge as much oxygen from the solution as possible. The masked halves of a coated "Pyrene" panel were immersed, one in the deaerated salt solution and the other in aerated solution. Impedance measurements were carried out regularly over a period of time from immersion. The visual appearance of the panels in the solutions was noted and photographed to show the differences in corrosion behaviour between the specimens.

2.10.3 The effect of temperature.

In these experiments, the temperature of the solution in which the test panel was immersed, was altered. The detached films showed little change at the higher glass transition temperature and no change at the lower Tg. These experiments were performed to see whether attached films behaved any differently at the lower Tg, than the detached films.

A vinylite specimen (VMCH) was immersed in 3% sodium chloride solution at room temperature and an impedance run carried out. The temperature of the solution was raised in small increments, using a thermostatically controlled glass covered immersion heater. (The glass covering avoids

possible contamination from the heating element.) After allowing the panel a few minutes to equilibrate at the new temperature, impedance measurements were made and the cycle repeated.

The converse experiment, where the solution was initially heated to above the lower Tg of the vinylite specimen, prior to initial immersion, was also performed. In this instance, impedance measurements were carried out over a period of hours, as the solution cooled down to ambient temperature. These temperature changing experiments, from below to above the Tg, or vice versa, were carried out at regular intervals from the initial immersion of the specimens, in order to show whether the length of time a specimen had been immersed, affected its impedance response at or above the glass transition temperature.

2.10.4 Effect of a pin hole.

In order to simulate damage to a coated specimen and to compare the response of attached and detached films to a pin hole, impedance measurements were carried out prior to and immediately after, the production of a 1mm diameter pin hole on an acrylic B panel. Further impedance measurements were made with time.

2.10.5 Effects of substrate preparation and coating thickness.

In this series of experiments, two different methods of substrate preparation, namely, citric acid pickling and degreasing "Pyrene" panels, were used. Multilayer coatings were applied, as described earlier and the specimens were exposed to 3% sodium chloride solution. Both acrylic and

vinylite specimens were examined and the substrate preparation and coating thickness are indicated in the results section.

2.10.6 Changes in the measured rest potential with time.

The rest potential of the immersed specimens, was monitored with time, against either a Calomel, or a silver/silver chloride reference electrode. It was thought that there may be some relationship between the rest potential of a specimen and its impedance behaviour. It was also possible that changes in the rest potential may be indicative of a corrosion or other process occurring on the specimen.

Chapter 3. Results.

Film characterisation.

3.1 Infra-red spectroscopy.

The infra-red traces obtained from each of the polymers, which are shown on the following pages, (figures 3.1-3.7), can be seen to have several peaks in common. The vinylites in particular, show great similarity to each other. The acrylic films are less similar, but markedly different from the traces from the vinyl based polymers. The infra-red absorption of many bonds and groups has been well characterised and it is possible to compare absorption peaks on the charts, with the published data. The table below summarises some of the absorbing groups and bonds, together with the wavenumber at their absorption peak.

Wave number (cm^{-1})	Bond or group absorbing I.R.
600-650	-C=C- , aromatics
700	aromatics.
825	-C=C-
950	-C-O- , aldehydes, vinyl.
1025	-OH
1100	-C-O- , esters, ethers.
1375	aldehydes, $-CO_2H$
1450	vinyls, alkanes.
1700-1750	$-CO_2H$, esters.
2900-3000	$-CO_2H$, H-Cl
3500-3600	-OH , -C C-H , -NH

Table 3.1 Infra-red data.

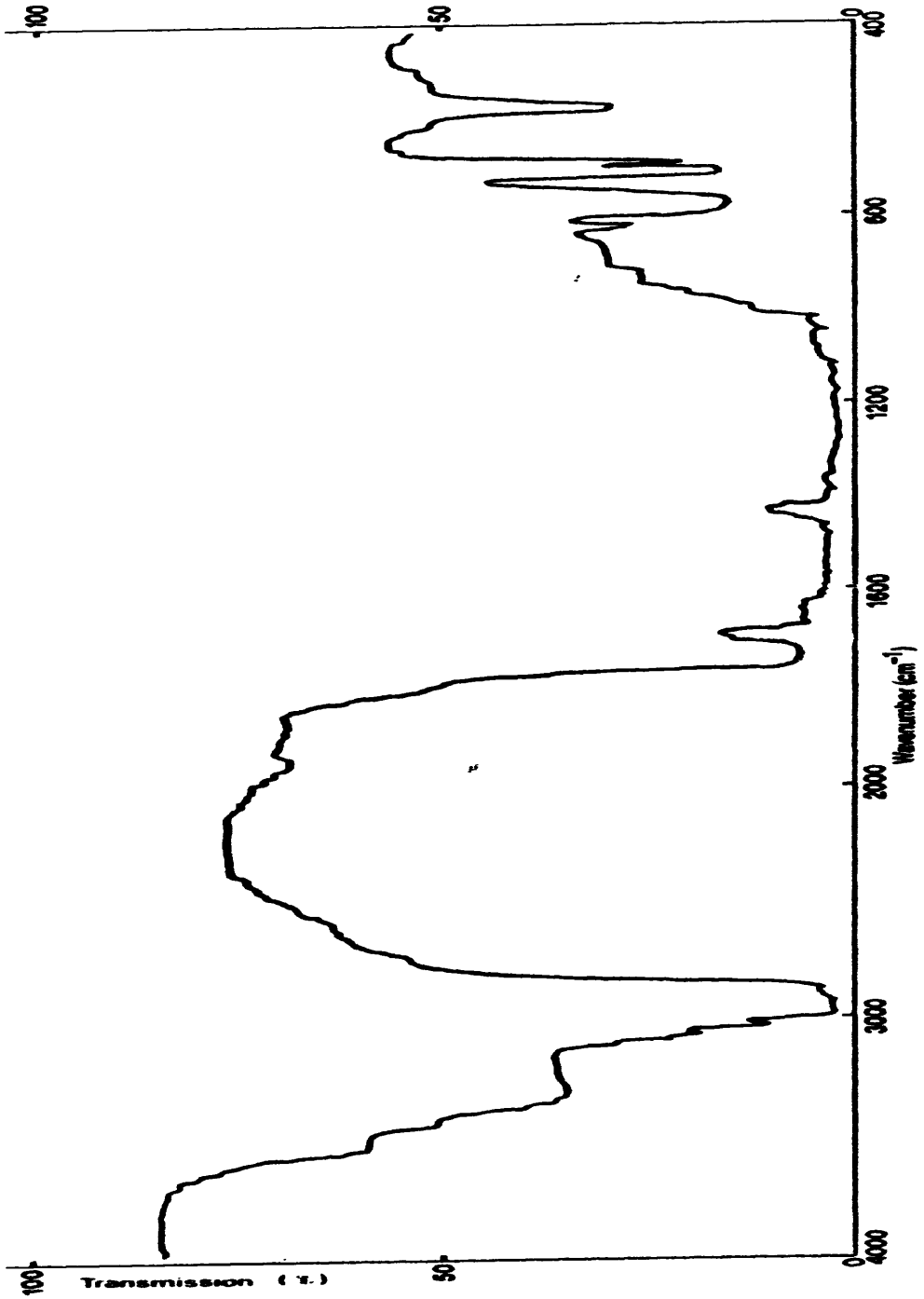

Figure 3.1 Infra-red absorption trace of VYHH (wet).

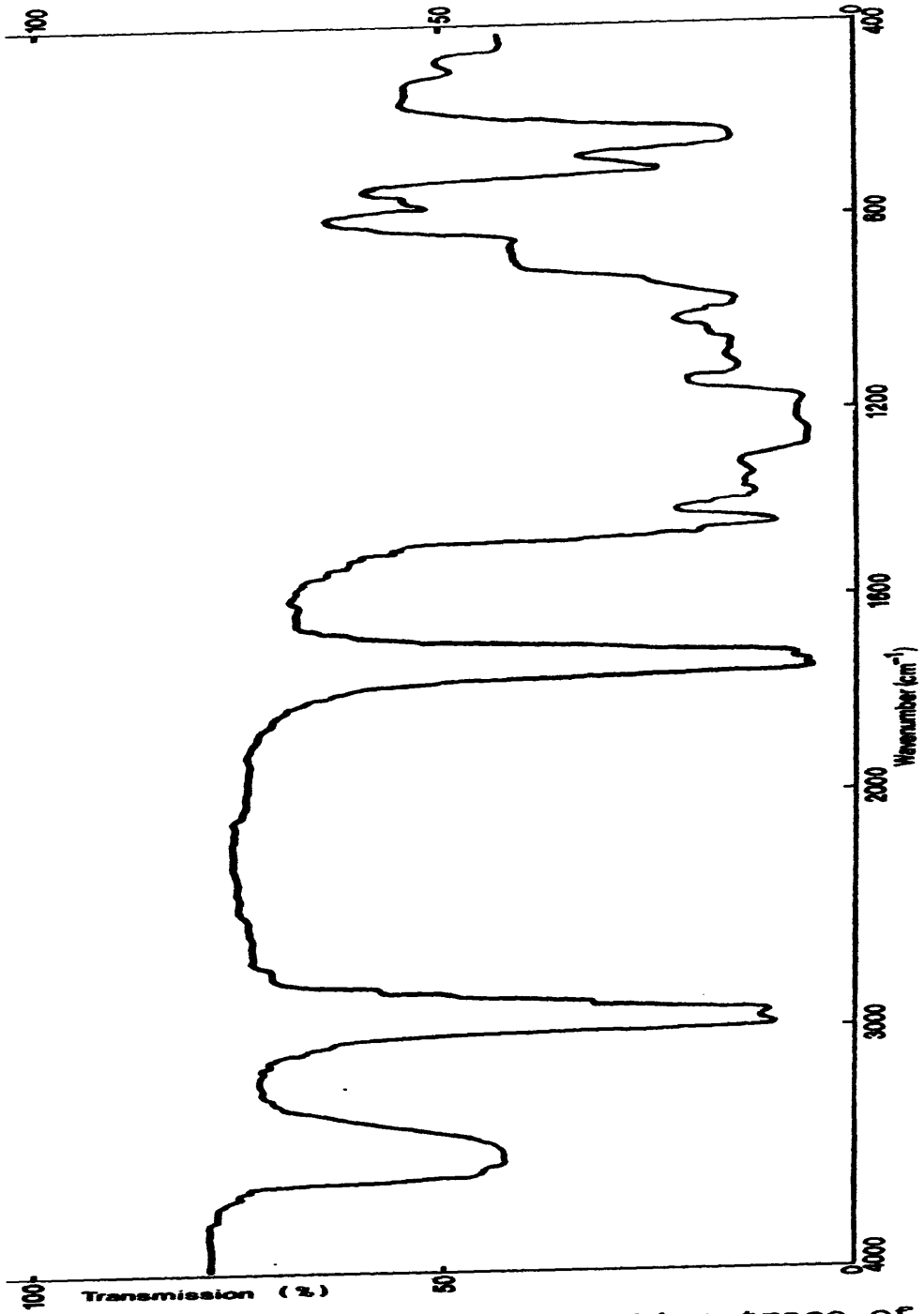

Figure 3.2 Infra-red absorption trace of VROH.

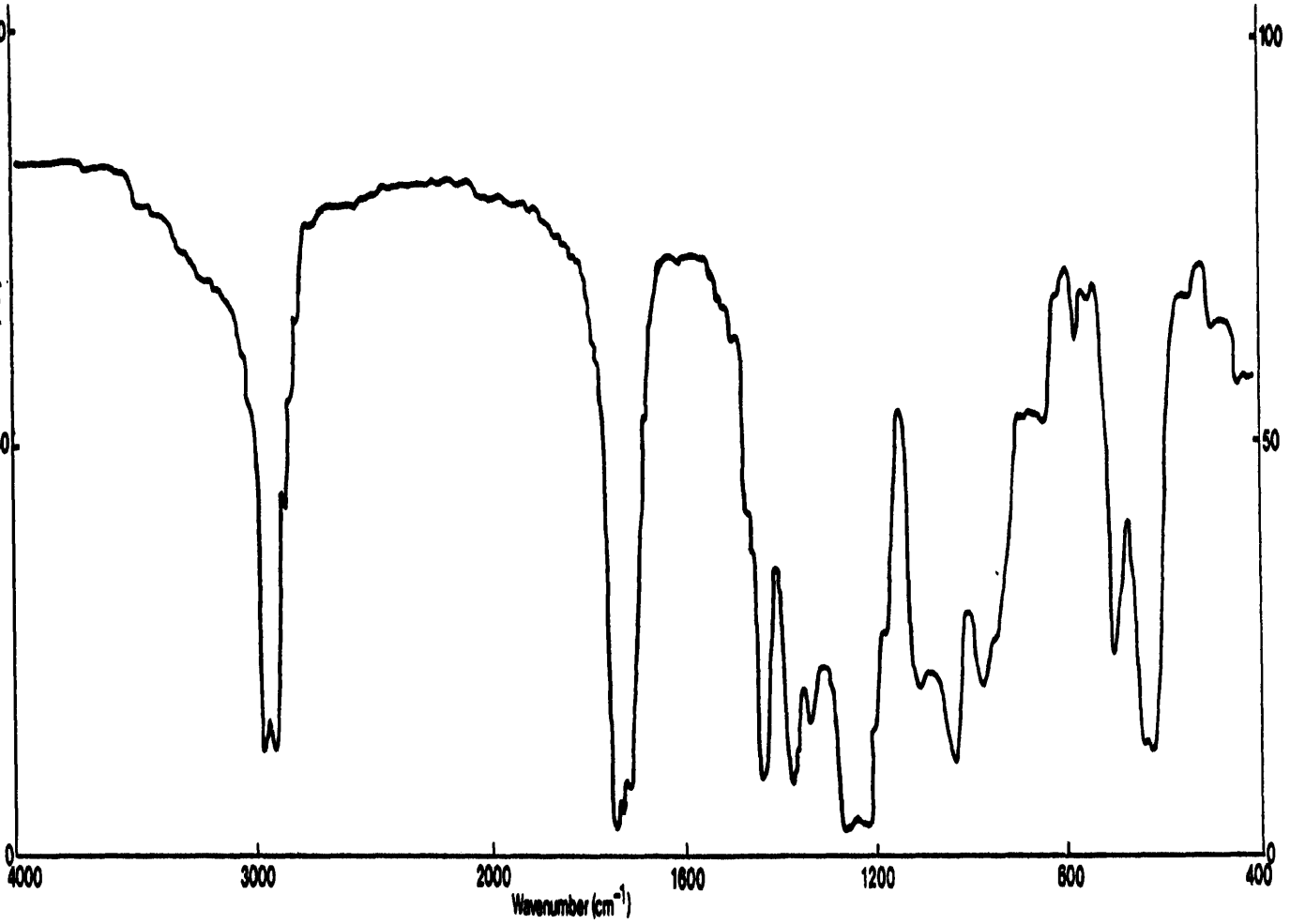

Figure 3.3 Infra-red absorption trace of VMCH.

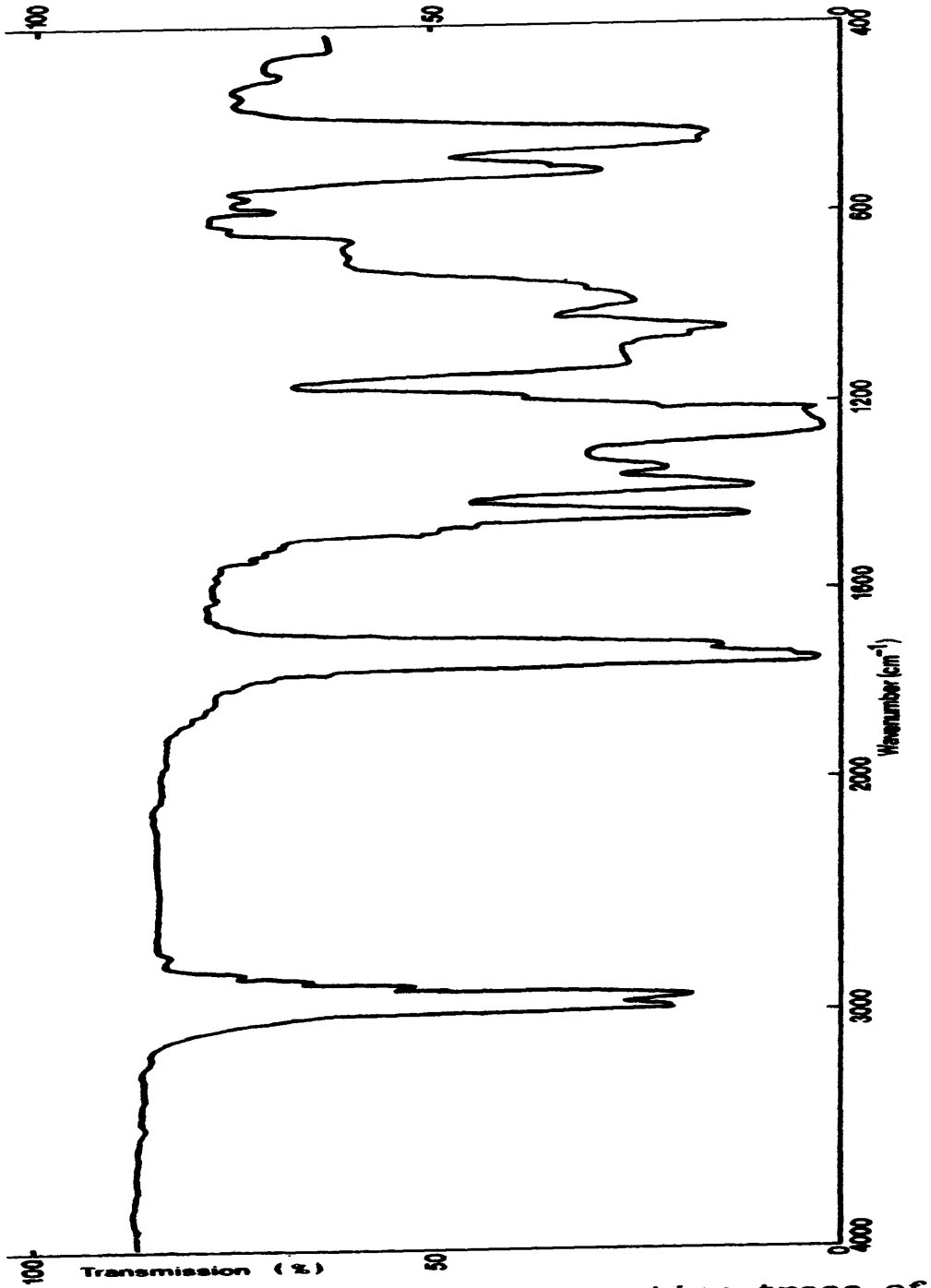

Figure 3.4 Infra-red absorption trace of VYHH.

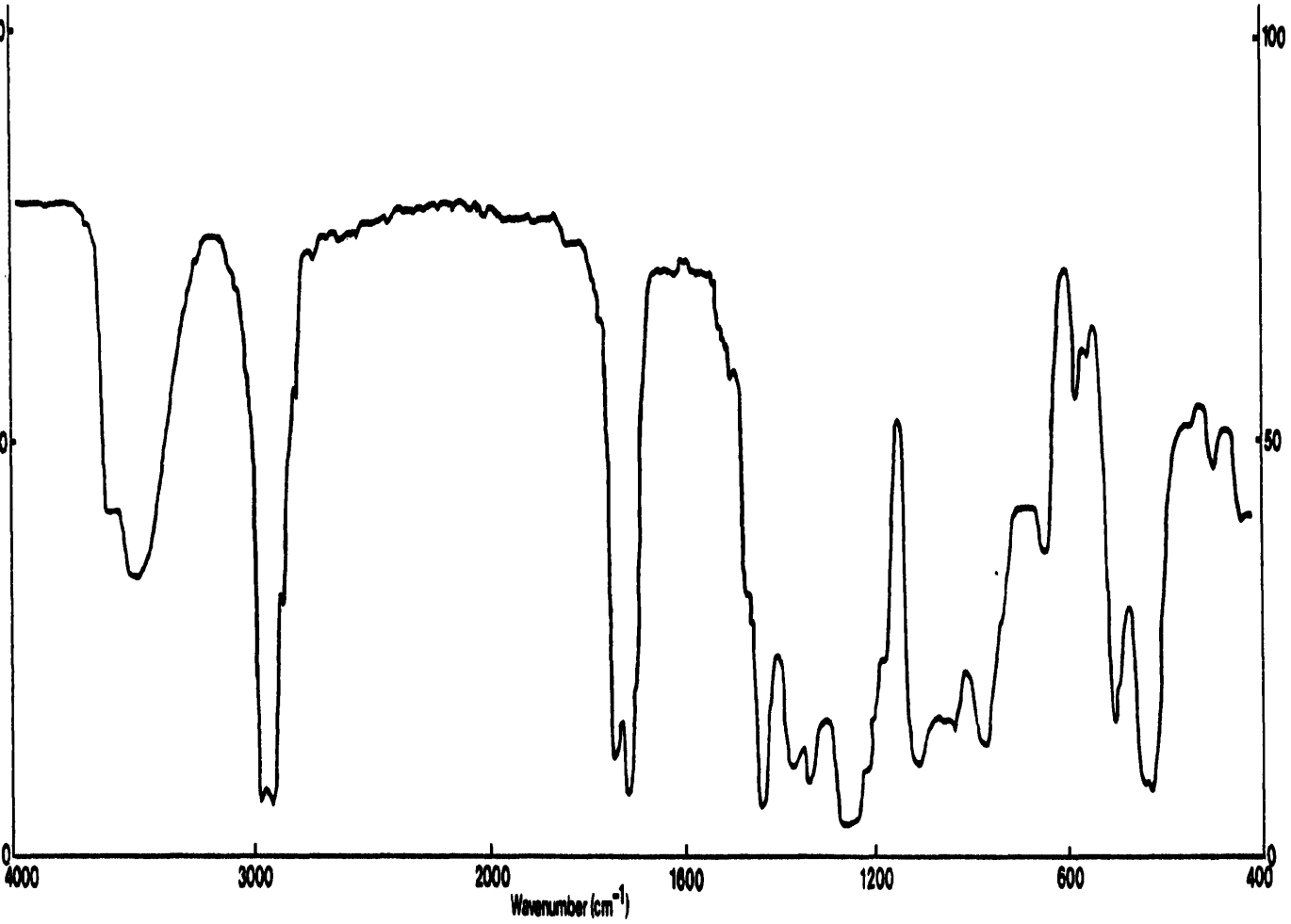

Figure 3.5 Infra-red absorption trace of VAGH.

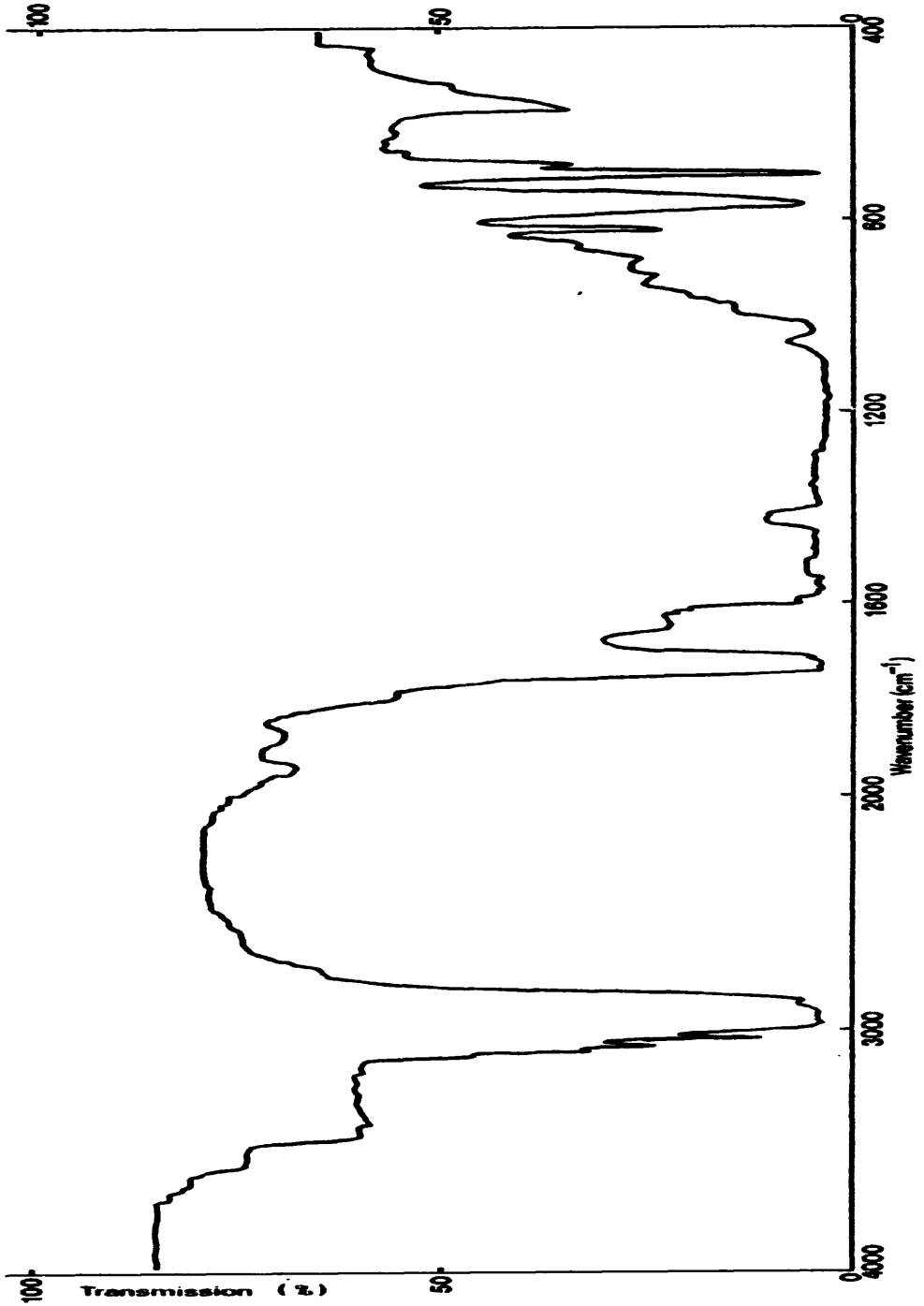

Figure 3.6 Infra-red absorption trace of Acrylic A.

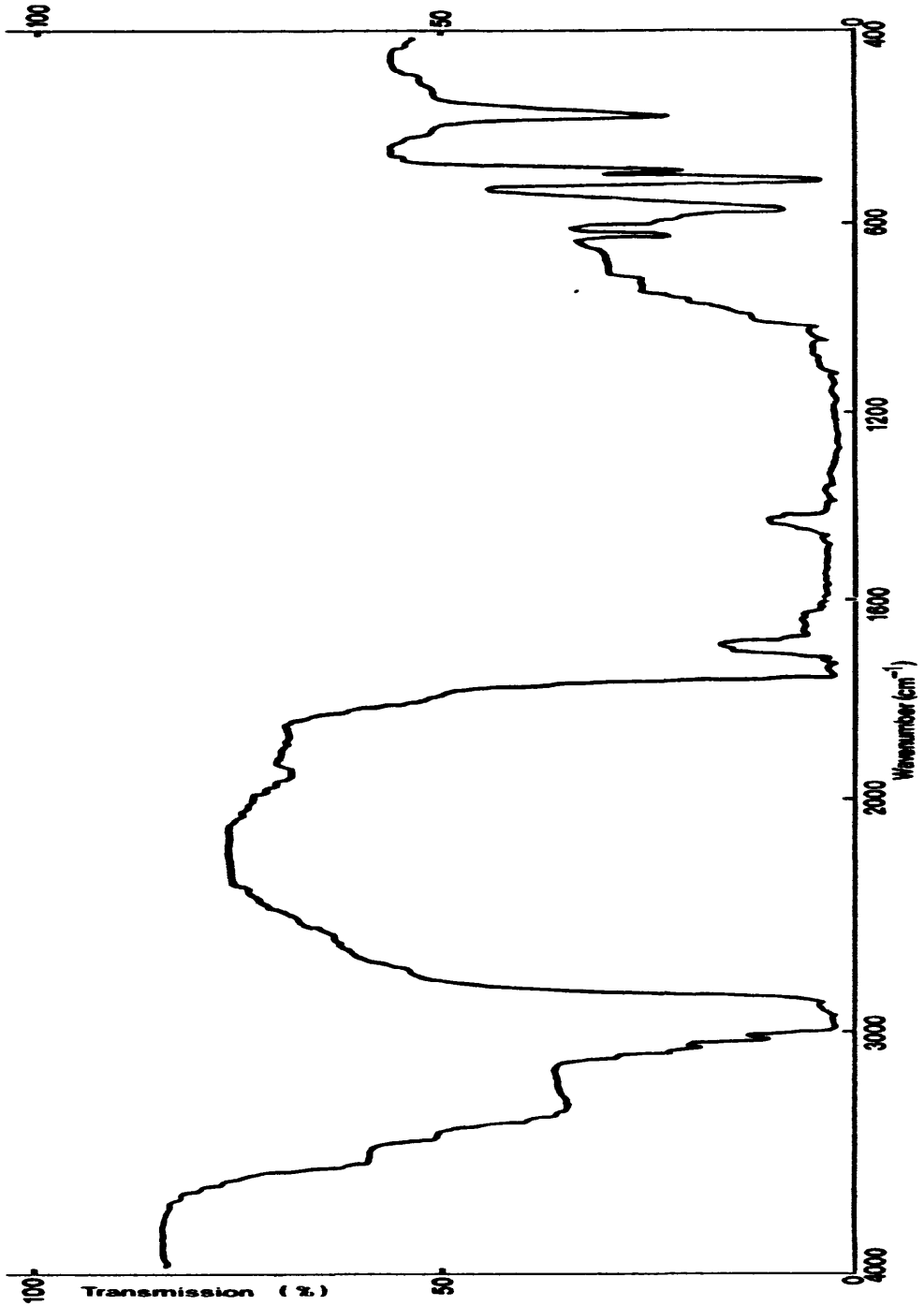

Figure 3.7 Infra-red absorption trace for Acrylic B.

From the table, it can be seen that groups such as $-CO_2H$, absorb infra-red light over a broad waveband, whilst others such as -C=C- absorb infra-red at several different and discrete wave numbers. The absorption at a particular wave number may, therefore, be due to any one, or to a combination of groups or bonds. In some cases, it is difficult to relate the absorption peaks on the graph directly to the group or bond responsible, however, by comparison of the possible groups with the polymer constituents, it may be possible to assume the occurrence of cross linking in some instances. Where a group is present as a polymer constituent and has a characteristic absorption wave number, if this peak does not appear in the trace from the cured film, it may be assumed that cross linking between this group and another part of the polymer chain has taken place.

There is, unfortunately, no information available using this technique, concerning the sequence of the side groups on the backbone of the polymer, or on their relative distribution. However, providing that all the films being examined by this method are of the same thickness, it is possible to relate the height of the absorption peaks to the relative quantities of absorbing groups in the film, bearing in mind that some groups and bonds absorb infra-red more strongly than others.

In the case of the four vinylite polymers, it is noted that the graphs obtained are very similar, each posessing absorption peaks corresponding to such groups and bonds as; -CO H; vinyl; esters; aldehydes; -CO; etc. The presence of a small quantity of an aromatic group is also observed

and this is probably due to the retention of a tiny amount of xylene (a strong infra-red absorber) in the films. Perhaps the most noticeable difference between the vinylite films, is the presence of a strong absorption peak at a wavenumber of about 3500 cm^{-1}, by VROH and VAGH. This absorption can be directly attributable to the presence of -OH groups in these polymers, since both the peak and the group are absent from VYHH and VMCH.

In contrast to the vinylites, the acrylic polymers contain a larger number of more complex constituents and although each each acrylic contains different compounds, the infra-red traces are very similar. This is probably due to the fact that the polymer constituents contain many of the same infra-red absorbing groups. Each contains styrene which absorbs in the aromatic regions, about 700cm^{-1}. The presence of ester linkages, -CO groups etc. could all originate from most of the original compounds in the polymers, or arise during stoving, as the polymers cross link and cure. The broad absorption bands in the 1000-1800cm^{-1} region, are likely to be caused by a large number of strong infra-red absorbing acrylate groups, since both acrylic polymers contain a number of acrylate compounds. Although these groups differ in size and in the exact composition of each acrylate compound, they all absorb infra-red in the same region, thereby making elucidation of particular groups in the polymers, impossible.

3.2 Glass transition temperature.

The glass transition temperatures (Tg) of the polymers was measured using two different techniques on both dry resin and cast films. The microindentation method was used on polymers cast onto aluminium sheet and the differential thermal analysis technique on dry resins and detached films. Both methods monitor the change in elasticity of the polymer which occurs at its Tg, the D.T.A. method by measuring the change in the heat capacity of the polymer, relative to that of glass beads. The indentation method, by the length of time between indentation and recovery of the film. The result of the two techniques are summarised in the table below and the graphs from which they are taken, are shown in Appendix 1.

	VYHH	VAGH	VROH	VMCH	Acrylic A	Acrylic B
Tg (°C)	29	29	34	29	-	-
Dry Resin	67	64	64	64	-	-
Detached	-	27	-	28	-	-
Film	60	-	54	54	43	33
Cast Film	30	30	39	30	43	34

Table 3.2 Tg's of the polymers.

From the table, it can be seen that the glass transition temperatures of the acrylic films are the same for both techniques, each polymer having only one Tg. The vinylites show the presence of two Tg's each and the presence of varying amounts of retained solvent. These features are

shown schematically in the diagram;

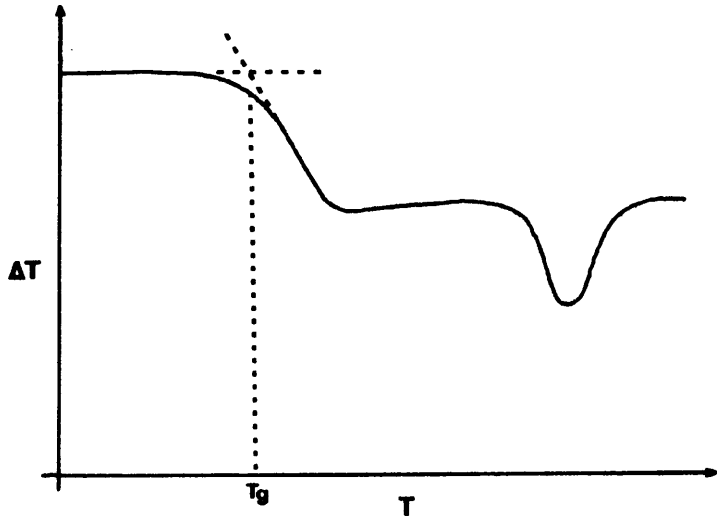

Figure 3.8 Schematic D.T.A. trace.

A tangent was drawn between the original baseline and the slope of the curve, as shown, the point of intersection being the glass transition temperature. Where the slope of the line changes, it is difficult to pinpoint the exact Tg accurately and several runs may be necessary if a precise Tg is required. Retained solvent in the film can be detected by a depression on the trace, followed by a return to the previous baseline, as shown in figure 3.8. When the same samples were re-run through the D.T.A. process, the second trace showed a higher Tg than the first, with no depression, as the trapped solvent had been removed. The increase in the measured Tg was caused by the loss of solvent from the polymer, which had a plasticising (Tg lowering) effect on the film.

The Tg of the vinylite polymers was measured three times, once as films cast on aluminium, by the indentation technique and twice by D.T.A.

as dry resins and detached films. Unlike the acrylic films, which show only one glass transition each and little or no retained solvent, the vinylites show two transitions in the dry resin state, with a small amount of retained solvent. Whilst in the cast state, microindentation shows the presence of the lower transition only. Using the D.T.A. method, the lower Tg of all the vinylites is very small, with a much larger transition around 65C in the dry resin. When measured as dry films, the presence of retained solvent in the film was readily apparent. When several of these films were re-run, the measured Tg increased by up to 15C. (The numbers quoted in the table, are the "first run" values.)

Although it was noted that the vinylite films contained retained solvent and therefore had a lowered Tg, it was decided to continue specimen preparation as before, that is casting the films and leaving them until the smell of solvent had disappeared. Since this is the curing method used "on-site", the corrosion behaviour of the polymers observed in the experiments reported here, may be related to any subsequent studies of these polymers under "natural weathering" conditions.

3.3 Detached films.

3.3.1 Analysis of impedance data.

After each impedance experiment was performed, the resulting data was produced in the form of punched paper tape. The information on this tape was loaded into the computer (HP85) and was stored on magnetic tape for future analysis or referral. The computer program generates several plots from the impedance data and details of this program have been given

elsewhere <107>.

The most commonly used plot, is the Nyquist plot. THis is a plot of the "imaginary" or capacitive part of the impedance (Z"), against the "real" or resistive part of the impedance (Z'). Each point on the curve, represents a measurement made at a particular frequency. From this plot, the value of the solution resistance (Rs), the charge transfer resistance (Rθ) or the polymer film resistance etc. may be obtained, together with information about diffusion processes occurring in the system. Such processes may be followed by studying the shape of the impedance plot. For example;

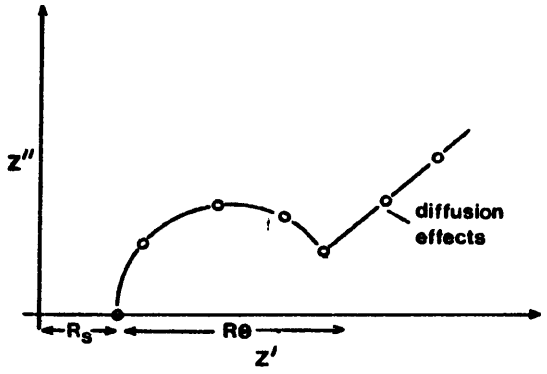

Figure 3.9 Schematic impedance plot.

On a coated specimen, the effects of the charge transfer resistance may not be seen. In this case, the effects of the polymer film will instead be observed and the capacitance values will relate to those of the film.

A second useful plot, is that of the imaginary part of the admittance (Y") against the angular frequency (ω). The slope of the plot is that of

the capacitance of the semicircle on the Nyquist plot. The numerical value of the capacitance provides information about the process under examination. For example, polymer films typically exhibit a capacitance measured in pF/cm; the electrochemical double layer in μF/cm and so on. Therefore, if more than one semicircle is observed on the Nyquist plot, it is possible to determine which is due to the polymer, for example and which is due to other processes.

3.3.2 Detached film results.

The impedance response of detached vinylite films was measured under several different experimental conditions. Firstly, the effect of time of immersion was studied using two films, VROH and VMCH, with 3% sodium chloride solution in each arm of the apparatus. Measurements were made at regular intervals over a period of time and the results are summarised in the following tables. The impedance response of VYHH over a short period of time is also presented. Following the table which summarises all the data concerning a particular specimen, are several of the more interesting impedance plots. The remainder of the plots from each experiment, have been located in the appendices at the end of this thesis.

The results indicate a difference in impedance behaviour between VROH and the other films, although all three polymers showed changes in the measured values of Rs, capacitance and specimen rest potential, with time.

Time	Rs Ωcm^2	Rsc Ωcm^2	Capacitance cm^{-2}	Nyquist Plot	Potential mV vs. S.C.E.
30min	7E4	-	3nF	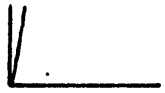	-410
2hrs	7E4	-	3nF		-540
1days	7E4	-	3.1nF	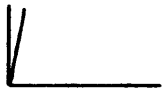	-630
2days	7E4	-	3.1nF		-660

Table 3.3 VYHH, intact, detached film.

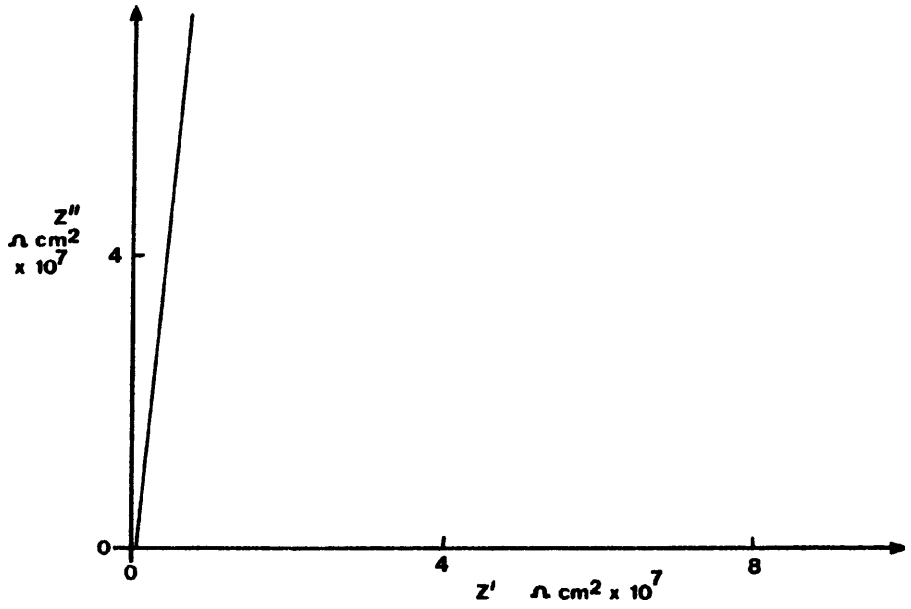

Figure 3.10 VYHH, detached film, 0-2 days immersion.

Time	Rs Ωcm^2	Rsc Ωcm^2	Capacitance cm^{-2}	Nyquist Plot	Potential mV vs. S.C.E.
0	7E4	-	3nF		-420
15min	7E4	-	2.8nF		-460
1-20hrs	7E4	-	2.8nF		-460
8days	3E4	-	16.2nF		-740
19days	1.3E6	-	312pF		-725
28days	1.1E6	-	360pF		-630
40days	3E4	-	13.1nF		-640

Table 3.4 VMCH, intact, detached film.

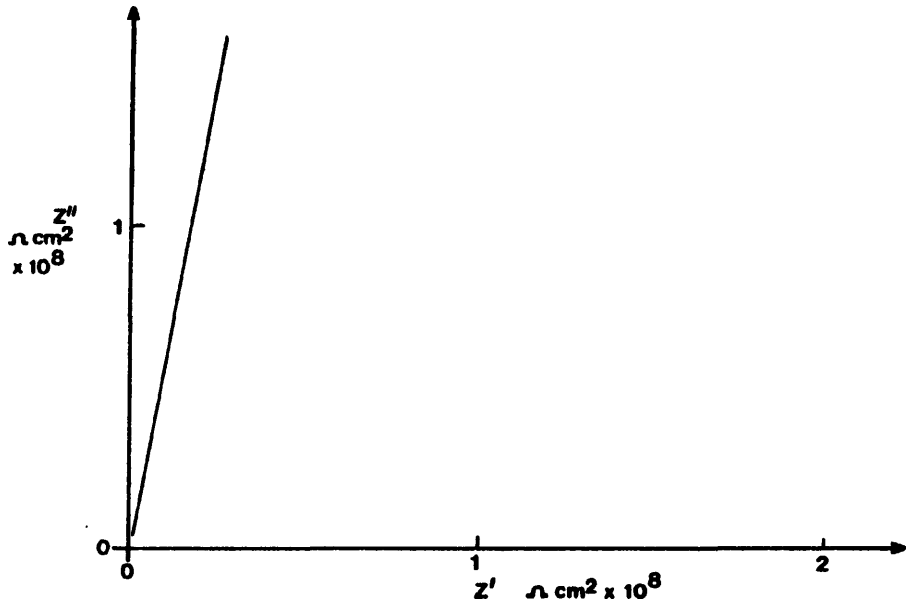

Figure 3.11 VMCH, detached film, 0-40 days immersion.

Time	Rs Ωcm^2	Rsc Ωcm^2	Capacitance cm^{-2}	Nyquist Plot	Potential mV vs. S.C.E.
0	2.3E4	3.5E5	14.4nF		-300
5min	2.3E4	2.4E5	14.6nF		-400
10min	2.3E4	1.9E5	14.7nF		-425
1hr	2.3E4	1.8E5	14.7nF		-480
5days	4.5E4	3.2E5	14.7nF		-620
12days	2.4E4	2.0E5	13.8nF		-620

Table 3.5 VROH, intact, detached film.

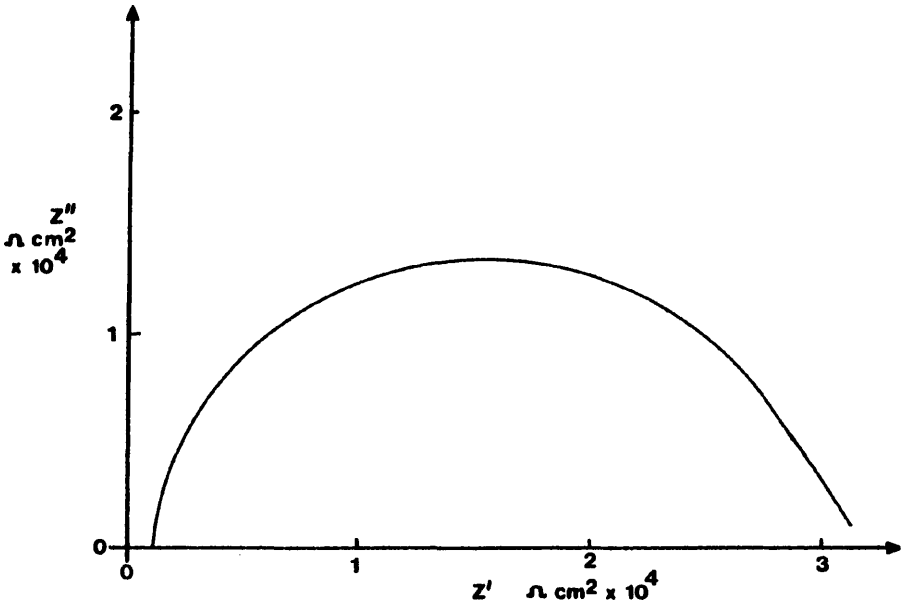

Figure 3.12 VROH, detached film, 0-12 days immersion.

After a period of time, a pinhole was made in each film by pushing a pin through the film. Again, the impedance response of the film was monitored with time. The results from these experiments are shown in the following tables and it can be observed that Rs (the solution resistance) decreases by several orders of magnitude when the pinhole is made in the film.The shape of the impedance plot also changes, from a "capacitive" type plot, to one typical of diffusion effects, with a corresponding change in the capacitance values. All the polymer films show an increase in Rs after a period of immersion.

Time	Rs Ωcm^2	Rsc Ωcm^2	Capacitance cm^{-2}	Nyquist Plot	Potential mV vs. S.C.E.
0	3.7E4	-	50.7μF		-610
5min	1.2E4	-	11.7μF	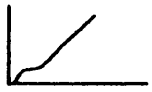	-230
15min	1.3E4	-	35.6μF		-560
30min	1.2E4	-	28.0μF	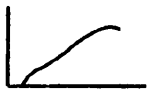	-640
7days	15.5	300	0.38mF		-740
18days	2.5	10	2.0mF		-550
30days	1.3	8.5E2	0.9mF	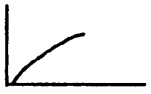	-620
43days	2.0	9.0E2	1.5mF	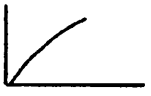	-620

Table 3.6 VYHH, detached film with pinhole.

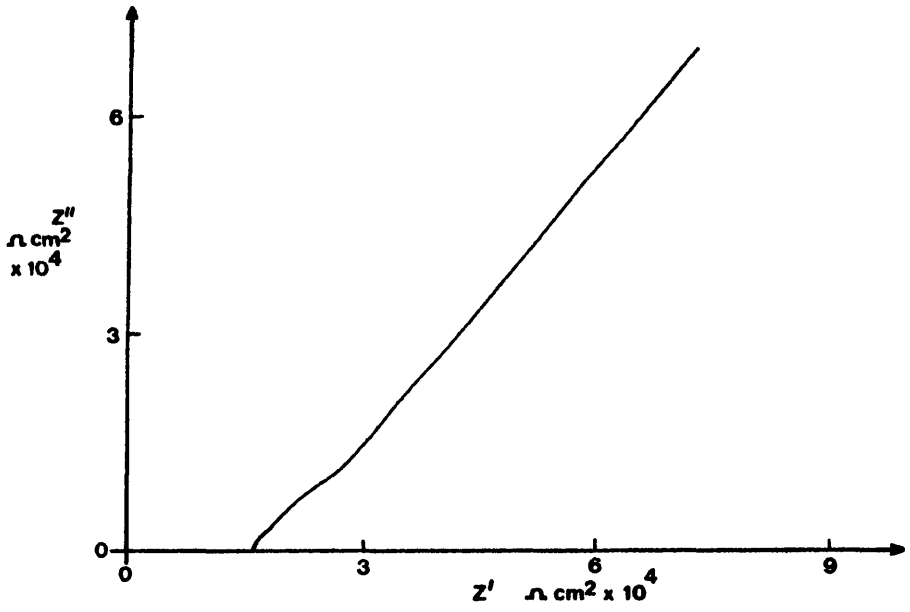

Figure 3.13 VYHH, 5 minutes after pinhole.

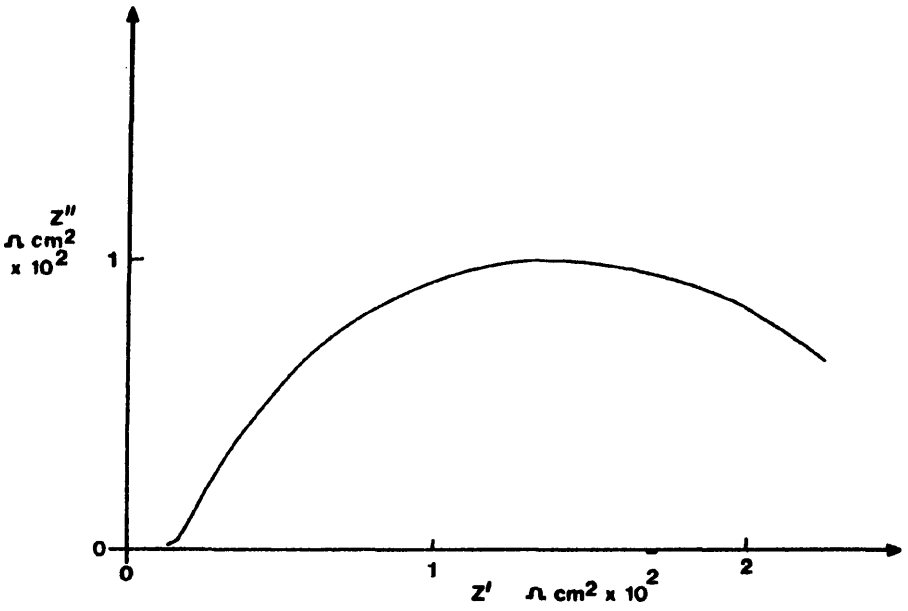

Figure 3.14 VYHH, 7 days after pinhole.

Time	Rs Ωcm^2	Rsc Ωcm^2	Capacitance cm^{-2}	Nyquist Plot	Potential mV vs. S.C.E.
0	39	-	1.1mF	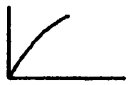	-640
2min	36	-	1.1mF	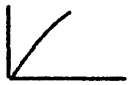	-640
5min	24	-	1.3mF	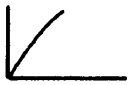	-640
10min	23.6	-	1.4mF	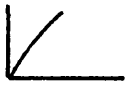	-640
30min	23.6	-	1.5mF	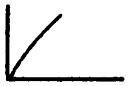	-640
1hr	23.4	-	1.2mF	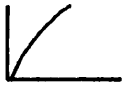	-640
1day	24.1	-	0.8mF	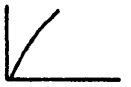	-645
3days	26	-	2.1mF	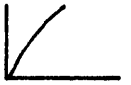	-620
9days	29	-	0.93mF		-620

Table 3.7 VMCH, detached film with pinhole.

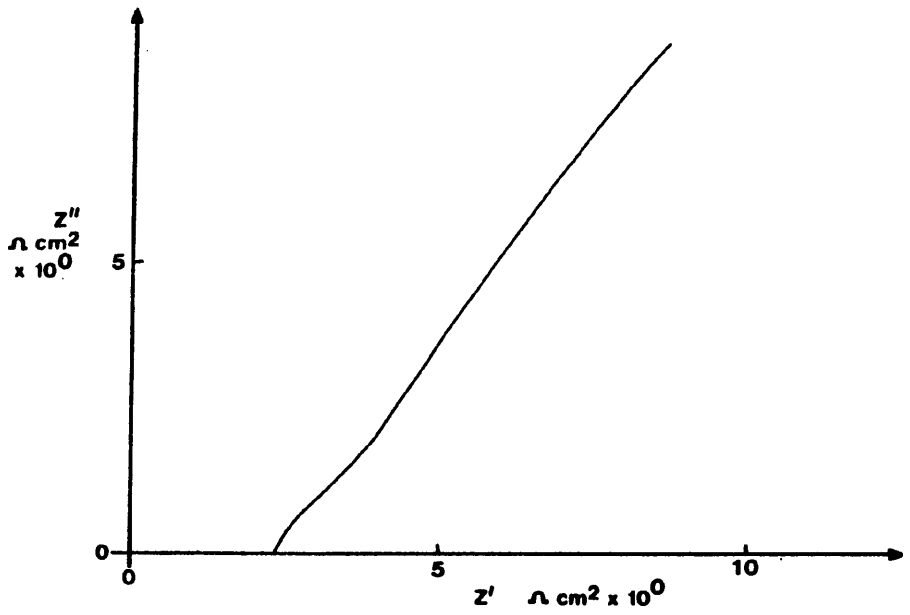

Figure 3.15 VMCH, detached film, 0-9 days after pinhole.

Time	Rs Ωcm²	Rsc Ωcm²	Capacitance cm⁻²	Nyquist Plot	Potential mV vs. S.C.E.
0	5	-	25μF		-585
2min	5	-	24.6μF		-585
5min	5	-	24.8μF		-585
10min	5	-	25μF		-590
30min	5	-	25.2μF		-590
1hr	5	-	25μF		-590
1day	5.3	-	30.9μF		-580
3days	4.5	-	31.7μF		-630
9days	7E4	-	3.2nF		-580

Table 3.8 VROH, intact detached film.

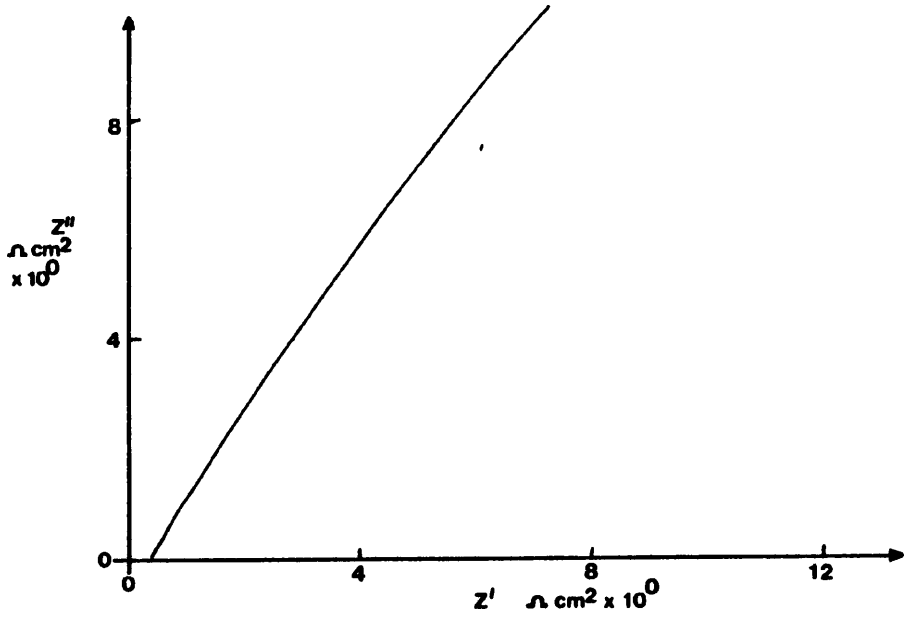

Figure 3.16 VROH, detached film, 0-9 days after pinhole.

In a third series of experiments, intact films were mounted in QVF fittings and placed in a water bath. The temperature of the bath was raised and impedance measurements carried out at each new temperature. The solution temperature in the QVF arms was measured, and the water bath heated in sucessive increments, until the salt solution temperature was above that of the Tg of the polymer. The results of these experiments are summarised, as before. Little change was observed in the impedance plot parameters with temperature, until the upper Tg of the polymers was reached, when there was an increase in both the measured rest potential and in the capacitance values of the films.

Temp °C	Rs Ωcm²	Rsc Ωcm²	Capacitance cm^{-2}	Nyquist Plot	Potential mV vs. S.C.E.
25	1.9E5	-	770pF	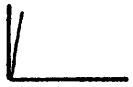	-650
28	1.9E5	-	780pF	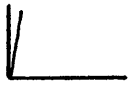	-650
30	1.9E5	-	780pF		-650
32	1.9E5	-	780pF		-650
35	1.9E5	-	820pF		-650
40	1.9E5	-	780pF		-650
45	1.9E5	-	780pF		-650
50	1.9E5	-	790pF		-645
55	1.9E5	-	780pF		-645
60	1.9E5	-	830pF		-620
63	1.9E5	-	830pF		-620
65	1.9E5	-	810pF		-620

Table 3.9 VMCH, detached film, effect of temperature.

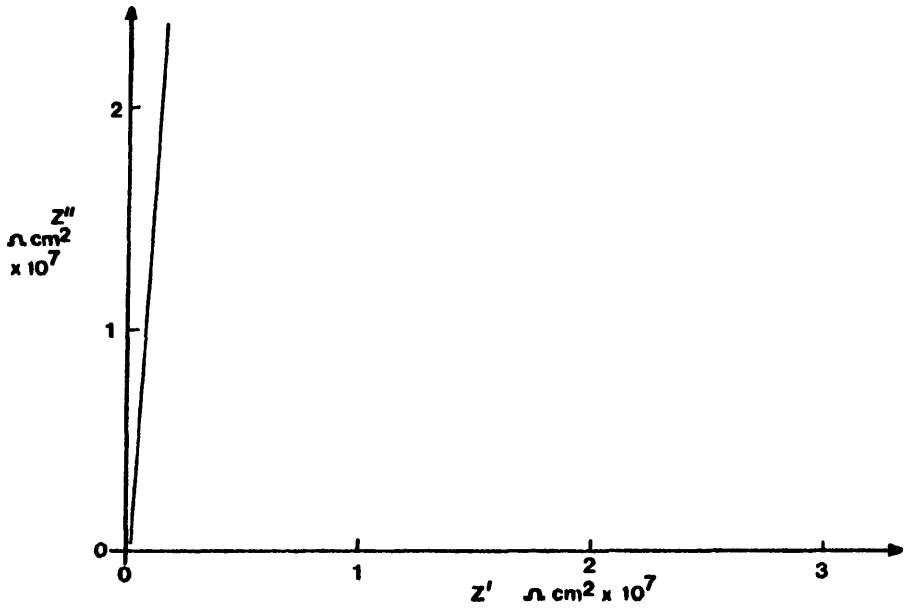

Figure 3.17 VMCH, 25-65°C.

Temp °C	Rs Ωcm²	Rsc Ωcm²	Capacitance cm^{-2}	Nyquist Plot	Potential mV vs. S.C.E.
22	2.2E5	-	670pF		-610
28	2.2E5	-	660pF		-610
30	2.2E5	-	680pF	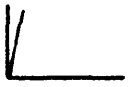	-610
32	2.2E5	-	680pF	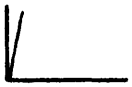	-610
35	2.2E5	-	660pF		-610
40	2.2E5	-	670pF		-610
45	2.2E5	-	660pF		-610
50	2.2E5	-	660pF		-610
55	2.2E5	-	660pF		-630
60	2E5	-	840pF		-650
65	2E5	-	790pF	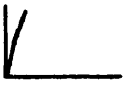	-650

Table 3.10 VROH, detached film, effect of temperature.

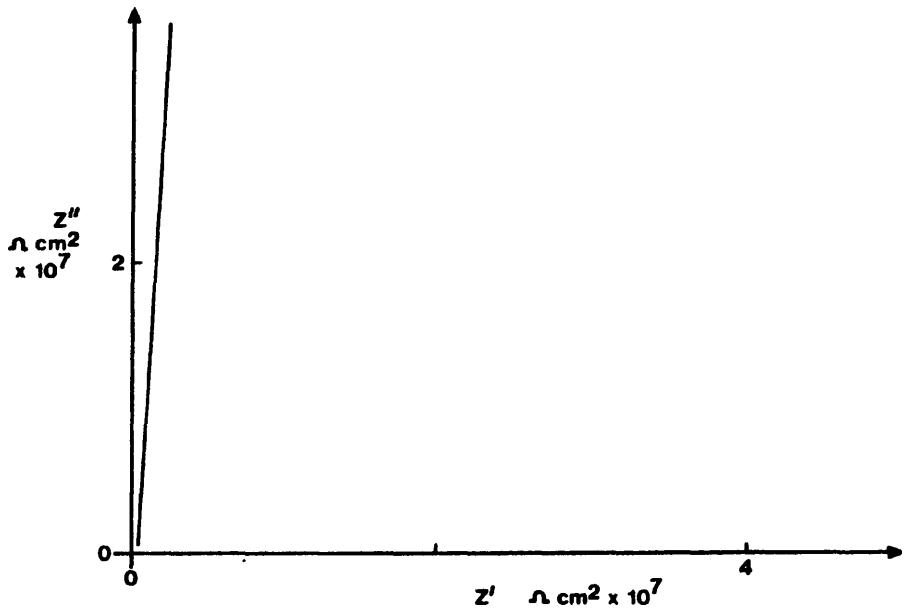

Figure 3.18 VROH, detached film, 22-65°C.

3.4 Agar.

It was observed that the pinhole produced in a detached film, became filled with a porous gel-like substance, which was thought to be composed of iron compounds and water. Experiments in which agar gel was placed on steel sheets and immersed in a beaker of salt solution, showed that the agar was capable of absorbing Fe compounds into itself. Specimens were made up by pouring agar solution into the wax troughs of pre-masked specimens. After immersion, impedance measurements were carried out over a period of time and the results are summarised in the following tables. It is noted that the solution resistance falls quickly at first and then more slowly with time. This is thought to be due to the ingress of water, sodium and chloride ions into the gel from the solution side and by iron ions from the substrate side.

Time	Rs Ωcm^2	Rsc Ωcm^2	Capacitance cm^{-2}	Nyquist Plot	Potential mV vs. S.C.E.
0	335	-	1.94μF	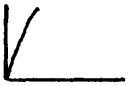	-370
5min	265	-	2.76μF		-370
10min	220	-	2.9μF	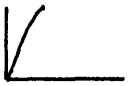	-370
15min	190	-	2.82μF	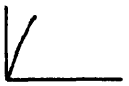	-370
30min	154	-	3.37μF	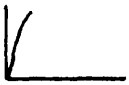	-360
45min	142	-	3.73μF	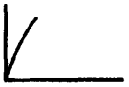	-390
1hr	136	-	4.12μF	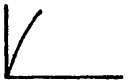	-390
1.5hrs	130	-	4.4μF	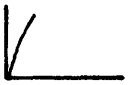	-320
2hrs	132	-	4.53μF		-320
2.5hrs	128	-	4.96μF	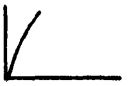	-320
3hrs	126	-	5.02μF	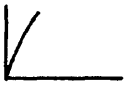	-330
4hrs	120	-	6.06μF	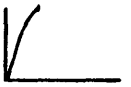	-370
19hrs	114	-	7.17μF	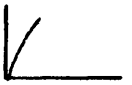	-580
7days	105	-	7.21μF	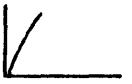	-470
22days	102	-	7.24μF	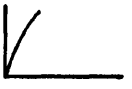	-370
36days	110	-	7.28μF	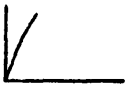	-650
63days	120	-	7.47μF	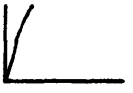	-320

Table 3.11 Agar 1, impedance response with time.

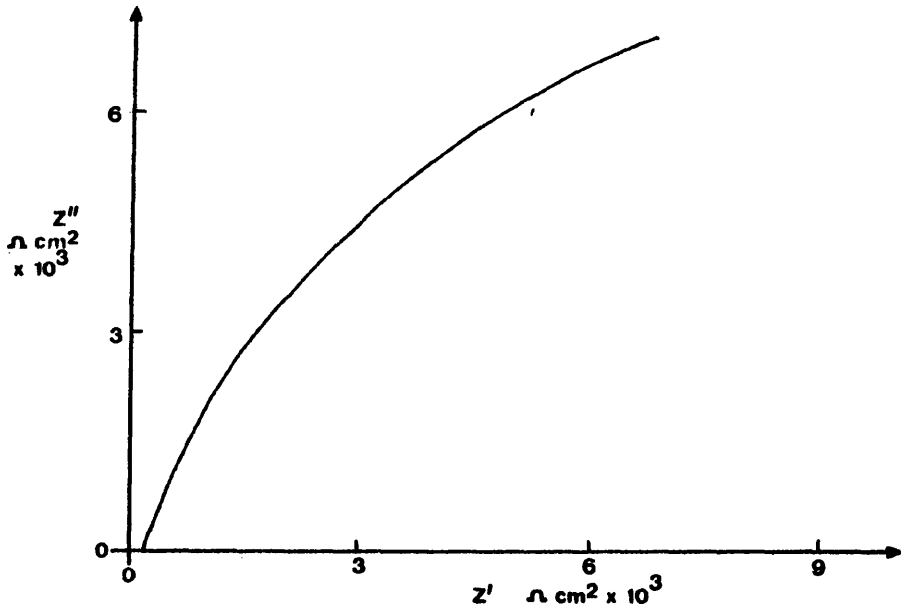

Figure 3.19 Agar 1, 0-63 days immersion.

Time	Rs Ωcm^2	Rsc Ωcm^2	Capacitance cm^{-2}	Nyquist Plot	Potential mV vs. S.C.E.
0	250	-	5.4μF	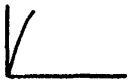	-380
5min	205	-	7.8μF	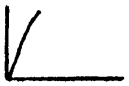	-380
10min	178	-	7.8μF	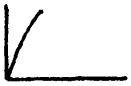	-380
15min	158	-	8.6μF	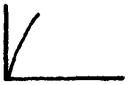	-380
30min	135	-	3.8μF	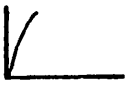	-360
45min	133	-	9.5μF	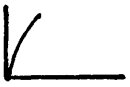	-360
1hr	128	-	7.1μF		-360
1.5hrs	128	-	7.1μF		-360
2hrs	127	-	7.5μF	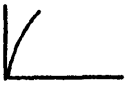	-360
3hrs	125	-	12.1μF	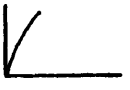	-410
18hrs	117	-	8.75μF	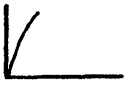	-500
7days	112	-	15.8μF	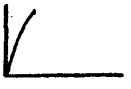	-310
22days	112	-	15.8μF	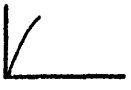	-340
36days	110	-	15.98μF	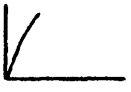	-340
63days	110	-	16.6μF	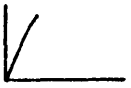	-350

Table 3.12 Agar 2, impedance response with time.

Plate 3.1 Agar specimen after 64 days immersion.

It can be seen that the orange compounds have permeated into the agar and that the surface of the metal is a bluish colour, as is the agar immediately adjacent to the steel. Both agar specimens were visually very similar on removal from the solution.

3.5 Dry film capacitance measurements.

The dry film capacitance of several films was measured by filling the wax trough of a specimen with mercury and then performing an impedance run. For each specimen measured in this way, the Nyquist plot was of a "capacitive" type, a schematic plot of which is shown overleaf.

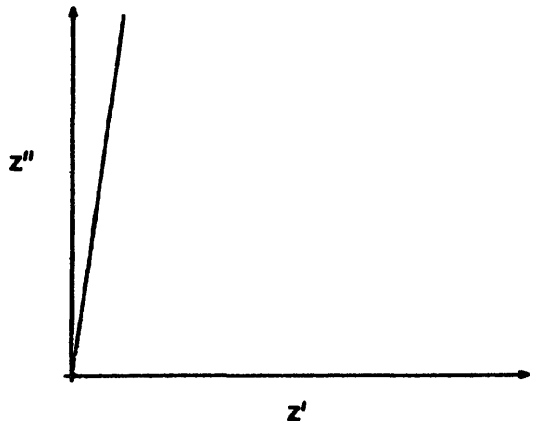

Figure 3.21 Schematic impedance plot.

From this plot it can be noted that the graph is not purely capacitive, as there is a very slight slope on the line. This is because the polymer film is not a perfect capacitor and may be considered (in terms of eqivalent circuit notation) to be "leaky", that is, to have a large resistor in parallel with it. It is also observed that the plot appears to have a "solution resistance", which is likely to be that of the polymer film. The results of the experiment are summarised in the following table.

Polymer	Thickness (μm)	Dry Capacitance (pF cm^{-2})	Dry Resistance (ohms cm^2)
VROH-B1	76	57.3	1.9E6
VROH-B2	76	57.8	1.9E6
VAGH-G1	35	64.7	1.1E6
VAGH-G2	36	63.8	1.1E6
Acrylic B	30	79.7	1.8E5
Acrylic A	70	37.5	3.4E5
VMCH-Y	33	73.7	3.3E6

Table 3.13 Dry capacitances and resistances of polymer films.

These results show that the dry capacitance and resistance measured, varied with the film thickness. The capacitance measurements varied inversely and the resistance values directly with the thickness of the coating. The measured resistance may vary with the type and structure of the film, some polymers being more conductive than others. The relationship between the film thickness and the capacitance will be discussed in Chapter 4.10.

3.6 Effect of the presence and absence of oxygen.

Previous work <112> had shown that an uncoated mild steel specimen placed in deaerated salt solution, did not undergo corrosion processes upon prolonged immersion and it was expected that similar results would be obtained using coated specimens. To test this hypothesis, the halves of prepared "Pyrene" panels were coated, masked and immersed in 3% sodium chloride solution. One half in aerated and the other in deaerated solution. Impedance measurements were carried out regularly over a period of time and the results are summarised on the following pages.

Time	Rs Ωcm^2	Rsc Ωcm^2	Capacitance cm^{-2}	Nyquist Plot	Potential mV vs. S.C.E.
0	9E4	-	79pF	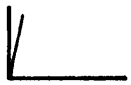	-610
5min	9E4	-	79pF		-610
15min	9E4	2.6E8	79pF		-315
30min	9E4	2.6E8	79pF		-400
1hr	9E4	2.3E8	79pF		-400
1day	1E5	2E8	79.3pF		-420
3days	9E4	1.8E8	79pF		-420
5days	9E4	1.7E8	79pF		-330
7days	9E4	2E8	79pF		-150
10days	9E4	1E8	79pF		-160

Table 3.14 VYHH-G, in aerated solution.

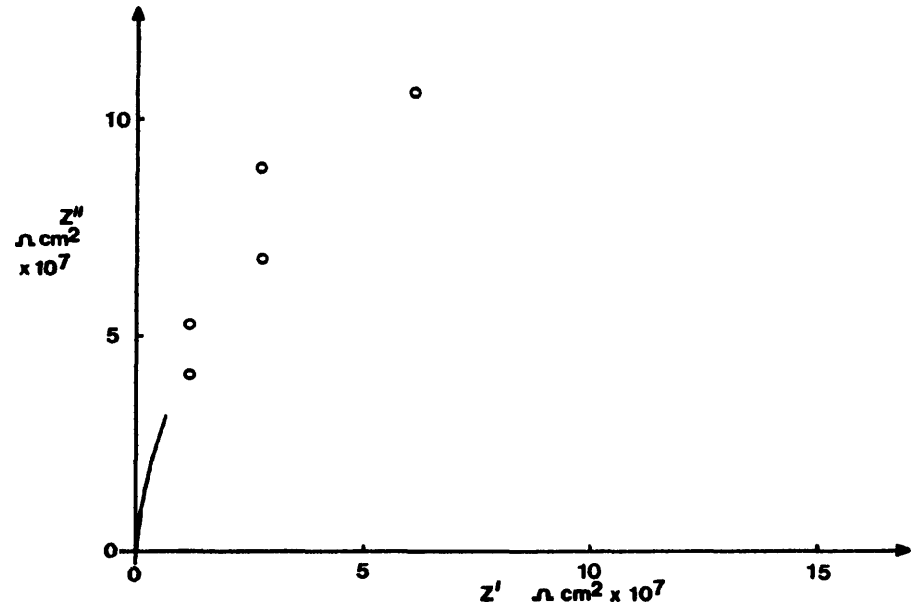

Figure 3.22 VYHH-G, 0-15 minutes immersion.

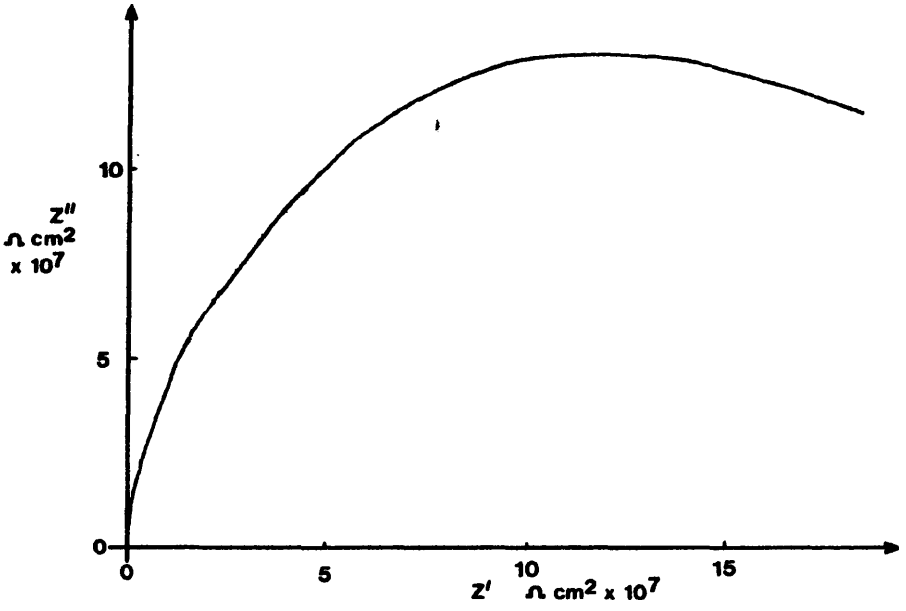

Figure 3.23 VYHH-G, 30 minutes to 10 days immersion.

Time	Rs Ωcm^2	Rsc Ωcm^2	Capacitance cm^{-2}	Nyquist Plot	Potential mV vs. S.C.E.
0	1E5	3.2E8	74pF		-610
5min	1E5	3E8	74pF		-610
15min	9E4	3.2E8	74pF		-350
30min	9E4	3.5E8	74pF		-340
1hr	9E4	3.5E8	74pF		-370
1day	1E5	3.5E8	74pF		-415
3days	1E5	3.8E8	77pF		-210
5days	9E4	4.6E8	74pF		-330
7days	9E4	4.7E8	74pF		-250
10days	6.6E5	7E7	21nF		-190

Table 3.15 VYHH-GN, in deaerated solution.

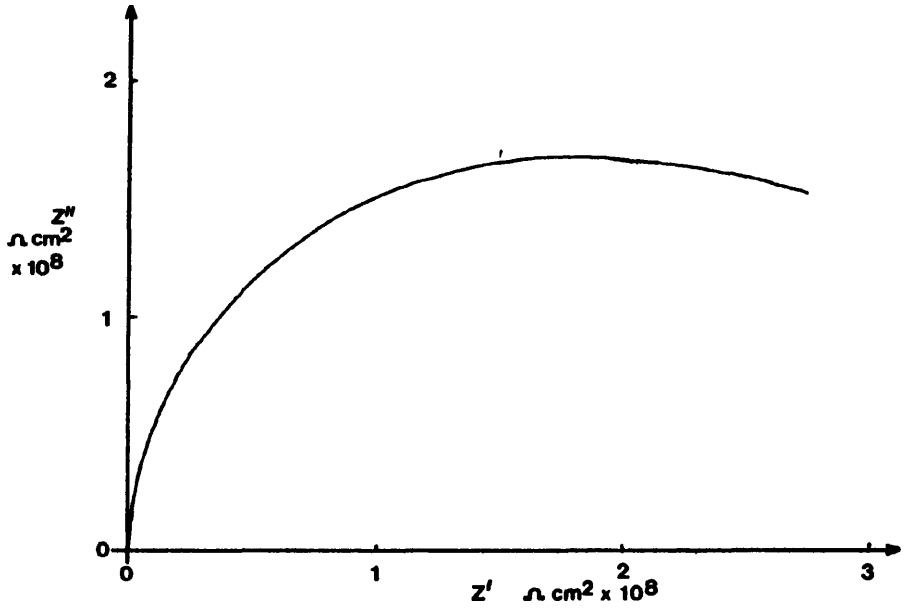

Figure 3.24 VYHH-GN, 0-10 days immersion.

Both specimens showed the same constant solution resistance over the test period and a similar series of impedance plots. The capacitance readings are also similar for the panels, those for the panel in aerated solution being slightly higher. The measured rest potentials were also close for the specimens and did not fall below -420mV (w.r.t. Calomel) during the test period. The photographs below, show the visual appearance of the specimens after five days immersion. It was observed that more extensive corrosion had occurred on the specimen in deaerated solution, than on the one in the aerated solution.

Plate 3.2 VYHH-G, 5 days in aerated solution.

Plate 3.3 VYHH-GN, 5 days in deaerated solution.

Specimens which had been coated with vinylite VAGH, showed similar results in terms of their impedance and corrosion behaviour.

Time	Rs Ωcm^2	Rsc Ωcm^2	Capacitance' cm^{-2}	Nyquist Plot	Potential mV vs. S.C.E.
0	7E4	-	94pF		-250
5min	7E4	2.6E7	94.6pF		-320
15min	7E4	2.5E7	102pF		-460
30min	7E4	2.5E7	101pF		-480
1hr	7E4	2.4E7	110pF		-460
1day	7E4	4.2E6	2.8nF		-400
3days	7E4	2.6E6	130pF		-525
5days	7E4	2.1E6	102pF		-545

Table 3.16 VAGH, in aerated solution.

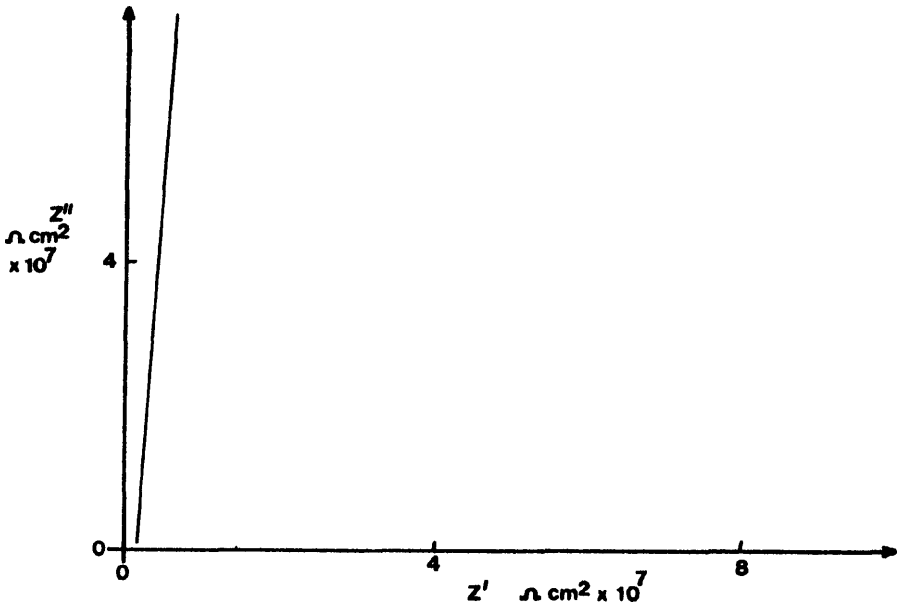

Figure 3.25 VAGH, on immersion.

Time	Rs Ωcm^2	Rsc Ωcm^2	Capacitance cm^{-2}	Nyquist Plot	Potential mV vs. S.C.E.
0	7E4	-	86.9pF		-610
5min	8E4	4.5E6	90.7pF		-220
15min	8E4	1.2E7	88.7pF		-500
30min	7E4	3.1E7	88.2pF		-470
1hr	7E4	4.6E7	87.4pF		-500
1day	7E4	2.4E6	0.21nF		-300
3days	8E4	4.7E6	110pF		-500
5days	7E4	4.9E6	99pF		-520

Table 3.17, VAGH-N, in deaerated solution.

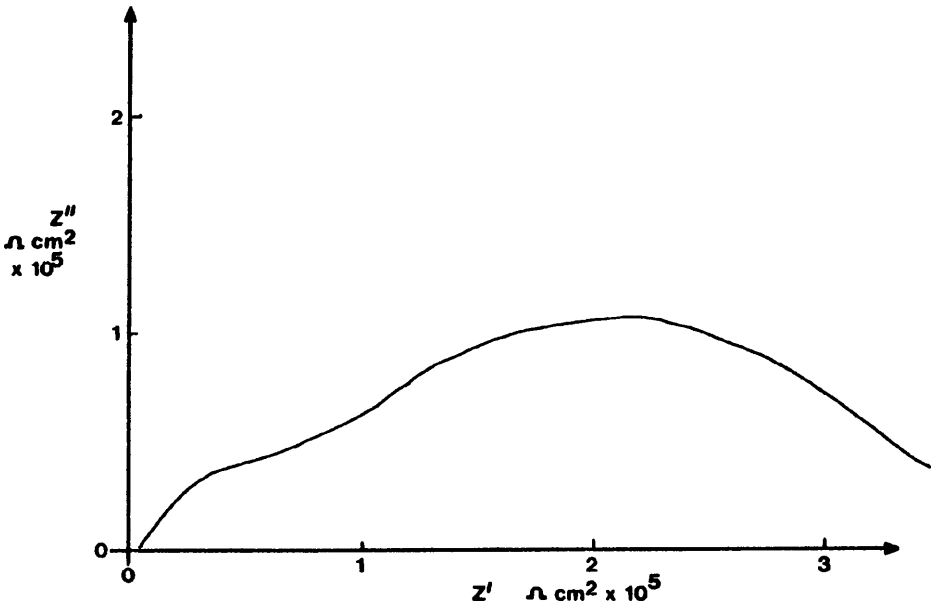

Figure 3.26 VAGH, 3 days immersion.

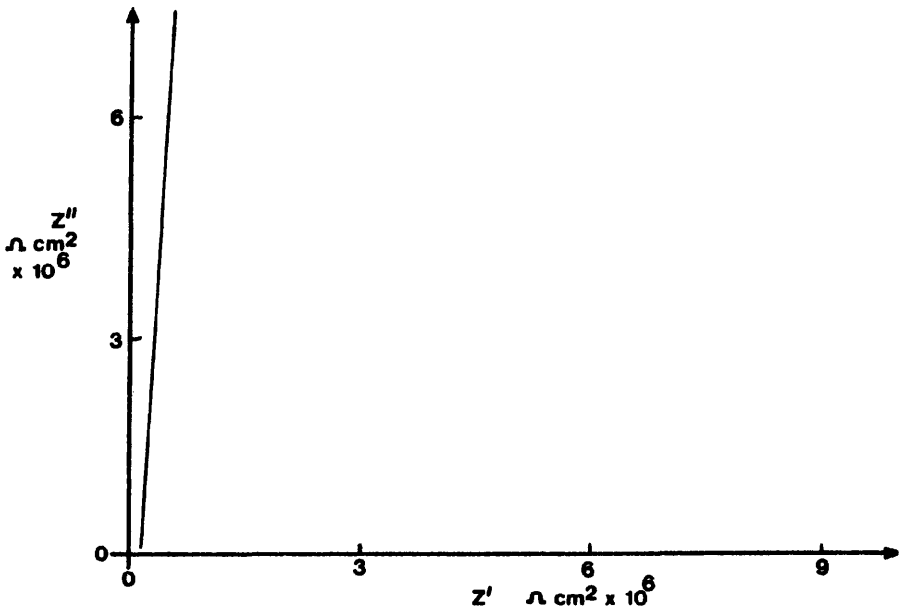

Figure 3.27 VAGH-N, on immersion.

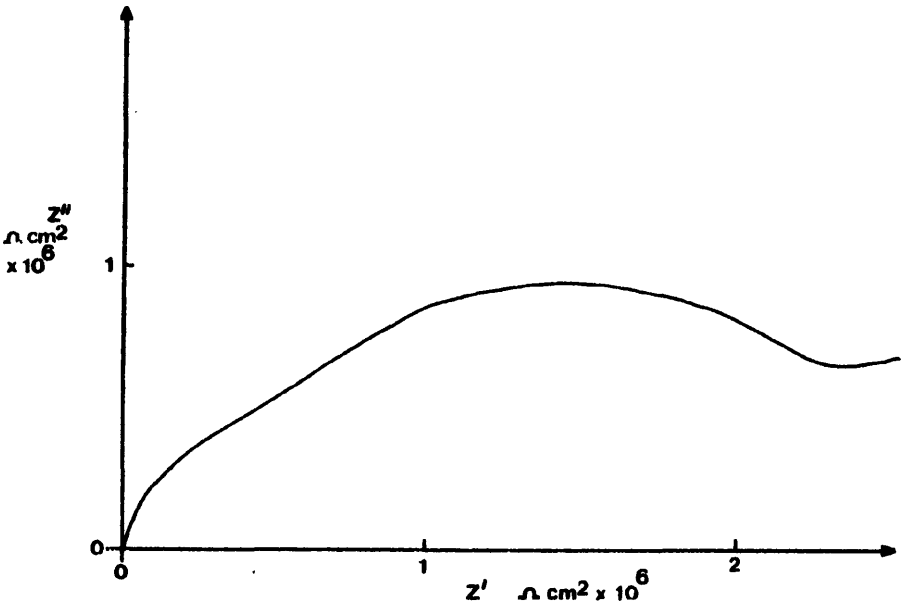

Figure 3.28 VAGH-N, after 30 minutes immersion.

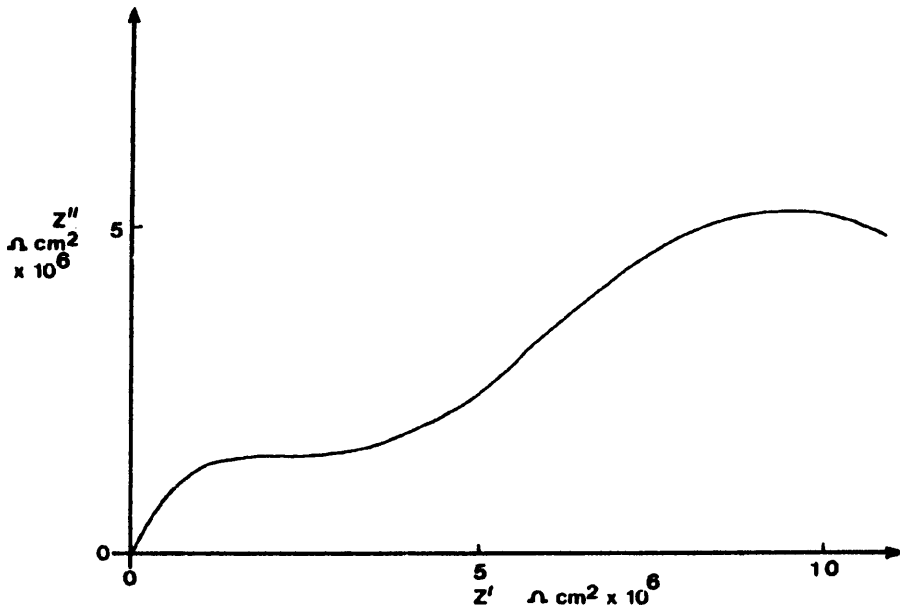

Figure 3.29 VAGH-N, after 3 days immersion.

As with the results of VYHH, the solution resistance measured was the same for both the specimens and did not vary over the test period. The capacitance measurements showed a general increase with time and again, the capacitance of the specimen in aerated solution was higher than in deaerated solution. The impedance plot shapes were more variable than those observed for VYHH as is the rest potential, which was generally lower than for the previous pair of specimens. The photographs of the VAGH pair are shown below.

Plate 3.4 VAGH, 5 days in aerated solution.

Plate 3.5 VAGH-N, 5 days in deaerated solution.

Again, it is noted that the specimen immersed in deaerated solution was the more corroded of the two.

The third vinylite studied in this way was VMCH. A different impedance and corrosion behaviour pattern was noted for this pair of specimens.

Time	Rs Ωcm^2	Rsc Ωcm^2	Capacitance cm^{-2}	Nyquist Plot	Potential mV vs. S.C.E.
0	1.5E5	-	52pF	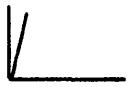	-610
5min	1.5E5	-	52pF		-610
15min	1.5E5	-	52pF	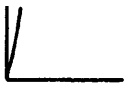	-610
30min	1.5E5	-	52pF		-610
1hr	1.5E5	-	53pF	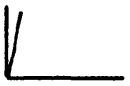	-610
1day	1.5E5	-	53pF	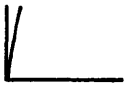	-610
3days	1.5E5	-	0.95nF	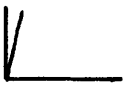	-610
6days	1.5E5	-	53pF	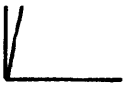	-610

Table 3.18 VMCH in aerated solution.

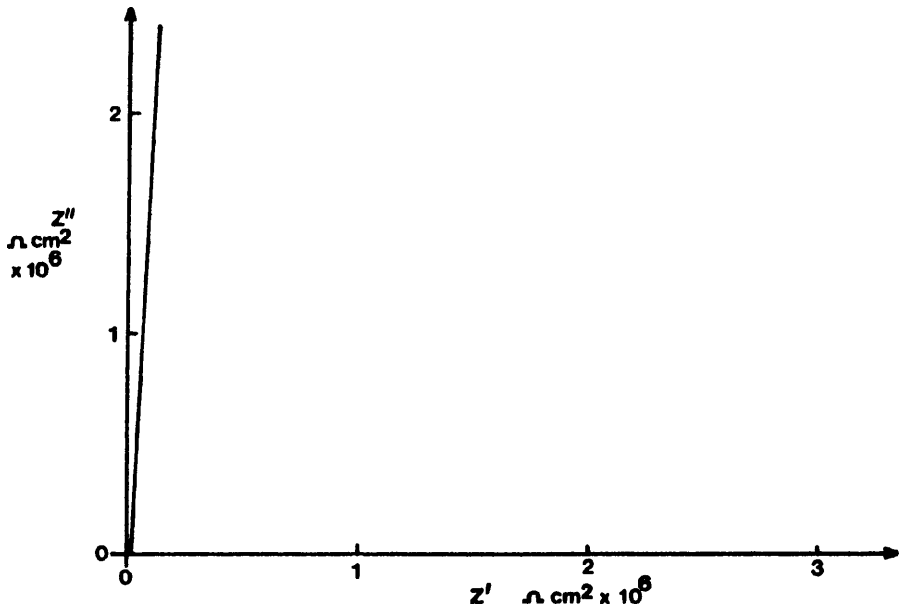

Figure 3.30 VMCH, 0-6 days immersion.

Time	Rs Ωcm²	Rsc Ωcm²	Capacitance cm⁻²	Nyquist Plot	Potential mV vs. S.C.E.
0	2E6	-	51pF		-610
5min	1.5E6	-	50pF		-610
15min	1.5E5	-	51pF		-610
30min	1.5E5	-	51pF		-470
1hr	1.5E5	-	50pF		-440
1day	1.5E5	-	50pF		-580
3days	1.5E5	-	51pF		-560
6days	1.5E5	-	51pF		-545

Table 3.19 VMCH-N in deaerated solution.

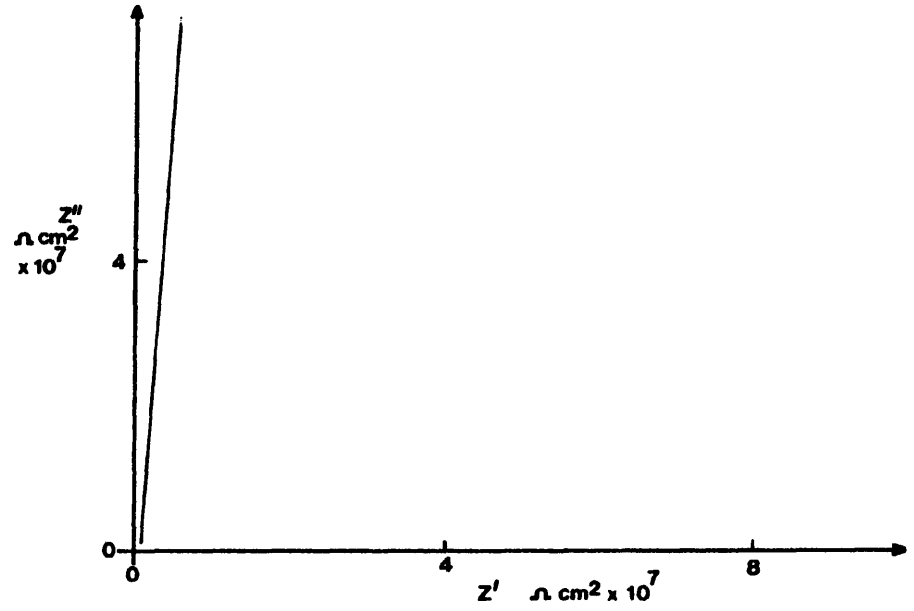

Figure 3.31 VMCH-N, 0-6 days immersion.

With this polymer, the impedance plot shows a particularly "capacitive" shape and again, is similar for both the specimens. As with the two previous vinylites, the solution resistance remains constant and identical for both, throughout the experiment. The capacitance, is higher in value for the specimen in aerated solution and increased slightly over the test period. In the deaerated solution, the capacitance of the specimen remained virtually constant during the experiment. Both of the samples were slow in taking up a measurable rest potential in comparison with the other specimens and the sample in aerated solution did not take up a stable rest potential after six days immersion. In common with the previously described vinylites, the specimen immersed in the deaerated solution showed the greater degree of corrosion attack.

Plate 3.6 VMCH, 5 days in aerated solution.

Plate 3.7 VMCH-N, 5 days in deaerated solution.

The fourth vinylite studied, VROH, again showed similar behaviour between the halves of the original panel, but different behaviour from the other three vinylites.

Time	Rs Ωcm^2	Rsc Ωcm^2	Capacitance cm^{-2}	Nyquist Plot	Potential mV vs. S.C.E.
0	8E4	4.7E6	81pF		-610
5min	8E4	4.5E6	81pF		-350
30min	8E4	4.5E6	82pF		-540
1hour	9E4	4.6E6	83pF	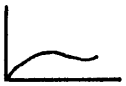	-550
1day	9E3	4.7E6	83pF	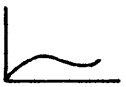	-540
3days	1E4	-	82pF	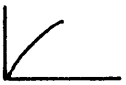	-540
5days	1E4	-	82pF	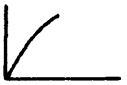	-560
7days	6.2E3	-	5nF	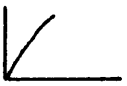	-610
10days	6.1E3	-	4.9nF	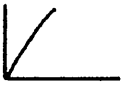	-500
15days	6.2E3	-	74pF	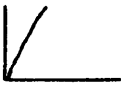	-560

Table 3.20 VROH in aerated solution.

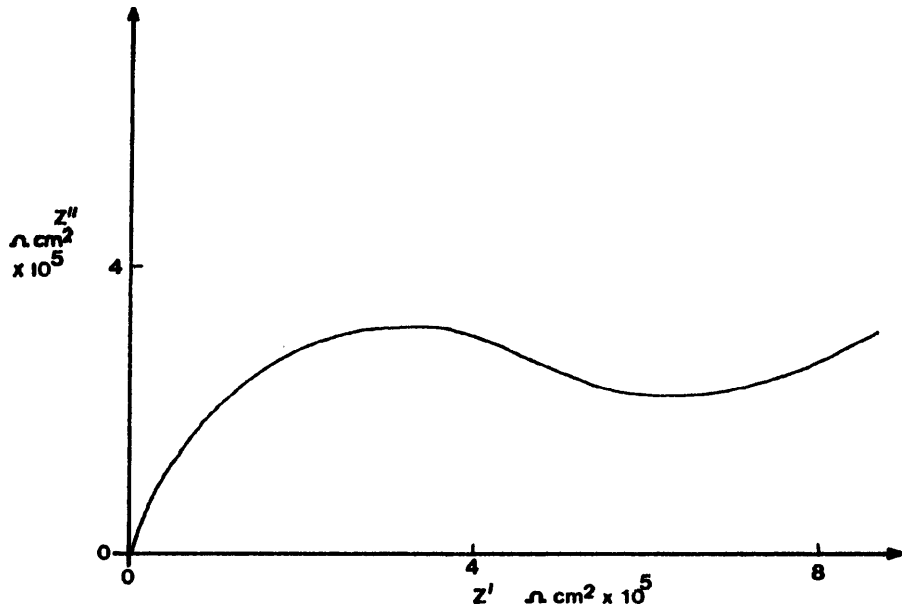

Figure 3.32 VROH, 0-1 day immersion.

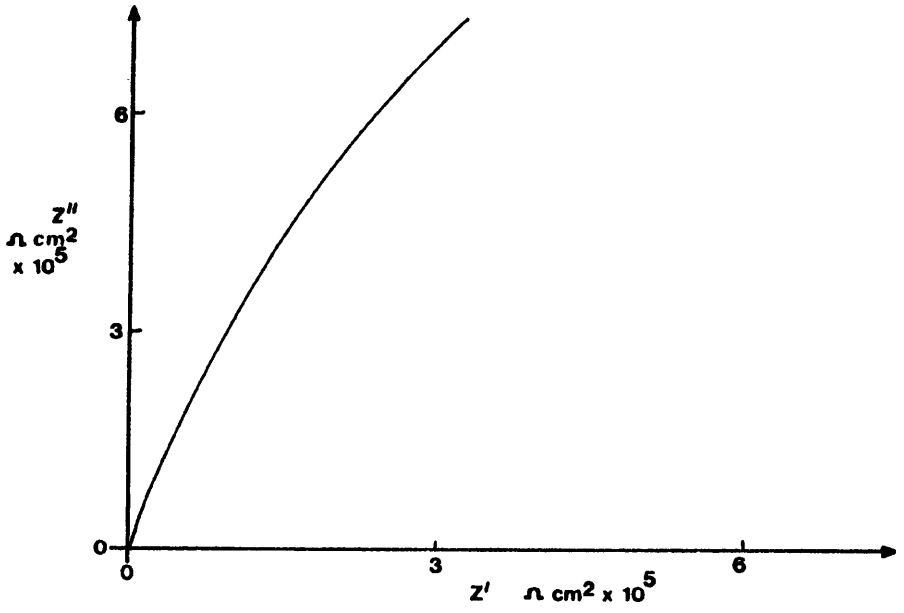

Figure 3.33 VROH, 3-15 days immersion.

Time	Rs Ωcm^2	Rsc Ωcm^2	Capacitance cm^{-2}	Nyquist Plot	Potential mV vs. S.C.E.
0	1E5	-	69pF	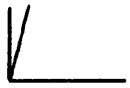	-380
5min	9E4	5.2E8	70pF	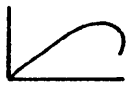	-440
15min	1.7E2	4.3E5	40nF		-490
30min	9E4	3.4E8	71pF		-540
1hr	9E4	3.9E8	71pF		-540
1day	9E4	-	71pF	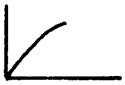	-580
3days	9E4	-	73pF	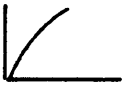	-550
6days	9E4	1.8E8	72pF		-550
9days	9E4	-	73pF	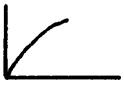	-440
15days	6.2E3	-	4.7nF	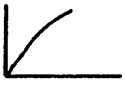	-525

Table 3.21 VROH-N in deaerated solution.

Figure 3.34 VROH-N on immersion.

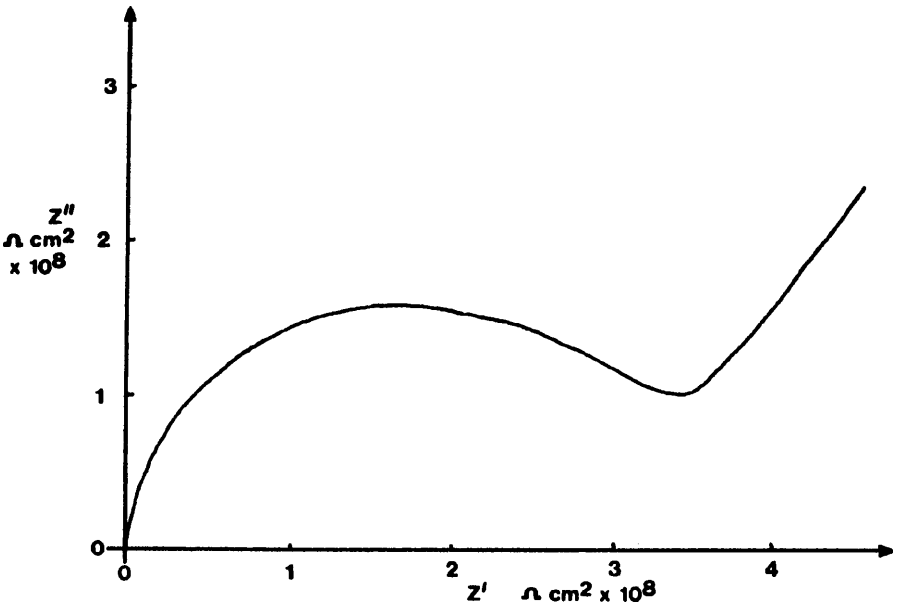

Figure 3.35 VROH-N 30 minutes after immersion.

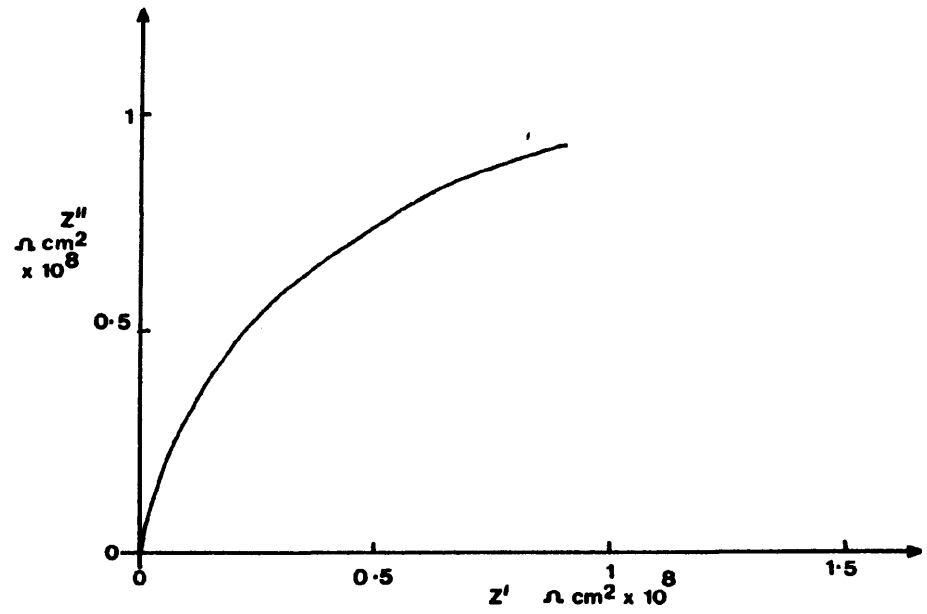

Figure 3.36 VROH-N, 3-15 days after immersion.

The results from the VROH specimens, show a different pattern of corrosion behaviour from those of the previous three polymers. The solution resistance, whilst being similar for both halves of the panel, varied over the test period. The capacitance values generally increased with time of immersion and as with the previous polymers, the specimen in aerated solution tended to exhibit a higher value for the capacitance than the specimen in deaerated solution. The measured rest potential was generally lower for these specimens than for any of the other vinylites and again, fluctuated with time. The shape of the impedance plots were also variable in shape for both of the VROH coated specimens, over the test period. The photographs show the visual appearance of the samples after five days immersion.

Plate 3.8 VROH, 5 days in aerated solution.

Plate 3.9 VROH-N, 5 days in deaerated solution.

From these photographs, it can be seen that there is very little

visual difference between these specimens, in contrast with the other polymers studied.

Generally, the results show that vinylite coated specimens undergo corrosion processes more quickly in deaerated than in aerated 3% sodium chloride solutions. Although the visual appearance of VYHH, VAGH and VMCH was similar after five days immersion, the corresponding impedance responses of the polymers are all different, as has been noted elsewhere <118>. The specimens immersed in aerated solution each exhibit a higher value of capacitance than their corresponding halves in deaerated solution, suggesting that there may be a greater quantity of water present in the specimens immersed in the aerated solution. For certain specimens, the capacitance increased by several orders of magnitude and in some cases, decreased again. This is possibly due to diffusion effects through pores in the films. It is likely that the black spots observed on the panels, occur under pores, or "D" areas in the films. With detached films, when a pore or pinhole was present in the film, the impedance plot was typical of that of a diffusional process. With the attached films, which are suspected of containing pores, a similar impedance response is observed. In this case, a combination plot, showing the effects of both the polymer and the diffusion processes. The relationship between the process occurring under and through the film, together with their impedance responses, has recently been reported <116>.

In a second series of experiments, two VROH coated specimens, which had been masked, were placed in a partially opened drawer. (This avoided contamination by spillages, etc. and allowed for air circulation around the panels). After thirty days, the specimens were removed from the

drawer and immersed in aerated and deaerated salt solution. The results from this experiment are summarised in tables 3.22 and 3.23.

Time	Rs Ωcm^2	Rsc Ωcm^2	Capacitance cm^{-2}	Nyquist Plot	Potential mV vs. S.C.E.
0	1.7E5	-	48pF	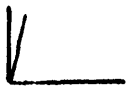	-610
5min	1.6E5	-	48pF	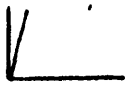	-610
10min	1.6E5	-	48pF	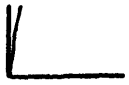	-610
15min	1.6E5	-	49pF		-610
30min	1.6E5	-	50pF		-610
45min	1.6E5	-	50pF	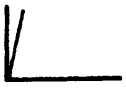	-550
1hr	1.6E5	-	50pF		-580
1day	1.6E5	9.2E5	84pF		-640
2days	2E5	-	136pF		-580
6days	1.4E5	-	69pF		-620
10days	1.4E5	-	194pF	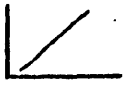	-580
16days	1.5E5	-	335pF	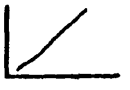	-580
22days	1.4E5	-	285pF	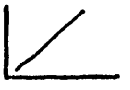	-570
30days	1.4E5	-	-	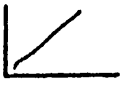	-560

Table 3.22 VMCH-Y (pre-rusted) in aerated solution.

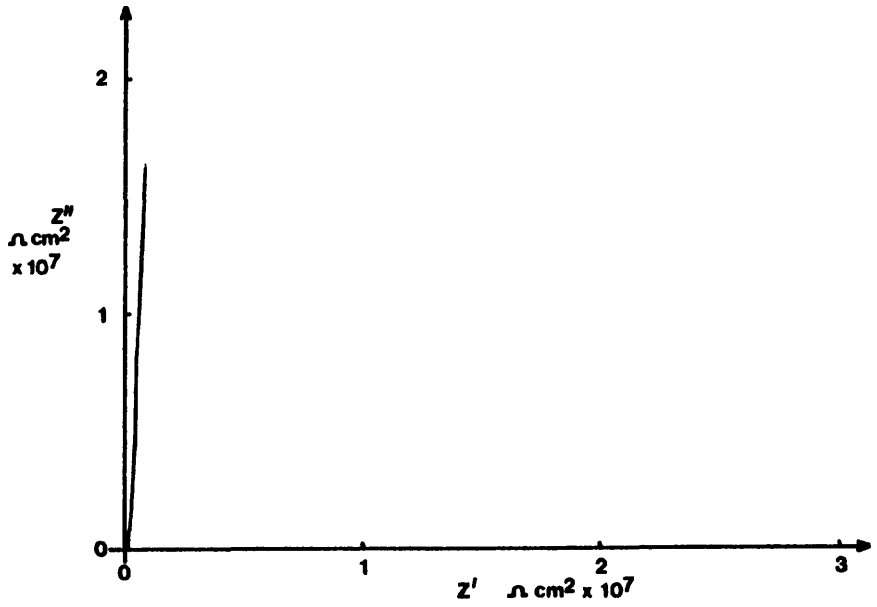

Figure 3.37 VMCH-Y, 0-1 hour immersion.

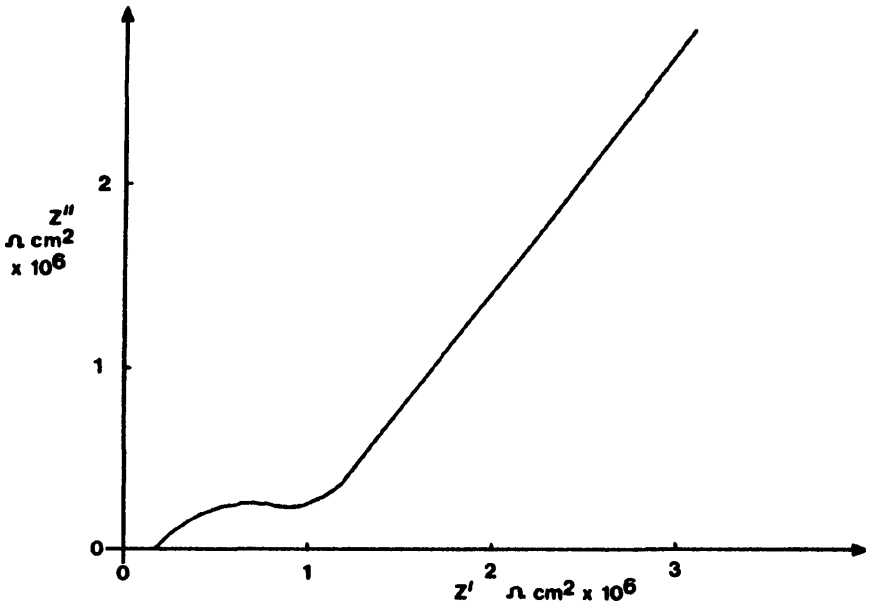

Figure 3.38 VMCH-Y, 1-6 days immersion.

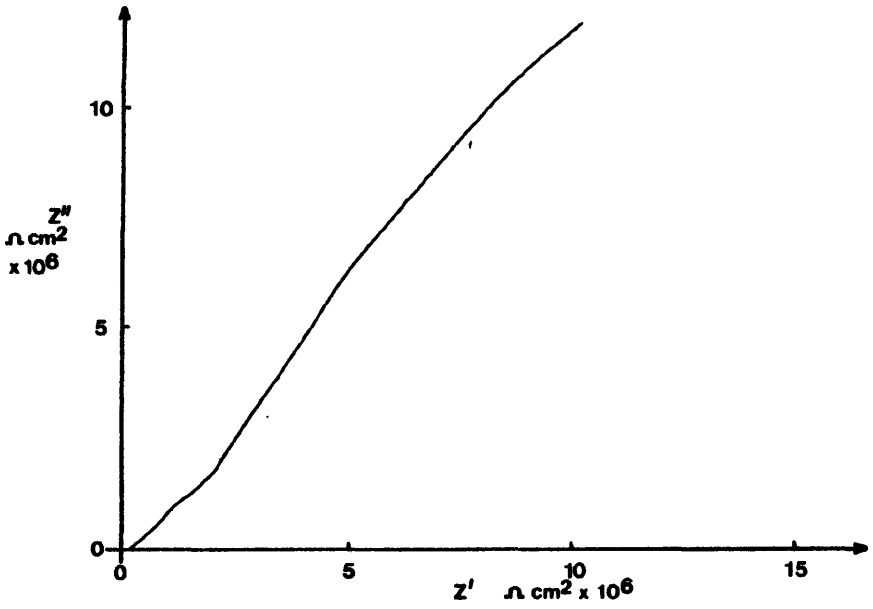

Figure 3.39 VMCH-Y, 10-30 days immersion.

Time	Rs Ωcm^2	Rsc Ωcm^2	Capacitance cm^{-2}	Nyquist Plot	Potential mV vs. S.C.E.
0	1.3E5	-	63pF	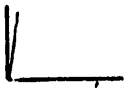	-610
5min	1.2E5	-	63pF		-400
10min	1.2E5	-	63pF	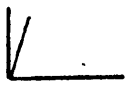	-400
15min	1.2E5	1.4E7	64pF		-610
30min	1.2E5	2.6E7	65pF		-530
45min	1.3E5	7.8E7	65pF		-580
1hr	1.2E5	2.2E7	65pF	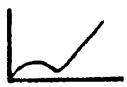	-620
1day	1.2E5	2.2E7	65pF	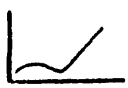	-660
2days	1.2E5	2E7	67pF		-580
6days	1.2E5	5.5E7	66pF		-450
10days	1.2E5	2E8	70pF		-560
16days	1.2E5	3.6E7	75pF	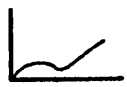	-500
22days	1.1E5	2E7	79pF		-520
30days	1.4E5	2.4E7	80pF		-470

Table 3.23 VMCH-YN (pre-rusted) in deaerated solution.

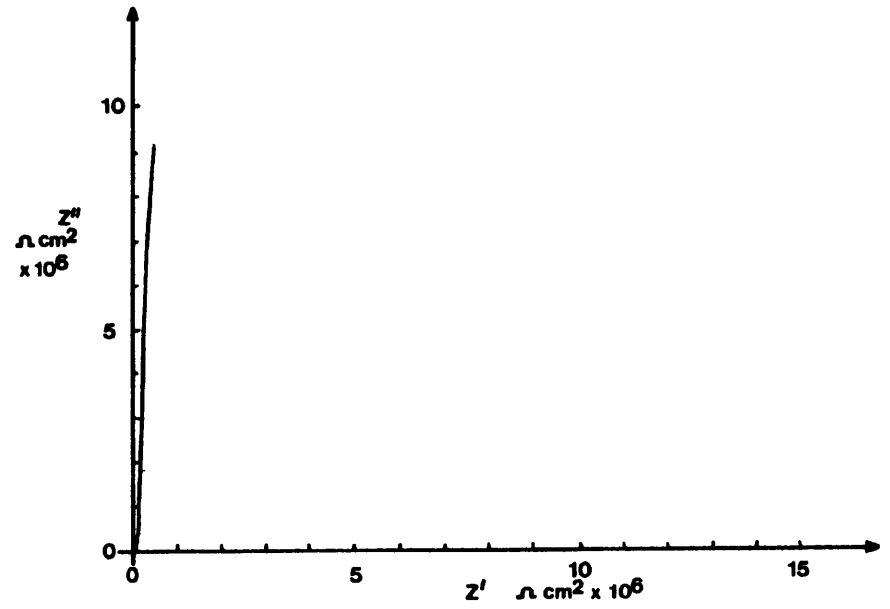

Figure 3.40 VMCH-YN, 0-15 minutes immersion.

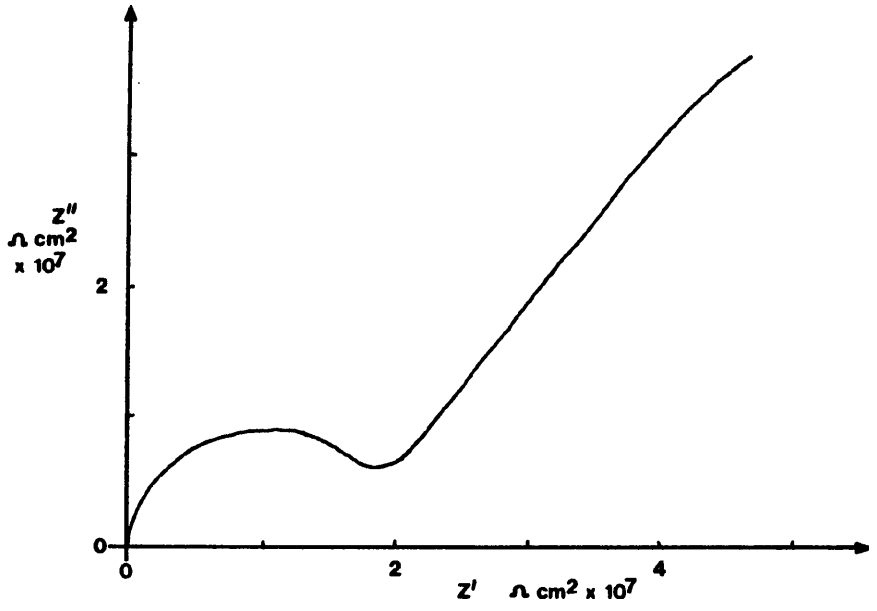

Figure 3.41 VMCH-YN, 1hour to 1 day after immersion.

The solution resistance of the specimen in the deaerated solution was

constant over the test period, whilst that of the other specimen was more variable. As with the previous series of experiments, the capacitance generally increased with time, although in this instance, the capacitance was higher for the specimen in deaerated solution, contrary to the previous results. The shape of the impedance plots differed between the two half panels, those from the specimen in the aerated solution exhibiting more diffusion type effects. Neither panel showed any visual evidence of corrosion prior to immersion, but after twenty-four hours in the salt solution, each showed a uniform corrosion pattern of tiny black spots over its surface. Unlike the previous experiments, both panels continued to have the same visual appearance, differing only in the colour of the spots. Those in the aerated solution became orange with time, whilst those in the deaerated solution became a blue-green colour. The size of the spots remained constant over the duration of the experiment.

3.7 Effects of temperature.

When detached films were subjected to changes in the external solution temperature, it was observed that there was a slight change in the rest potential at the upper glass transition temperature, with apparently no change in the impedance (or any other) response, at the lower Tg. With this in mind, it was decided to investigate the effect of changing the temperature of the salt solution in the region of the lower Tg, more closely.

One half of a masked VMCH coated panel (VMCH-1), was immersed in 3% sodium chloride solution at 37°C and the solution allowed to cool slowly.

Impedance measurements were performed after each 1°C decrease in the solution temperature and the results are summarised in table 3.24. The rest potential, which the specimen took up immediately upon immersion, remained constant during the experiment. Small changes in the shape of the impedance plots, resulted in variations in the values of the resistance and capacitance measurements.

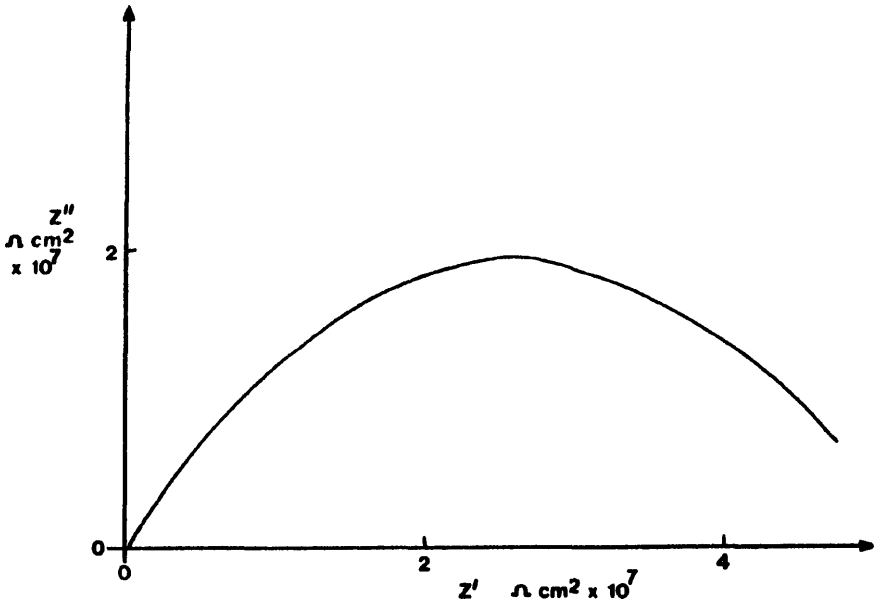

Figure 3.42 VMCH-1, 37-16°C.

Temp °C	Rs Ωcm²	Rsc Ωcm²	Capacitance cm⁻²	Nyquist Plot	Potential mV vs. S.C.E.
37	1.6E5	5E7	139pF		-560
36	1.6E5	5E7	128pF		-560
35	1.6E5	5E7	127pF		-560
34	1.6E5	4.5E7	126pF		-560
33	1.5E5	4.5E7	148pF		-560
32	1.6E5	4.6E7	132pF		-560
31	1.6E5	4.6E7	140pF		-560
30	1.6E5	3.6E7	137pF		-560
29	1.6E5	3.5E7	145pF		-560
28	1.6E5	3E7	144pF		-560
27	1.6E5	3.2E7	143pF		-560
26	1.6E5	3.5E7	153pF		-560
24	1.6E5	2E6	129pF		-560
22	1.6E5	2E6	121pF		-560
21	1.6E5	1.7E7	121pF		-560
20	1.6E5	1.7E9	122pF		-560
18	1.6E5	1.7E7	123pF		-560
16	1.6E5	1.7E7	122pF		-560

Table 3.24 VMCH-1, impedance response with temperature.

A further temperature changing experiment was performed after twenty-one days immersion in salt solution and these results are presented in table 3.25. During this time, the specimen had developed small black spots over its surface and it was possible that the presence of corrosion products under the film, may have some effect upon the impedance response.

Temp °C	Rs Ωcm²	Rsc Ωcm²	Capacitance cm^{-2}	Nyquist Plot	Potential mV vs. S.C.E.
35	1.1E5	1.3E6	81pF		-420
34	1.1E5	1.5E6	80pF		-420
33	1.1E5	1.7E6	80pF		-420
32	1.1E5	1.8E6	80pF		-420
31	1.E5	2E6	80pF	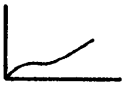	-420
30.5	1.1E5	1.7E6	79pF	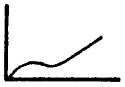	-420
29.5	1.1E5	2E6	79pF		-420
29	1.1E5	1.8E6	78pF		-420
28	1.1E5	2E6	78pF		-420
27	1.1E5	1.9E6	78pF		-420

Table 3.25 VMCH-1, impedance response after 21 days immersion.

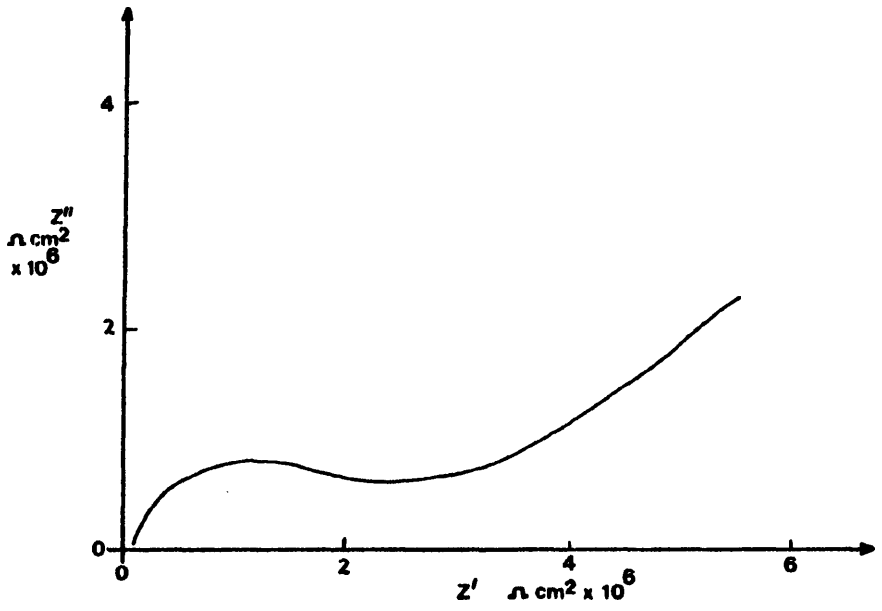

Figure 3.43 VMCH-1, 35-27°C.

After twenty-one days immersion, the rest potential, impedance plot shape and its resulting parameters, remained almost constant throughout the experiment. As with the previous run and in common with with the results from the detached film experiments, there was no obvious change in the impedance response at the polymers lower glass transition temperature.

The other half of the panel (VMCH-2), was immersed in salt solution at room temperature and the solution heated in small increments. The results from this experiment are given in table 3.26.

Temp °C	Rs Ωcm²	Rsc Ωcm²	Capacitance cm^{-2}	Nyquist Plot	Potential mV vs. S.C.E.
15	1E5	-	78pF		-640
16	1E5	-	81pF		-640
17	1E5	-	79pF		-640
20	1E5	-	78pF	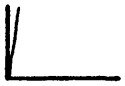	-560
25	1E5	-	79pF		-560
27	1E5	-	80pF		-560
28	1E5	-	80pF		-560
29	1E5	-	81pF		-560
30	1E5	-	82pF	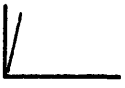	-560
31	1E5	-	83pF		-560
33	1E5	-	84pF		-560

Table 3.26 VMCH-2, impedance response with temperature.

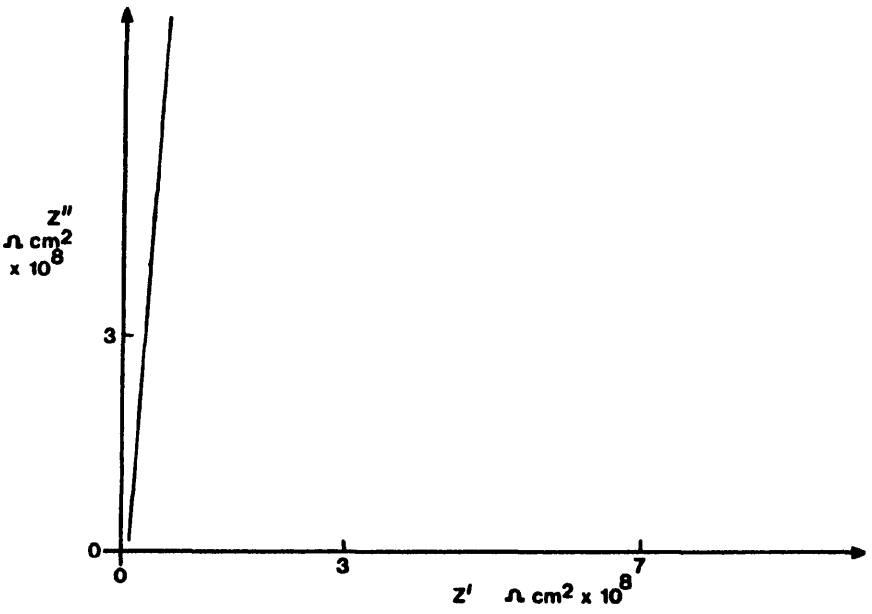

Figure 3.44 VMCH-2, 15-34°C.

Comparison of the data obtained from the half panels, shows that there is a difference in both the plot shape and in the capacitance values obtained from the films. The specimen immersed in salt solution at a temperature above that of its Tg, showing a much higher initial capacitance. Both the specimens exhibit approximately the same solution resistance and take up a similar rest potential (-560mV w.r.t. Calomel) on immersion.

The temperature changing experiments were repeated on VMCH-2 after four, twelve and twenty-five days immersion. The results are presented in the following tables.

Temp °C	Rs Ω cm²	Rsc Ω cm²	Capacitance cm^{-2}	Nyquist Plot	Potential mV vs. S.C.E.
20	1E5	4E7	78pF		-410
22	1E5	4E7	79pF		-410
24	1E5	4E7	79pF		-410
26	1E5	4E7	80pF		-410
27	1E5	4E7	81pF		-550
28	1E5	4E7	82pF		-550
30	1E5	4E7	83pF		-550
32	1E5	4E7	84pF		-550

Table 3.27 VMCH-2, 4 days after immersion.

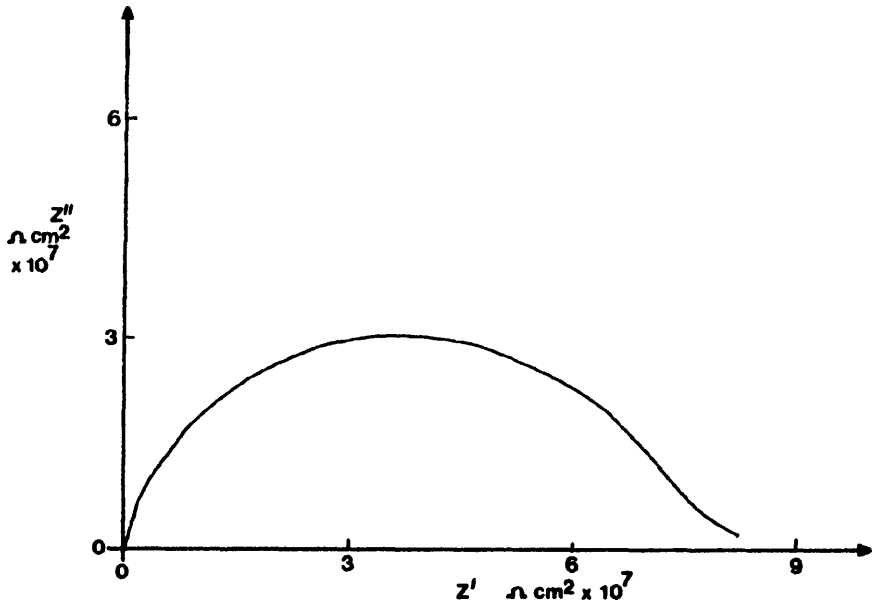

Figure 3.45 VMCH-2, 20-32°C.

Temp °C	Rs Ω cm²	Rsc Ω cm²	Capacitance cm⁻²	Nyquist Plot	Potential mV vs. S.C.E.
33	1E5	3E7	85pF		-580
32	1E5	3E7	84pF		-580
31	1E5	3E7	83pF		-580
30	1E5	3E7	83pF		-580
29	1E5	3E7	82pF		-580
27.5	1E5	3E7	81pF		-580
26	1E5	3E7	81pF		-580

Table 3.28 VMCH-2, 12 days after immersion.

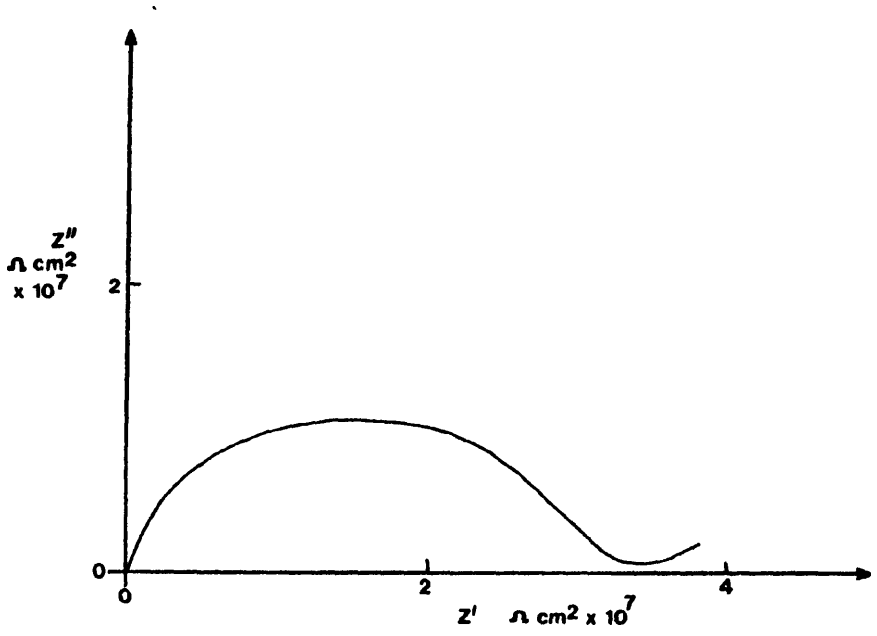

Figure 3.46 VMCH-2, 33-25°C.

Temp °C	Rs Ωcm^2	Rsc Ωcm^2	Capacitance cm^{-2}	Nyquist Plot	Potential mV vs. S.C.E.
18	8E4	2E6	79pF		-620
35	8E4	2E6	81pF		-620

Table 3.29 VMCH-2, 25 days after immersion.

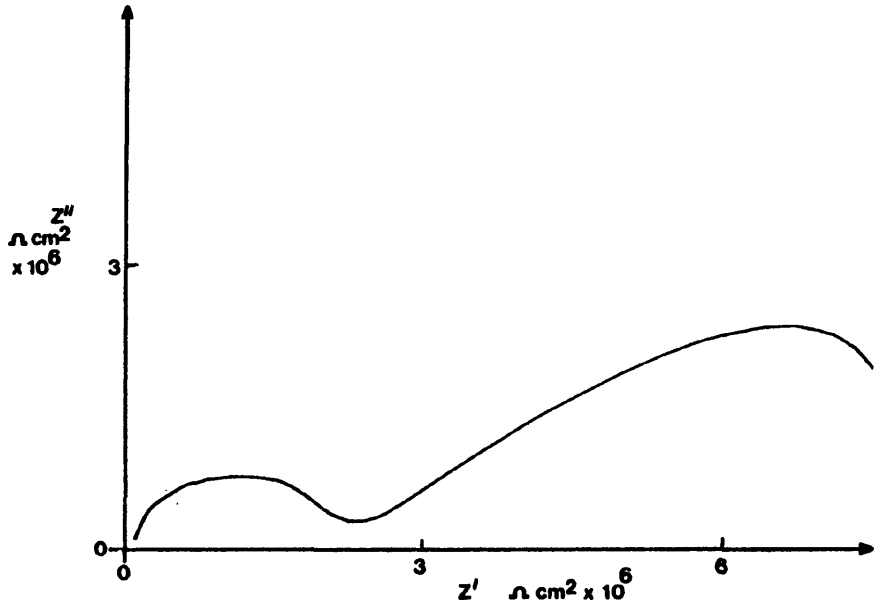

Figure 3.47 VMCH-2, impedance response at 18°C and 35°C.

These results, from VMCH-2, show a consistant increase in the measured capacitance as the solution temperature increased. When the converse experiment was performed, that is, decreasing the temperature, the same pattern of higher capacitances at higher temperatures was apparent. During each run, the capacitance only varied by a few pF/cm^2 and remained at 79-80pF/cm^2 (at room temperature) during the first twelve days of the experiment. After twenty-five days immersion, as with VMCH-1, the

capacitance showed a slight decrease in value (although this was more pronounced for VMCH-1) and again, corrosion processes were observed under the film.

3.8 The impedance response of a pinhole.

The effects of creating a pinhole in an attached film, were also monitored using the impedance technique. The pinhole was made on an acrylic B specimen and the impedance response of the panel followed with time. Table 3.30, summarises the response of the specimen before the creation of the pinhole and the impedance behaviour with time.

Time	Rs Ωcm^2	Rsc Ωcm^2	Capacitance cm^{-2}	Nyquist Plot	Potential mV vs. S.C.E.
**	2E5	-	-		-110
0	1.2E3	500	1.69μF		-540
3min	1.3E3	550	0.63μF		-540
7min	1.2E3	650	0.64μF		-590
11min	1.2E3	700	0.4μF		-605
16min	1.2E3	720	0.34μF	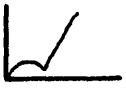	-605
22min	1.2E3	720	0.29μF	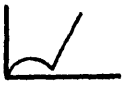	-605
75min	1.3E3	780	0.16μF		-620
28hrs	1.5E3	340	0.12μF	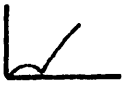	-670
2days	1.5E3	450	0.08μF	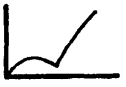	-670
3days	1.7E3	500	0.08μF		-665
** Before creation of pinhole.					

Table 3.30 Acrylic B. Impedance response after the creation of a pinhole.

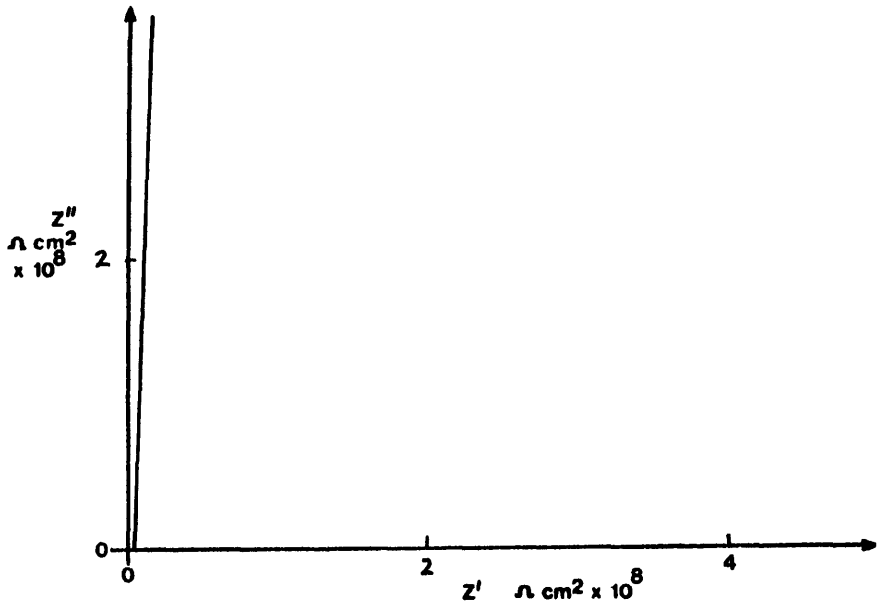

Figure 3.48 Acrylic B, before the pinhole was created.

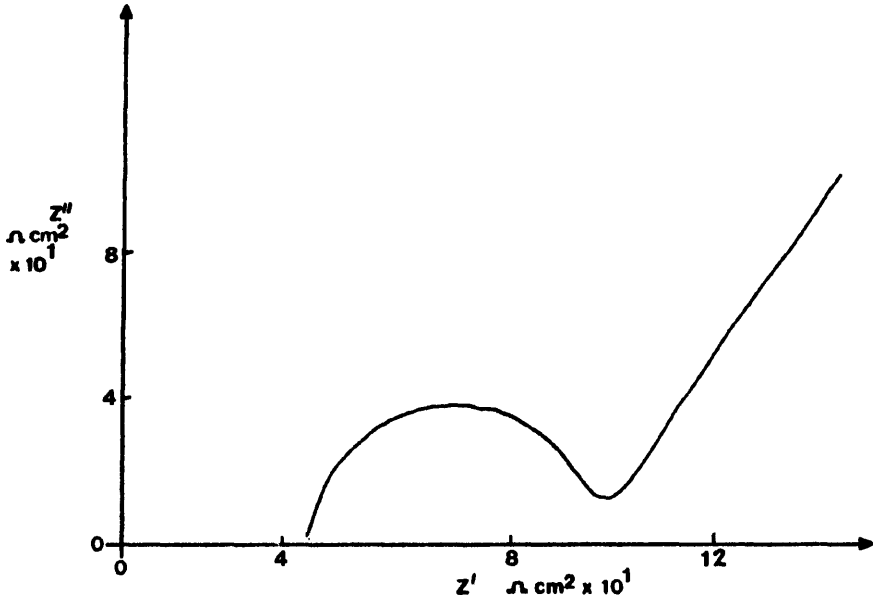

Figure 3.49 Acrylic B, 0-3 days after the pinhole was created.

3.9 Effect of substrate preparation and coating thickness.

Vinylite and acrylic coated specimens were exposed to 3% sodium chloride solution and were monitored with time, using the impedance technique. The results of these experiments are presented in the following tables. As with the previous data, sketches of the impedance plots obtained are presented with the results, larger, scaled impedance plots are shown after the tables and in appendix 4.

Acrylics A1 and B1.

Both the acrylic A1 and B1 specimens exhibited "capacitive" type impedance plots throughout the duration of the experiment. The specimen rest potentials were extremely unstable over the first 78 days of immersion, although the solution resistance and capacitance values remained constant for each panel.

Time	Rs Ωcm^2	Rsc Ωcm^2	Capacitance cm^{-2}	Nyquist Plot	Potential mV vs. S.C.E.
0	3.2E5	-	57pF		-
7days	3.2E5	-	57pF		-
23days	3.2E5	-	57pF		-
78days	3.2E5	-	57pF		+40
85days	3.2E5	-	60pF		-20
101days	3.2E5	-	60pF		-20
119days	3.2E5	-	58pF		-55
128days	3.2E5	-	59pF		-160
136days	3.2E5	-	59pF		-140

Table 3.31 Acrylic A1, 48μ on degreased steel.

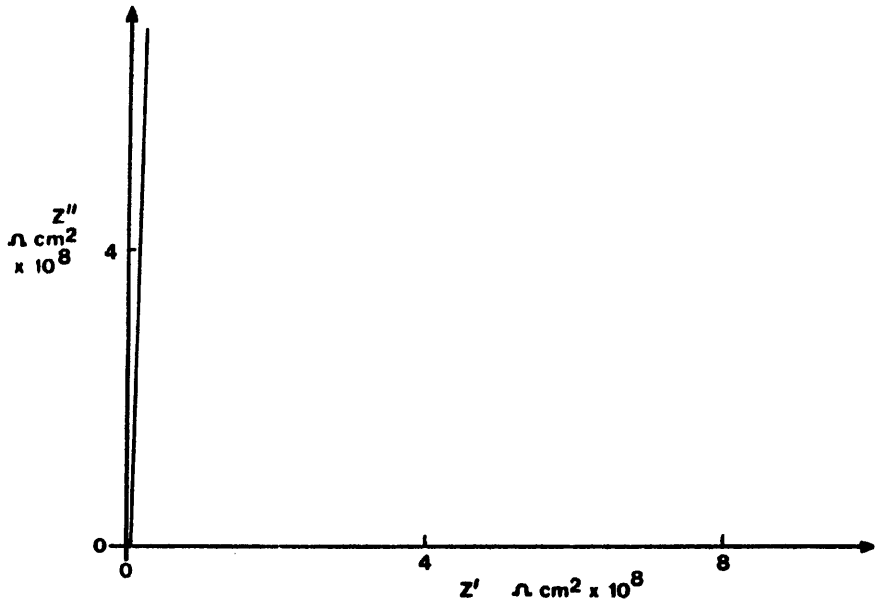

Figure 3.50 Acrylic A1 0-136 days immersion.

Time	Rs Ωcm^2	Rsc Ωcm^2	Capacitance cm^{-2}	Nyquist Plot	Potential mV vs. S.C.E.
0	4E5	-	34pF		-
7days	4E5	-	34pF		-
23days	4E5	-	34pF		-
78days	4E5	-	35pF		-50
85days	3.8E5	-	35pF		-110
101days	3.8E5	-	36pF		-15
128days	4E5	-	35pF		+10
136days	3.8E5	-	40pF		-15

Table 3.32 Acrylic B1, 83μ on degreased steel.

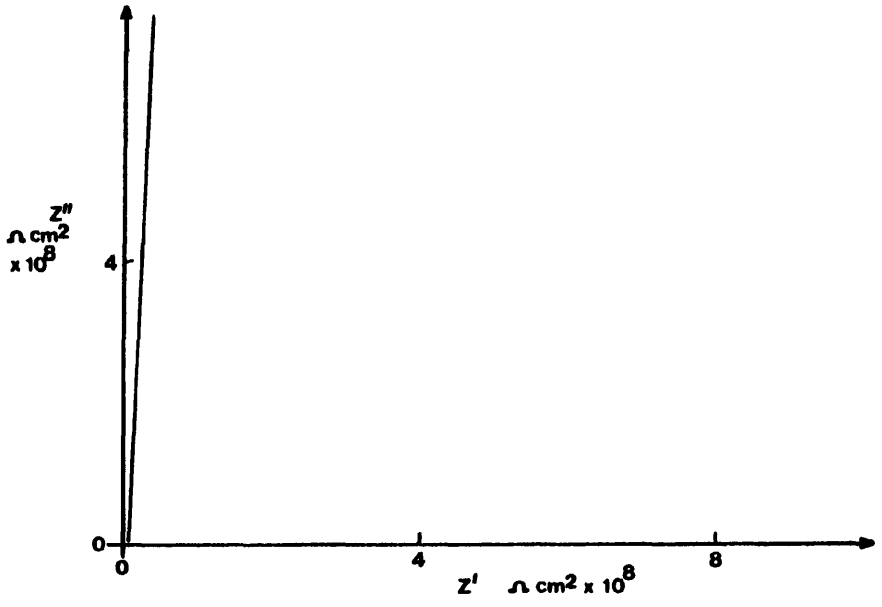

Figure 3.51 Acrylic B1, 0-136 days immersion.

No visible corrosion occurred on acrylic A1, whilst on B1, three very small black spots became apparent after 78 days immersion. At this time, a rest potential was measured on the specimens, although it was not completely stable. The capacitance of the films increased slightly over the test period and the rest potential continued to be unsettled.

Acrylics A2 and B2.

The previous pair of acrylic coated specimens showed few visual signs of corrosion after prolonged immersion in salt solution. Consequently, it was decided to repeat the experiment, using thinner films. The results are shown in the following tables.

Time	Rs Ωcm^2	Rsc Ωcm^2	Capacitance cm^{-2}	Nyquist Plot	Potential mV vs. S.C.E.
0	1E4	-	53pF		-610
10min	1E4	-	53pF	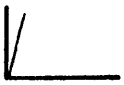	-610
30min	1E4	-	55pF	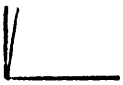	-610
1hr	1E4	-	56pF	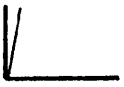	-610
2hrs	9E3	7E5	98pF		-610
1day	1E4	-	55pF	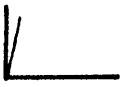	-610
7days	1E4	-	56pF	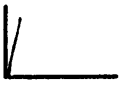	-610
13days	1E4	-	61pF	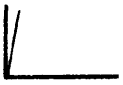	-610
21days	2.2E5	7E5	33pF		-610
48days	2E5	7E5	40pF		-560
73days	2E5	6E5	43pF		-660
92days	2E5	7E5	43pF		-660

Table 3.33 Acrylic A2,50μm on degreased steel.

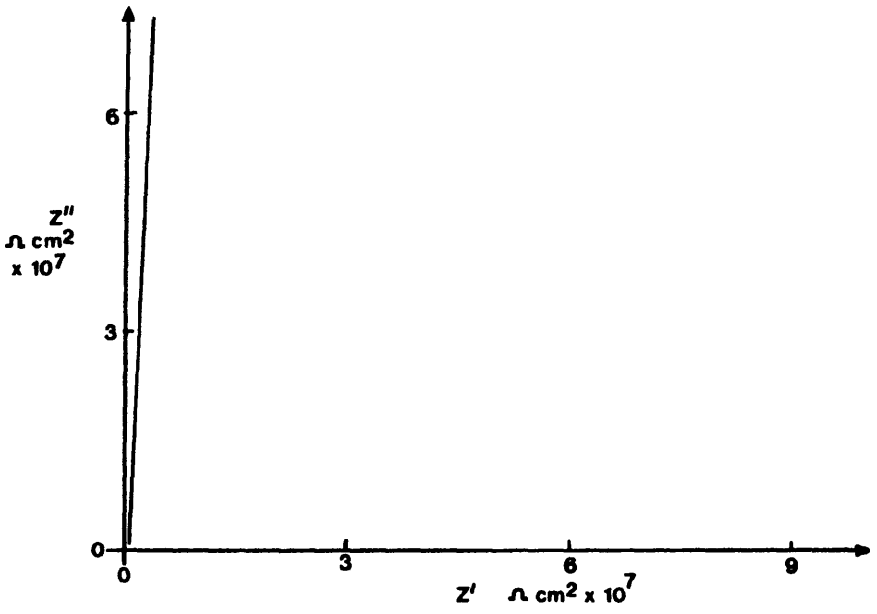

Figure 3.52 Acrylic A2, 0-1 hour and 1-13 days.

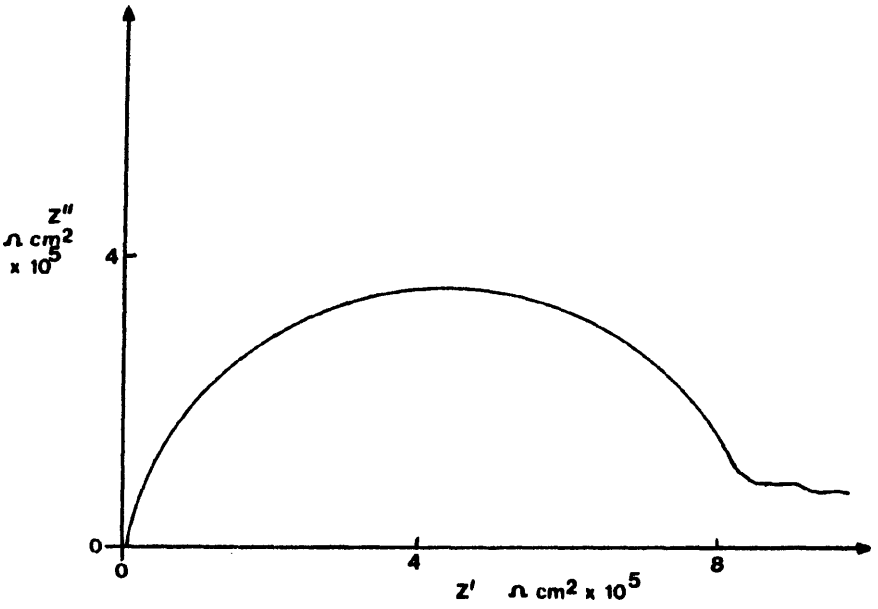

Figure 3.53 Acrylic A2, 2 hours.

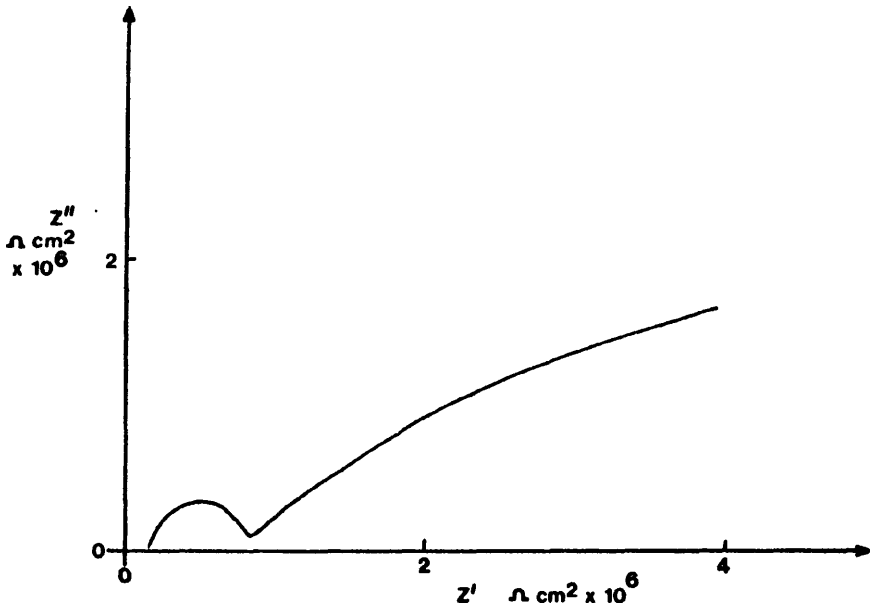

Figure 3.54 Acrylic A2, 21-92 days.

Time	Rs Ωcm^2	Rsc Ωcm^2	Capacitance cm^{-2}	Nyquist Plot	Potential mV vs. S.C.E.
0	1E4	-	101pF		-610
10min	1E4	-	99pF		-610
40min	1E4	7.5E5	97pF		-610
2hrs	1E4	-	55pF		-610
1day	7E4	6.5E5	100pF		-610
3days	7E4	5.5E5	98pF		-610
8days	7E4	3.8E5	98pF		-610
13days	7E4	2.6E5	105pF		-610
21days	7.5E4	-	-	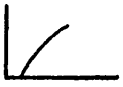	-610
48days	7E4	2E5	98pF		-420
73days	7E4	1.8E5	98pF		-460
92days	7E4	1.5E5	97pF		-460
134days	7E4	1.5E5	83pF		-520

Table 3.34 Acrylic B2, 30μm on degreased steel.

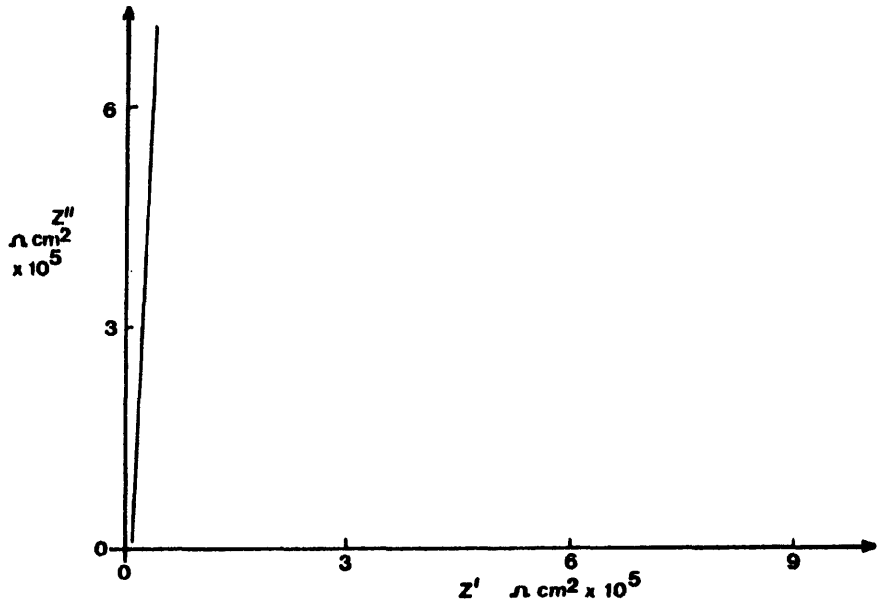

Figure 3.55 Acrylic B2, 0-10 minutes after immersion.

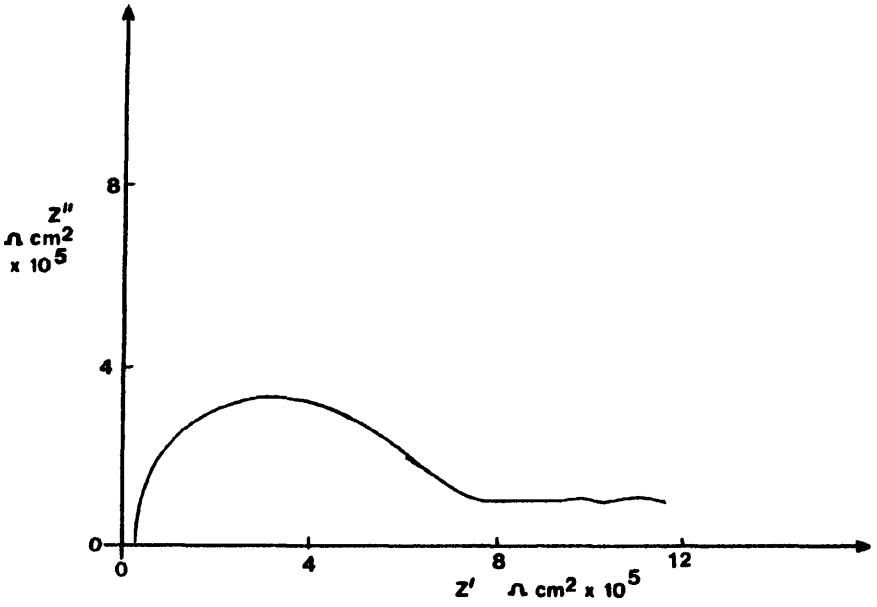

Figure 3.56 Acrylic B2, 40 minutes after immersion.

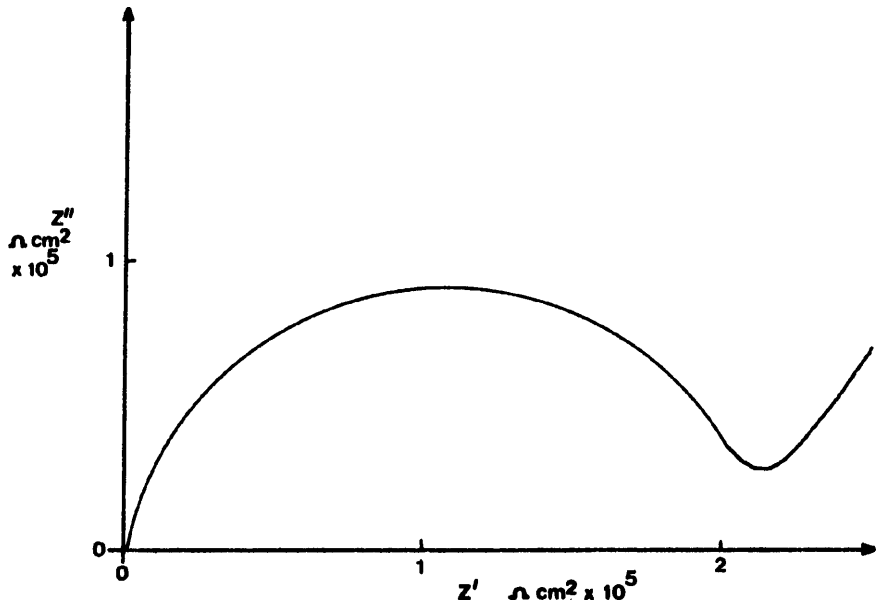

Figure 3.57 Acrylic B2, 48 days after immersion.

As with the previous acrylic A specimen, the impedance plots were mainly of the capacitive type. A few small black spots were observed on the specimen after eight days immersion, but there was no change in the shape of the impedance plot until twenty-one days had elapsed. After this time, it was observed that the corrosion spots had begun to increase in size, very slowly.

Plate 3.10 Acrylic A2 after 48 days immersion.

After forty-eight days immersion, a filiform type growth had become apparent. Again, a slow rate of growth was observed. The onset of growth of corrosion phenomena, appeared to coincide with the change in shape of the impedance plots and an increase in the solution resistance.

For the acrylic B2 specimen, the impedance plots were semicircular in shape after twenty-four hours immersion and remained this shape, with some scatter of the data points, throughout the experiment. The diameter of the semicircle slowly decreased with time, indicating that there may be some corrosion process occurring. The capacitance of the film also varied with time. Although the impedance data implied that there was a corrosion process operating, there was no visual evidence of corrosion products. However, several small, fluid filled blisters were observed on the specimen, on its removal from the test solution. The contents of these blisters appeared, from their pH, to be water.

Vinylite VAGH.

Three VAGH specimens were examined in this experiment. Specimen (1), was three coats of polymer, on a citric acid pickled panel, number (2), three coats on a degreased panel and number (3), two coats of polymer on a degreased specimen. The results from these specimens,are given in the tables.

Time	Rs Ωcm^2	Rsc Ωcm^2	Capacitance cm^{-2}	Nyquist Plot	Potential mV vs. S.C.E.
0	9E3	1.2E8	35pF		-
1day	9E3	1.2E9	38pF		-
2days	9E3	1.4E9	38pF		-
7days	9E3	7.8E8	38pF		-
9days	9E3	9.4E8	39pF		-
13days	9E3	7.3E8	38pF		-
17days	9E3	6.8E8	38pF		-
28days	9E3	6.3E8	39pF		-640
59days	9E3	1E8	44pF		-488
84days	9E3	9.9E7	48pF		-640
107days	9E3	-	-	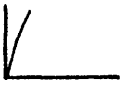	-440
134days	9E3	5E5	360pF		-330
142days	9E3	3.2E5	50pF		-180

Table 3.35 VAGH-1, 88μm on pickled steel.

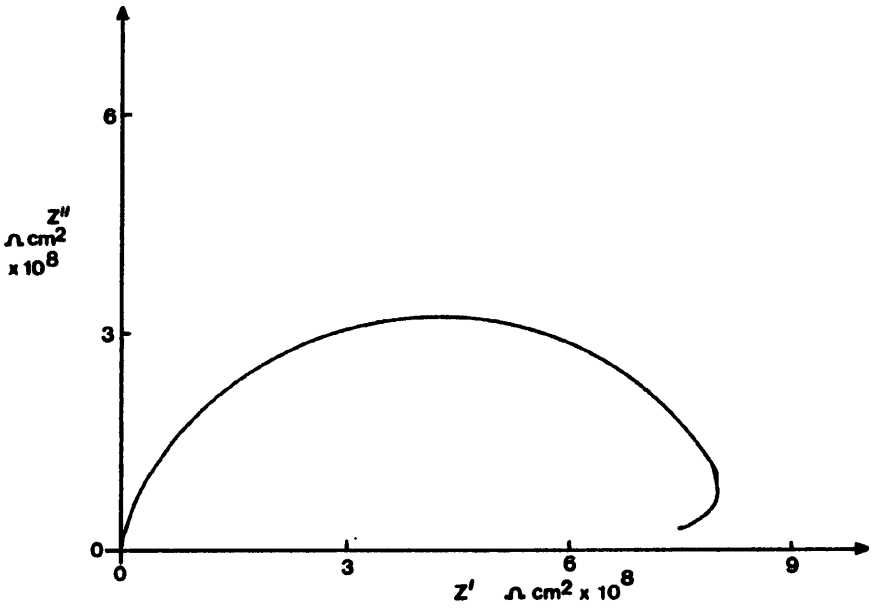

Figure 3.58 VAGH-1, 1-7 days after immersion.

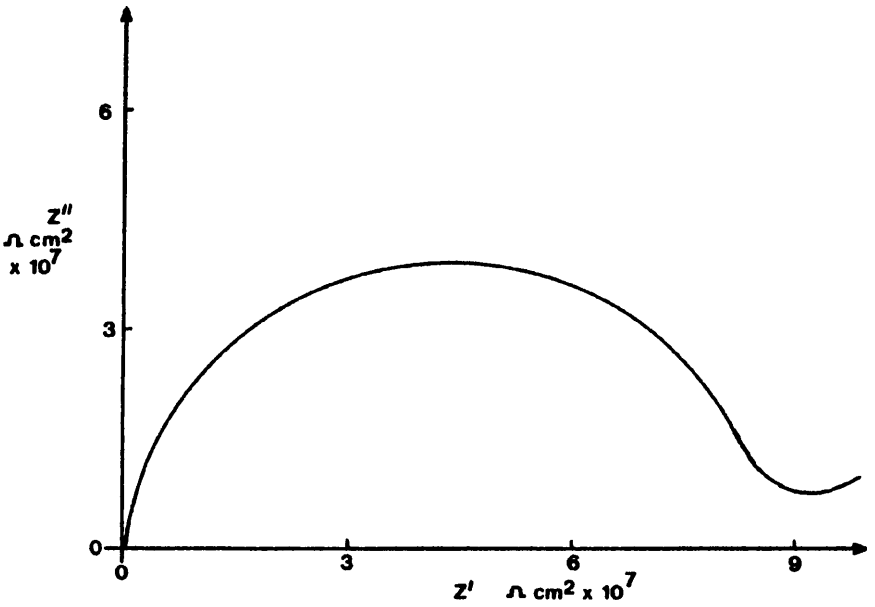

Figure 3.59 VAGH-1, 28-59 days after immersion.

Time	Rs Ωcm²	Rsc Ωcm²	Capacitance cm⁻²	Nyquist Plot	Potential mV vs. S.C.E.
0	3E4	-	40pF		-
1day	3.1E4	-	43pF		-610
6days	2.5E4	-	44pF		-620
13days	2.5E4	-	44pF		-660
29days	3E4	-	55pF		-560
47days	2.5E4	-	43pF		-400
56days	3E4	-	-		-430
64days	2.5E4	-	44pF		-585

Table 3.36 VAGH-2, 80μm on degreased steel.

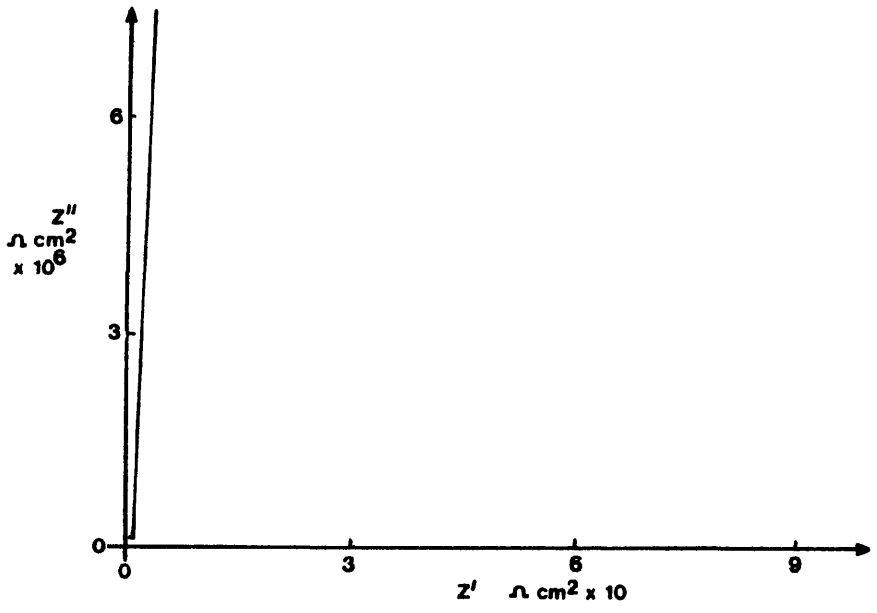

Figure 3.60 VAGH-2, 0-64 days after immersion.

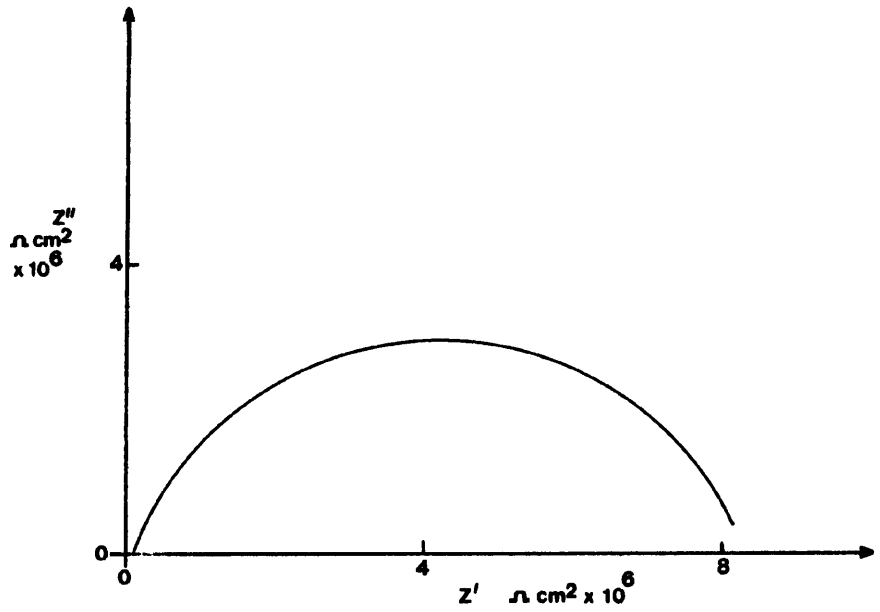

Figure 3.61 VAGH-2, 56 days after immersion.

Time	Rs Ωcm²	Rsc Ωcm²	Capacitance cm⁻²	Nyquist Plot	Potential mV vs. S.C.E.
0	3.2E5	-	59pF		-
1day	3.2E5	-	61pF		+90
6days	3.2E5	-	62pF		-
13days	3.2E5	-	64pF		-35
29days	3.2E5	-	64pF		-620
47days	3.2E5	-	62pF		+50
56days	3.2E5	-	63pF		+170
64days	3.2E5	-	63pF		+45

Table 3.37 VAGH-3, 60μm on degreased steel.

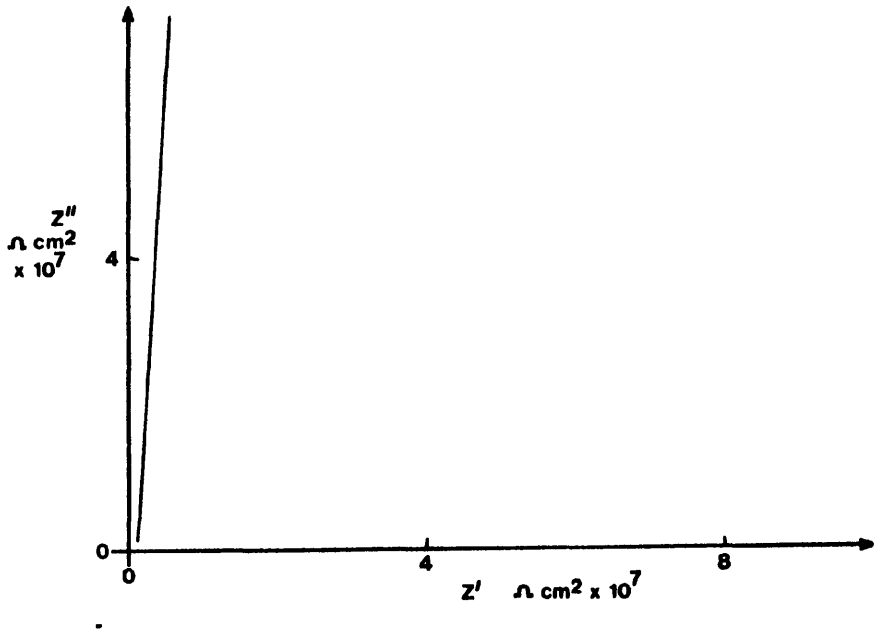

Figure 3.62 VAGH-3, 0-64 days after immersion.

The impedance data obtained from VAGH (1), showed semicircular plots of variable shapes. The solution resistance, Rs, remained relatively constant, whilst the diameter of the semicircle decreased steadily over the test period. The capacitance value increased with time and after one hundred and thirty-four days, appeared to be influenced by a diffusion process, as the value increased by several orders of magnitude. However, after one hundred and forty-two days, a "capacitive" type plot was observed. The rest potential, which was unstable for the first twenty-eight days of immersion, varied considerably with time.

Specimens VAGH (2) and (3), exhibited very similar impedance behaviour with time. Both showed an increase in the capacitance values with time and both exhibit "capacitive" type impedance plots. On (2), a semicircular plot was observed after fifty-six days immersion, but this quickly returned to the previous shape. A few fluid filled blisters were

observed on this specimen after six days in solution, but no corrosion product was noted. Several small black spots were observed on specimen (3) after six days immersion, which increased slightly in size up to thirteen days in solution, after which, no further apparent growth of these sites, or initiation of new sites, occurred.

Vinylite VMCH.

The results obtained from impedance studies on a VMCH coated degreased specimen, are shown in the table.

Time	Rs Ωcm^2	Rsc Ωcm^2	Capacitance cm^{-2}	Nyquist Plot	Potential mV vs. S.C.E.
0	2.5E5	-	34pF		-
1day	2.5E5	-	36pF		+290
6days	2.5E5	-	36pF		-200
13days	2.4E5	-	37pF		-190
29days	2.5E5	-	37pF		+155
47days	2.5E5	-	37pF		-340
56days	2.5E5	-	37pF		+105
64days	2.5E5	-	37pF		-350

Table 3.38 VMCH, 90μm on degreased steel.

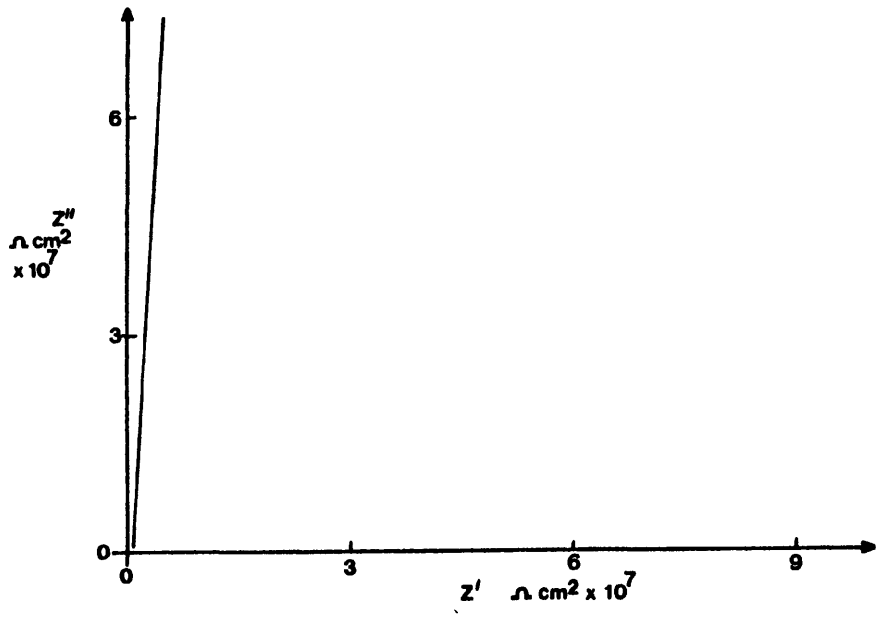

Figure 3.63 VMCH, 0-64 days after immersion.

As was observed with the acrylic specimens, the impedance plots from this panel, were of the capacitive type. The solution resistance remained constant throughout the experiment and the measured capacitance increased over the test period. The specimen rest potential, did not become settled and varied considerably with time. The consistantly "capacitive" impedance plot and the unstable rest potential, suggested that the polymer film is intact and that the impedance response, is that of the film alone. This theory was reinforced by the fact that small black corrosion spots initiated under the polymer film. The presence of the corrosion process on the specimen was not detected by the impedance technique. However, it must be noted that the spots, after initiating, did not increase in size during the remainder of the experiment.

Vinylite VYHH.

Three coats of this vinylite polymer was cast onto a citric acid pickled panel. The specimen was then immersed in salt solution and its impedance response noted. The results are presented in the following table.

Time	Rs Ωcm^2	Rsc Ωcm^2	Capacitance cm^{-2}	Nyquist Plot	Potential mV vs. S.C.E.
0	3E6	1.1E8	30pF		-
1day	3E6	1.1E8	31pF	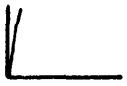	-
2days	3E6	-	31pF		-
7days	3E6	-	31pF		-
9days	3E6	7.5E9	31pF		-
13days	3E6	-	31pF		-
20days	3E6	3.9E9	31pF		-
29days	3E6	5.6E8	31pF		-400
84days	3E6	-	31pF		-100
107days	3E6	-	31pF		-60
125days	3E6	-	32pF	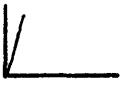	-30
142days	3E6	-	32pF	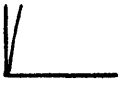	-10

Table 3.39 VYHH, 100μm on pickled steel.

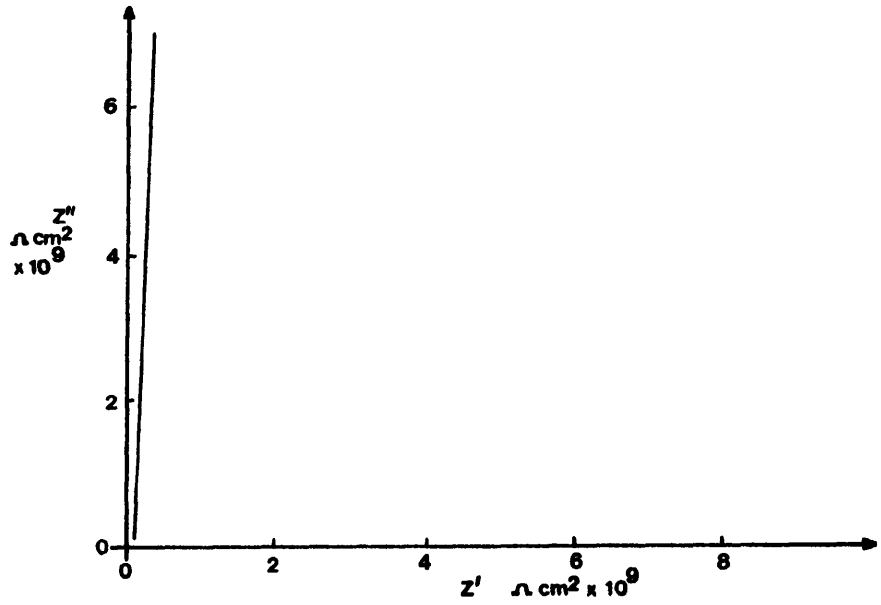

Figure 3.64 VYHH, 0-142 days immersion.

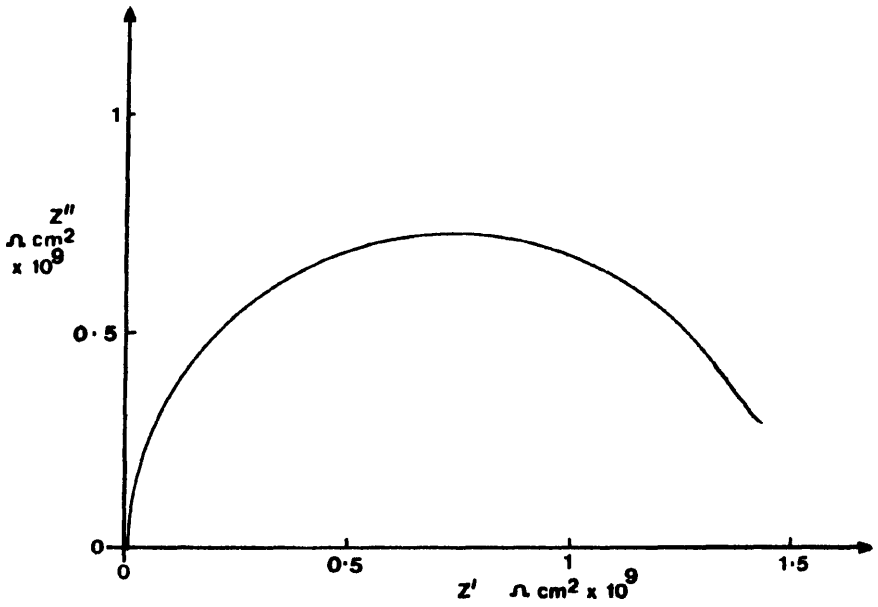

Figure 3.65 VYHH, 9,20 and 29 days immersion.

Initially upon immersion, the specimen exhibited a "capacitive" type

behaviour, which remained for the first nine days immersion. After this time, a semicircular plot was observed and small black spots were noted under the film. The impedance response of the specimen alternated between capacitive and semicircular type behaviour over the duration of the experiment. After twenty days, a second series of black spots initiated (neither set of spots increased in size with time), coinciding with a semicircular plot. The capacitance of the film increased slightly over the experimental period.

Vinylite VROH.

Three coatings of this vinylite polymer were applied to a citric acid pickled panel, which was immersed in 3% sodiun chloride solution. The impedance responses of this specimen with time, are presented in the table.

Time	Rs Ωcm²	Rsc Ωcm²	Capacitance cm⁻²	Nyquist Plot	Potential mV vs. S.C.E.
0	4.5E5	2.2E9	45pF		-
1day	4.5E5	2.2E9	45pF		-
6days	4.5E5	1E8	46pF		-
13days	4.5E5	1.3E8	46pF		-
20days	4.5E5	5E7	46pF		-
27days	4.5E5	1E7	60pF		-710
36days	4.5E5	1E5	55pF		-680
57days	5E5	6E5	43pF		-575
65days	6E4	6.5E5	1.6μF		-575

Table 3.40 VROH, 74μm on pickled steel.

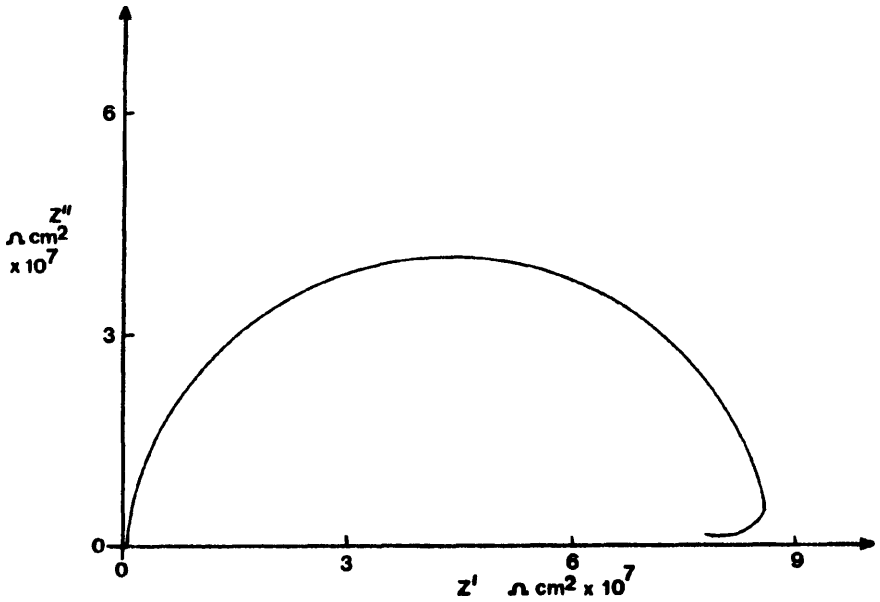

Figure 3.66 VROH, 0-20 days immersion.

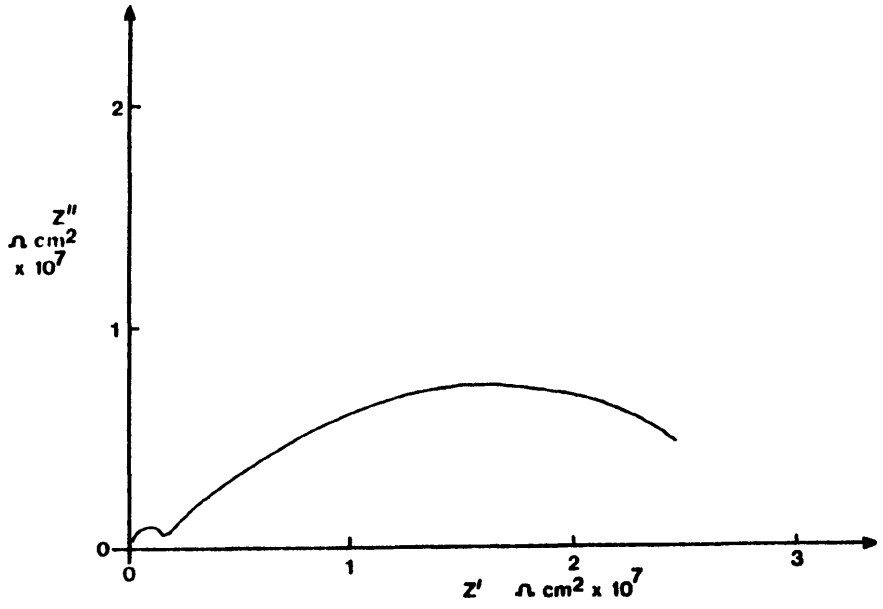

Figure 3.67 VROH, 27 days after immersion.

It can be noted that a semicircular impedance plot was obtained immediately upon the immersion of this specimen. After nine days in the solution, several tiny black spots were noticed under the film, but there was no change in the impedance response. After twenty-seven days immersion, a double semicircle was observed, the first semicircle corresponding to the polymer film and the second, it was thought, to the electrochemical double layer. The rest potential, which was taken up immediately upon immersion, fell quickly to a relatively low value,(-710mV w.r.t. silver/silver chloride reference electrode) and remained at about this value for the duration of the experiment. After thirty-six days in solution, orange coloured corrosion product had pushed through the film at several places on the specimen surface. These places corresponded to the sites of initiation of the black spots, which had increased in size with time. Orange corrosion product was not observed

until the polymer film was ruptured. After eighty-four days, the specimen surface was covered in corrosion product and the impedance response of the film was only partly observed.

3.10 Capacitance and coating thickness.

The capacitance of the specimens was measured immediately upon immersion and these results (shown in the table), were plotted against the reciprocal of the thickness of the film, as shown in the graph. As has been previously observed, <128>, a straight line relationship was obtained.

Polymer	Thickness (μm)	$\frac{1}{\text{Thickness}}$ (μm^{-1})	Initial Capacitance (pF/cm^2)
VAGH	88	114	35
VAGH	80	125	40
VAGH	60	166	59
VYHH	100	100	30
VYHH	43	230	79
VROH	74	135	45
VROH	60	166	48
VROH	58	172	62
VMCH	90	111	34
Acrylic A	48	202	57
Acrylic A	70	143	38
Acrylic B	84	119	34
Acrylic B	30	333	88

Table 3.41 Polymer thickness and capacitance data.

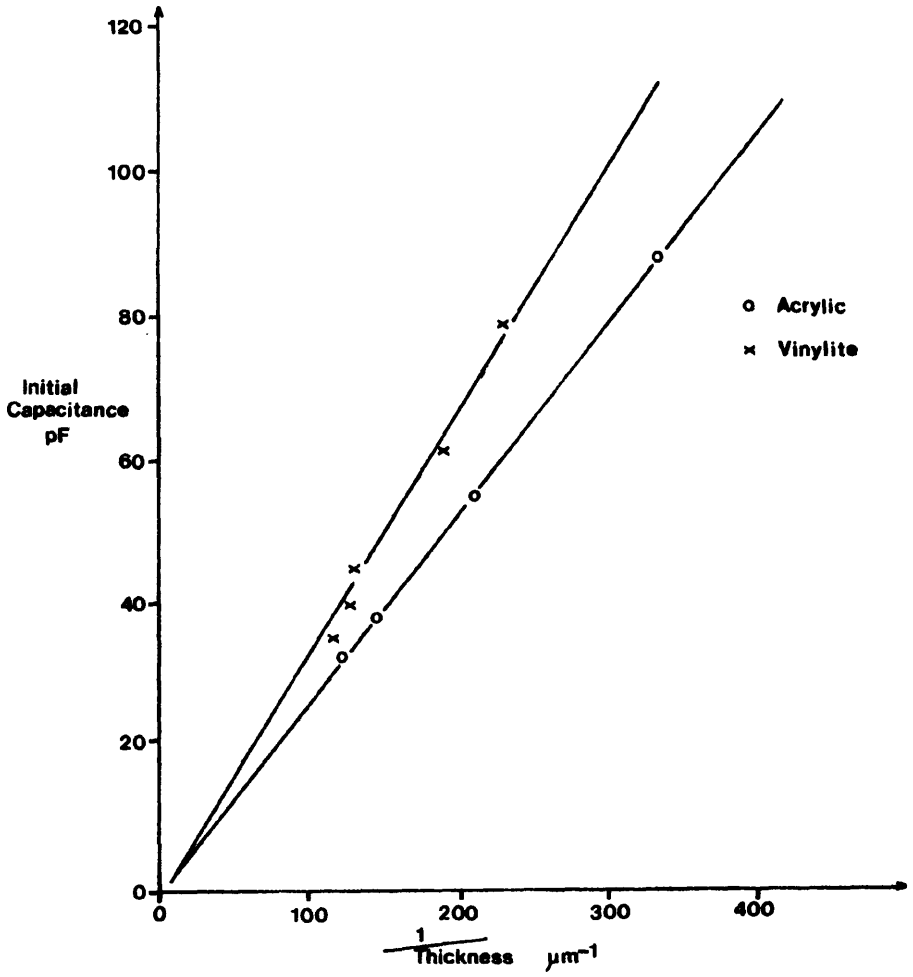

Figure 3.68 Relationship between coating thickness and capacitance.

3.11 Water uptake into polymer films.

The impedance data obtained from the Nyquist plots, may be used to obtain information concerning the behaviour of the polymer film with time. The uptake of water into a coating, may be related to the type and structure of that coating, in terms of the polymer constituents, degree of cross linking, etc. Several methods of determining the amount of water absorbed by a film are available and perhaps the simplest, is that of Brasher and Kingsbury <20>.

$$\%\text{water uptake} = \frac{125 \times \log(C / C_o)}{\log 80}$$

where: C = capacitance after given time
C_o = initial capacitance
125 = swelling factor
80 = dielectric constant of water

This formula makes several assumptions as to the distribution of water within the polymer film. Some assumptions are necessary for any calculation and the results of the calculations here are for comparison purposes only and not for the calculation of absolute quantities of water in the films.

The assumptions made are;

1)The capacitance values refer only to the polymer films. This is probable if the film is intact.

2)Changes in the capacitance are due to water uptake.

3)The permittivity of the water is 80. If water is bound to entities within the films, this value will be different.

4)The distribution of water within the film is random and uniform. This is not necessarily so, but some form of distribution must be assumed.

5)No polar solvent is retained in the film. Tg experiments showed that

a little xylene may be retained in the films, but it is not a polar molecule.

The percentage water uptake into the films had been calculated for several specimens and the results are shown in the following table.

Polymer	Immersion time (days)	Initial capacitance pF/cm^2	Capacitance after x days pF/cm^2	% Water uptake
VYHH	6	30	31.2	1.16
VYHH	142	30	32.4	2.2
VROH	7	45	46.2	0.78
VROH	84	45	48	1.84
VAGH	6	58.8	62.5	1.8
VAGH	64	58.8	63	1.98
VMCH	6	52.1	54.6	1.34
Acrylic A	7	57.5	57.5	0
Acrylic A	121	57.5	59.4	0.93
Acrylic B	7	34	34	0
Acrylic B	107	34	35.3	1.07

Table 3.42 Water uptake into polymer films.

3.12 Changes in the rest potential with time.

The rest potential of the specimens was monitored with time. It was noted that no specimen exhibited a constant rest potential and that for some polymers, a potential could not be measured for some time after immersion. In general, it was found that a relatively low rest potential (-560mV w.r.t. Calomel, or lower), coincided with a semicircular impedance plot. A more noble rest potential, often accompanied a

diffusion type plot. Where a "capacitive" plot was observed, a stable rest potential could not be monitored at all, for some polymers. The results from several specimens reported here, have been plotted on the following graph.

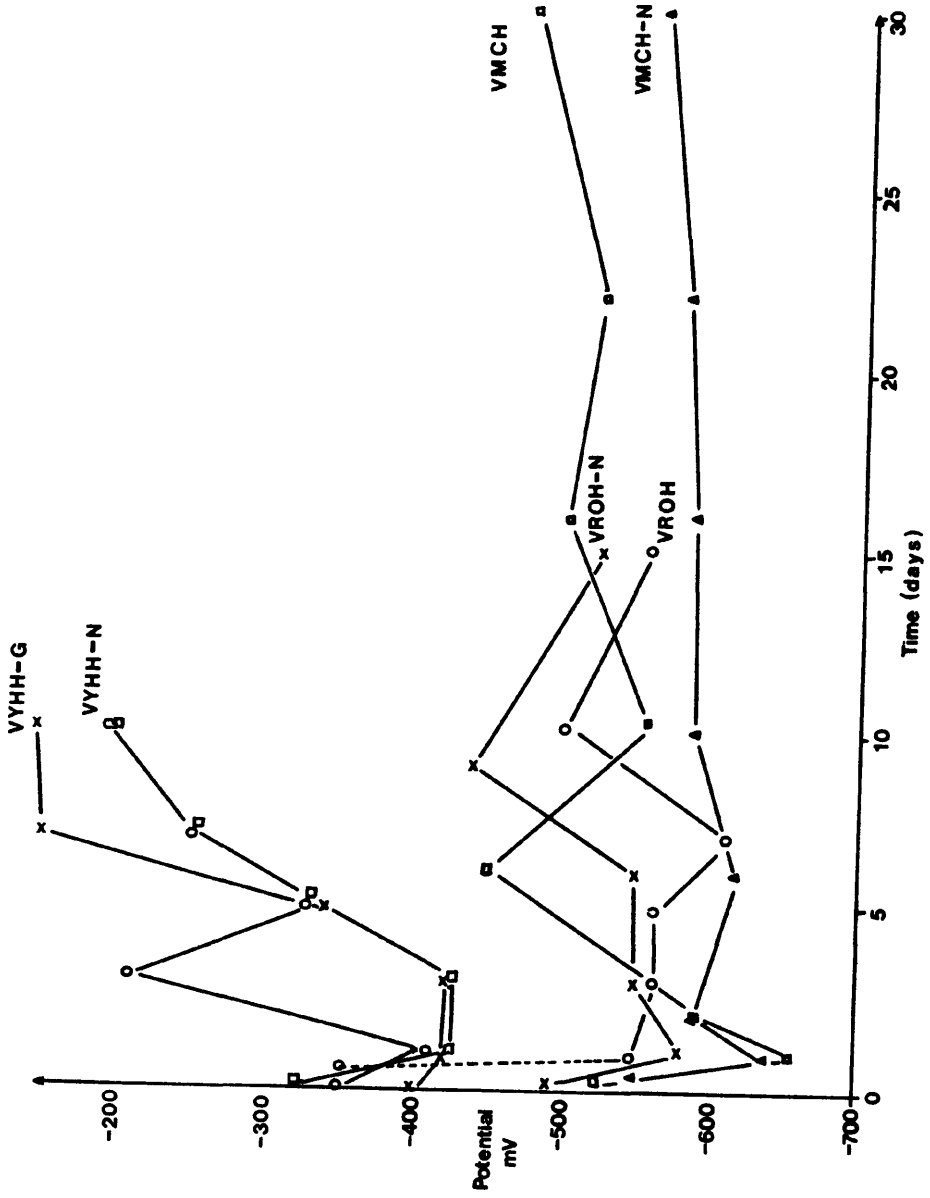

Figure 3.69 Specimen potential against time.

Chapter 4. Discussion.

4.1 Introduction

One major objective of this work was to assess the suitability of the impedance technique as an investigative tool in the study of polymer coatings for corrosion protection. The data presented in this thesis, indicates that the impedance method is able to distinguish between a protective film and a non-protective film, but that it is unable to detect the presence of small areas of corrosion under an intact film. It was noted that the rest potential of the specimen followed the corrosion trends indicated by the impedance data.

The other major objective was to determine whether the structure of a polymer film affected its protective ability. The results suggest that it does; and that it is the number of defects within a film that governs its protective properties. The number of defects can be related to the degree of crosslinking of the polymer and the number of coats applied. The method of surface preparation also affects the degree of protection afforded by the polymers.

4.2 Initial Experiments

Previous work using the impedance technique on coated substrates, <112> had suggested that it is a useful method for the examination of the protective abilities of polymer films. Ho used thick pigmented films and exposed only a small ($1 cm^2$) area to the test solution. His results

indicated that the corrosion behaviour of the painted specimen could be followed by the change in the impedance data, in particular, that the diameter of the semicircular part of the plot, could be directly substituted for the polarisation resistance Rp, in the Stern-Geary equation (page 17) and was directly related to the corrosion rate of the substrate. This finding appeared to provide a useful basis for examining the protective abilities of polymers with different structures, by comparing the corrosion rates obtained from each polymer.

Initially, a number of simple experiments were set up, using several different transparent polymers, which were exposed to 3% salt solution and run in a two electrode format, against a platinum counter electrode as shown on page 49. Although all the specimens experienced the same environment, it was not possible to reproduce Ho's observations using these polymers. The series of curves obtained by Ho are shown below, together with a variety of the many shapes obtained from the vinyl films.

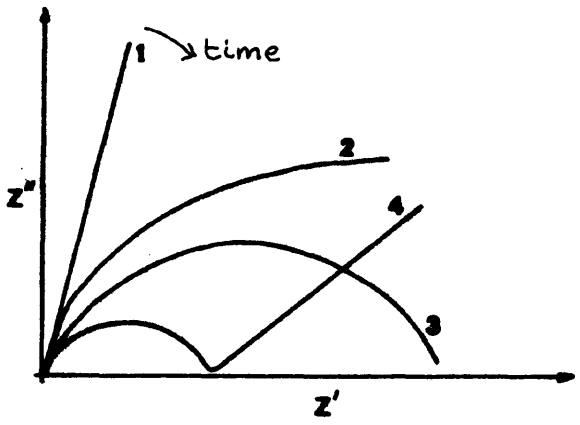

Figure 4.1 Ho's Series of Curves. <112>

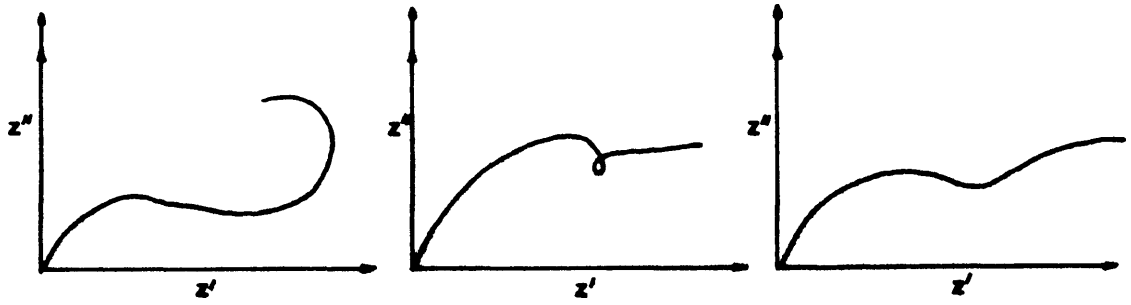

Figure 4.2 Curves from Vinyl Specimens.

Whilst the progression observed by Ho appears to be true for coal tar epoxy and chlorinated rubber paints, no such orderly change was noted for vinyl or acrylic polymers, where the shapes of the plots change with time and may even revert to a previously obtained shape, for example, VAGH (page 137), VROH(page 101), and acrylic B2 (page 130). After several experiments, it became apparent that the conclusions drawn by Ho, were not applicable to these polymers and were therefore, not a true indication of the corrosion events occurring on these specimens. The results could be interpreted on the basis that it was the polymer film which was being observed and that the defects in the film were giving rise to the observed semicircular type behaviour.

Visual examination of the specimens after some time of immersion, revealed that there was a wide variety of areas on the substrate, some bright metal, a number of small rust spots and a few larger sites. From a comparison of the visual and impedance results it could be inferred that the impedance technique was not a reliable method of indicating either the presence or the extent of underfilm corrosion. A capacitive type plot, for example, may be obtained, whilst corrosion products may be visible under the film, (e.g. VAGH-N page 98 and acrylic A2 page 130). Alternatively, there may be no observable corrosion after some time, but a semi-circular plot is obtained, (e.g. VMCH page 115 and acrylic B2 page 133).

It was therefore decided to perform a series of experiments in order to determine whether the origin of the impedance response in these experiments, was the corrosion process itself (as had been previously assumed) or, whether it was due to some film effect, in this case, the presence of defects within the film.

The components of the Nyquist plot have been traditionally assumed to be those of the corrosion processes taking place on the metal, as described on page 23.

Whilst these parameter assignments have been shown to be true for an uncoated substrate <98>, it was observed that the semicircle parameters were usually related to the film and not to the corrosion process. In order to support this conclusion, the following model was constructed, which illustrates the various parameters examined in this work. Each factor was studied separately and its effect on the impedance data included in the appropriate sections.

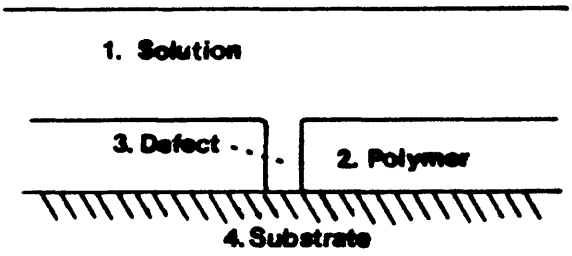

Figure 4.3 Schematic Diagram of Experimental System.

1) Solution effects;
   (i) no solution.
   (ii) solution temperature.
   (iii) oxygen concentration.

2) Polymer effects;
   (i) physical properties.
   (ii) structure.
   (iii) thickness.
   (iv) water uptake.
   (v) film resistance and capacitance.

3) Film defects;
   (i) degree of crosslinking.
   (ii) deliberate damage.

4) Substrate effects;
   (i) substrate preparation.
   (ii) no substrate.

Other practical considerations were the method of making the impedance measurements and the influence of the rest potential.

The rest potential of several specimens was monitored with time and in some cases, found to vary with the shape of the impedance plot. For example, with VAGH, a rest potential of -250mV (S.C.E.) was measured and a capacitive type plot was observed. With a semicircular plot, the same specimen showed a rest potential of -480mV (S.C.E.). These figures are typical of many of the experiments. Whilst the presence of corrosion products was often noted at the more active potentials (e.g. -480mV), it was usually absent when the specimen potential was more noble (for example -200mV). However, with an intact film, it was also noted that corrosion products may be observed under the film, whilst the potential remained relatively noble. The specimen potential was shown by Scantlebury and Callow <115> to affect the shape of the impedance plot

and it was therefore considered important, that the specimen be kept at its measured rest potential throughout the frequency sweep, neccessitating the use of a three electrode system of measurement. The latter system also produced a decrease in the scatter of the data.

4.3 Variation of Solution Parameters.

4.3.1 No Solution.

It was originally assumed that the part of the impedance plot ascribed to the solution resistance (Rs), was of a constant value <112>. However, this was shown <128> to vary with the concentration of the solution, a higher value for Rs being observed with solutions of low conductivity.

In this work, a novel system of examining the solution resistance was devised, by replacing the aqueous solution with mercury, thereby creating a "metal sandwich" with the polymer as the "filling". The results (page 85), showed that the film capacitance varied with the inverse of the film thickness, as was observed for specimens immersed in aqueous solution. The dry, film resistance, which varied directly with the coating thickness, appeared to vary between the polymer types, suggesting its dependance on the ability of the film to conduct electrons. As there is no solution present in this experimental system and hence no ions, the current which flows around the circuit must be electronic in nature. For some polymers, conduction of electrons is easier than for others, resulting in differences in the film resistance. The vinyl films, contain simple co-polymerised compounds, with no double

bonds, ring structures, etc. As there are no constituents of the polymer which could assist in electron transport, the resistance of the vinyl films was high. In comparison, the acrylic polymers are composed of a larger number of compounds, including the ring compound, styrene. The crosslinking agent used in the acrylic polymers is Cymel 301 (whose structure is shown below). It is also a ring structure and is not always fully crosslinked.

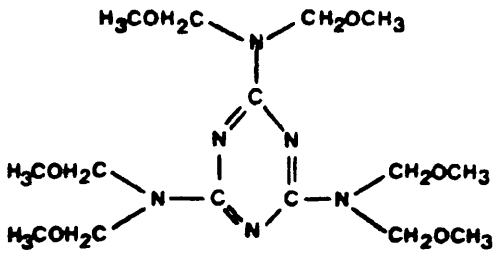

Figure 4.4 The Structure of Cymel 301.

It is suggested that the presence of the unconjugated double bonds (-C=C-) and the ring structures in the acrylic polymers, allow for the easier passage of electrons through these films and hence a lower film resistance is observed.

4.3.2 Solution Temperature.

It was thought that if the presence and diffusion of water and ions into a film, was affected by the temperature of the solution, this could become apparent in the impedance response of the specimens. However, in a series of experiments using attached and detached films, there was no marked change in either the impedance plot shape, or in its parameters, at either the upper or lower glass transition temperatures (Tg) of the vinyls studied.

It is probable that there were no major defects in the specimen immersed in solution above its Tg, as it showed a high constant solution resistance over the temperature range under study. The diameter of the semicircle observed on the impedance plot decreased with decreasing solution temperature. Ho suggested that this is due to an increase in the corrosion rate of the substrate as the temperature decreases. This phenomenon and explanation has been observed and reported elsewhere <51>. From the results in this work, it is proposed that the decrease in the diameter of the semicircle is due to a decrease in the ionic resistance of the film, caused by the entry of water and ions into the coating. At temperatures above Tg, the polymer chains are considered to possess a greater freedom of movement and thus to allow an increased quantity of aqueous species into and through the film. It would therefore be expected that the film resistance would decrease as the temperature increased, the opposite of this particular result. However, only in this experiment did the resistance decrease with a decrease in solution temperature and it is suggested that this is due to the permeation of water into the coating at temperatures above the polymers Tg. As the temperature decreased, the solution became trapped within the now more rigid polymer chains in greater quantity than would be usual at a particular temperature, thus lowering the film resistance abnormally.

In general the experiments with the solution temperature showed that there was no marked change in either the impedance plot shape, or in its parameters, at the Tg of the vinyl polymers examined. There was also no increase in the amount of underfilm corrosion which occurred during these experiments, as compared with specimens at 25° C. Although an increase might have been expected, due to the higher temperatures and easier permeability of aqueous bourne corrodants into the film, it was

possible that there was a decrease in the dissolved oxygen concentration at higher temperatures, which compensated for the increased permeability. Oxygen is generally considered to be neccessary for corrosion to occur and Ho showed that bare steel which was exposed to deaerated 3% sodium chloride solution, did not corrode. It was therefore assumed that coated mild steel under the same conditions would also exhibit no corrosion.

4.3.3 Oxygen Concentration.

Contrary to the expected results, those specimens immersed in deaerated solution, exhibited a greater degree of corrosion attack, than their aerated counterparts. The reason for this apparent anomaly, may lie in the nature of the corrosion reactions, in particular, with the cathodic reaction. In aerated solution, it is the reduction of molecular oxygen, in deaerated solution, the reduction of hydrogen ions to molecular hydrogen.

The following steps have been proposed <129> for the corrosion of mild steel in deaerated solution, the anodic process being;

$$Fe + H_2O \longrightarrow FeOH_{ads} + H^+ + e^- \qquad (1)$$

$$FeOH_{ads} + H_2O \longrightarrow Fe(OH)_2 + H^+ + e^- \qquad (2)$$

In a deaerated solution, the cathodic process is simply;

$$2H^+ + 2e^- \longrightarrow H_2 \qquad (3)$$

The hydrogen gas produced, diffuses into the solution. This may be illustrated diagramatically, as shown overleaf.

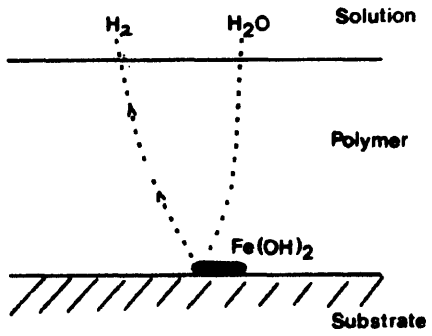

Figure 4.5 Schematic Corrosion Process in Deaerated Solution.

Water molecules diffuse into the film quickly <58> and react at suitable sites on the mild steel surface. Such sites can be under pores or "D" areas in the film, or can occur where the polymer does not adhere to the metal, or where there is an inclusion or imperfection in the film. The water molecules combine with the steel, forming the hydroxide, which is a blue/green colour. The hydrogen ions and electrons released during this process, combine with each other to form hydrogen gas. The hydrogen molecule is small and mobile and can easily escape from the film into the solution. This process will continue until sufficient corrosion product has built up to block the pore, or to fill the disbonded area under the film. At this stage, the impedance plot ceases to be due to diffusion at a pore and reverts to that of the total polymer film area. Once this situation of blocked pores, etc. is reached, new corrosion sites initiate and the process is repeated.

For aerated solutions, the proposed corrosion process is more complicated. The anodic process, equations (1) and (2) remains unchanged, but the cathodic process is now the reduction of oxygen. Two possible pathways for the reduction of oxygen are presented here, the first involving the reaction of oxygen with water and the second, the reaction between oxygen and hydrogen ions, involving a peroxide intermediate.

Pathway A <130,131>.

$$O_2 \longrightarrow O_{2ads} \qquad (4)$$

$$O_{2ads} + e^- \longrightarrow O^-_{2ads} \qquad (5)$$

$$O^-_{2ads} + H_2O \longrightarrow HO_{2ads} + OH^- \qquad (6)$$

$$HO_{2ads} + e^- \longrightarrow HO^-_2 \qquad (7)$$

$$HO^-_2 \longrightarrow OH^- + \tfrac{1}{2}O_2 \qquad (8)$$

Pathway B <129>.

$$O_2 \longrightarrow O_{2ads} \qquad (9)$$

$$O_{2ads} + e^- \longrightarrow O^-_{2ads} \qquad (10)$$

$$O^-_{2ads} + H^+ \longrightarrow HO_2 \qquad (11)$$

$$HO_2 + e^- \longrightarrow HO^-_2 \qquad (12)$$

$$HO^-_2 + H^+ \longrightarrow H_2O_2 \qquad (13)$$

$$H_2O_2 + e^- \longrightarrow OH_{ads} + OH^- \qquad (14)$$

$$OH_{ads} + e^- \longrightarrow OH^- \qquad (15)$$

Both pathways require electrons for the reduction of various intermediates, as well as a supply of water molecules (in A) and hydrogen ions (in B). It is possible that the "in-situ" mechanism may depend upon the pH of the solution at the polymer-metal interface, pathway A being preferred under neutral or alkaline conditions, when few hydrogen ions are present, pathway B if acid conditions, that is a plentiful supply of hydrogen ions, prevail.

Equations (1) and (2) can be combined with pathway A as follows;

$$Fe + H_2O \longrightarrow FeOH_{ads} + H^+ + e^- \qquad (A)$$

$$O_2 \longrightarrow O_{2ads} \qquad (B)$$

$$O_{2ads} + e^- \longrightarrow O_{2ads}^- \qquad (C)$$

$$O_{2ads} + H_2O \longrightarrow HO_{2ads} + OH^- \qquad (D)$$

$$FeOH_{ads} + H_2O \longrightarrow Fe(OH)_2 + H^+ + e^- \qquad (E)$$

$$HO_{2ads} + e^- \longrightarrow HO_2^- \qquad (F)$$

$$HO_2^- \longrightarrow OH^- + \tfrac{1}{2}O_2 \qquad (G)$$

From these equations, it can be seen that the electrons produced at steps A and E are required for steps C and F, as well as for possible combination with hydrogen ions to form hydrogen molecules. Competition for water molecules between iron and oxygen intermediates, steps D and E, is also possible.

A similar combination of equations is proposed for pathway B; (Bockris mechanism) <1298>

$$Fe + H_2O \longrightarrow FeOH_{ads} + H^+ + e^- \qquad (a)$$

$$O_2 \longrightarrow O_{2ads} \qquad (b)$$

$$O_{2ads} + e^- \longrightarrow O_{2ads}^- \qquad (c)$$

$$O_{2ads}^- + H^+ \longrightarrow HO_2 \qquad (d)$$

$$FeOH_{ads} + H_2O \longrightarrow Fe(OH)_2 + H^+ + e^- \quad (e)$$

$$HO_2 + e^- \longrightarrow HO_2^- \quad (f)$$

$$HO_2^- + H^+ \longrightarrow H_2O_2 \quad (g)$$

$$H_2O_2 + e^- \longrightarrow OH_{ads} + OH^- \quad (h)$$

$$OH_{ads} + e^- \longrightarrow OH^- \quad (i)$$

For this process, electrons are again required at several stages, in this case, c,f,h and i. As before, this competition restricts the number of electrons which are available for combination with hydrogen ions. The hydrogen ions are also required at steps d and g, thereby reducing the possibility of hydrogen molecule formation.

As the oxygen reduction process is more complex than that of hydrogen ion reduction, it will result in a slower corrosion rate in aerated solution, than in deaerated solution.

4.4 Variation of Polymer Films.

4.4.1 Film Thickness.

The effect of film thickness was examined using multicoat systems and single films of approximately the same total thickness. It has been noted <53> that the greater the number of coats, the more protective the paint layer. In the present work, it was observed that fewer rust sites initiated and that the growth of spots was much slower for the multicoat specimens. It is proposed that this is due to there being fewer pores or defects in the finished coating when a number of layers are applied.

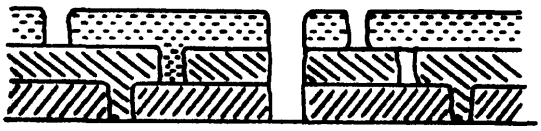

Figure 4.6 Defects in a Schematic Multicoat System.

After the application of three layers, only one of the original pores remains, the others being filled or blocked off by susequent layers. In this work, one, two and three layer specimens were made up using the vinyl polymers. Only single layer acrylic specimens were cast, as the latter polymer showed a much greater degree of protection towards the substrate, as a single layer, than the multicoated vinyl polymers, again thought to be due to the crosslinking nature of the acrylic films. As expected, the number of sites initiated decreased with the number of layers of polymer applied. The rate of growth of the underfilm corrosion sites was also much slower for the multicoated specimens than for those with only a single polymer layer. This suggests that the diffusion and permeation of water and ions is occurring more slowly through the multilayered films, there being fewer pores or defects present in these films. These results are in agreement with the generally accepted view, that a number of thin layers are more protective than one layer of the same total thickness. Whilst this is true within a particular coating type, in this case, vinyl polymers, it is not possible to assume that several coats of paint A will be more protective than one coat of paint B, as was shown by comparing the vinyl and acrylic polymers.

4.4.2 Film Capacitance and Water Uptake.

The straight line relationship between the reciprocal of film thickness and the capacitance of the film on initial immersion, has been previously observed <128>. Thus on the assumption that there is no swelling of the film, then the slope of a plot of capacitance against reciprocal of film thickness, will have a slope equal to that of the dielectric constant of the polymer. It can be seen from figure 3.68 (page 150), that straight line plots were obtained for both the vinyl and acrylic polymers, but that the slopes of the lines were different, showing that the dielectric constants of the polymers also differed. The dielectric constant for the vinyls was of a higher value than that measured for the acrylic films and this can be ascribed to the more hydrophillic nature of the vinyl polymer, the chains exhibiting a greater degree of polarity than would occur in the acrylic films. Therefore, the dielectric constant (which is affected by the polarity of the molecule) is higher for the vinyl polymers.

The capacitive data can also be used to estimate the uptake of water into the film. The calculations on page 152 show that some films appear to absorb a greater quantity of water than others. This must be related to the thickness and structure of the films. When a specimen is initially immersed in the test solution, it is likely that there is a greater uptake of water within the first few minutes. This is the "fast change" described by Maitland and Mayne <58>. Evidence to support this theory is obtained from the comparison of the "dry" capacitance values, with those obtained on the initial immersion of the specimen. The capacitance in aqueous solution was found to be higher, suggesting that there had been a change in the dielectric constant of the polymer, which

was probably caused by the uptake of water into the film. On prolonged immersion, the capacitance increased slowly and it is likely that this is the "slow change", that is, the exchange of ions within the film, accompanied by the uptake of further quantities of water. It is possible that the ions entering the film, are surrounded by a "shell" of water molecules <62> and small changes in the measured capacitance values may be recorded as these ions exchange for others originally associated with the polymer, causing small amounts of water to become temporarily "free" within the polymer.

The film structure and its degree of crosslinking are important in that they act as a barrier between the substrate and the environment, in this case, the test solution. The acrylic films exhibited only a slight increase in capacitance (and therefore water uptake) over the test periods, whilst the vinyl polymers showed a much greater absorption of water. The acrylic films, being chemically crosslinked, are likely to contain fewer defects and pores than the vinyl coatings. Very few underfilm corrosion sites were observed on the acrylic specimens and they generally produced "capacitive" type impedance plots, with unstable rest potentials, again showing that the acrylic films were the least defective of the polymer types examined. However, they do produce brittle films which can be easily damaged mechanically and they therefore have some practical limitations. The vinyl polymers, whilst providing a lesser degree of protection are more flexible, hence they offer a practical advantage.

4.4.3 Physical Properties of the Polymers.

In an attempt to determine whether the relative protective properties of the polymers under study were due to the presence or absence of a particular group, or groups, on the polymer backbones, infra-red spectroscopy was carried out to try and identify the groups present. The results showed one group to be missing from two of the vinyls; that is an -OH group was present only in the VROH and VAGH. The acrylic films produced similar traces, not surprising when it is considered that they both contained similar compounds, varying mainly in chain length, a feature which is not easily observed using this technique. Although the vinyl and acrylic infra-red traces showed some small differences, this technique provided no data to account for their different protective abilities.

A second physical property, the glass transition temperatures of the polymers was also examined, this data showed a greater number of differences between the polymers.

The acrylic films appear to contain only one glass transition temperature, whilst the vinyl polymers, which contain a fewer number of constituent compounds, show the presence of two transitions. This apparent anomaly arises because of the structure of the polymers. If a polymer is made up from two constituents co-polymerised together, the resulting polymer may vary in structure. Under particular conditions of manufacture, the monomers may polymerise either with themselves, or with the second monomer. This results in the formation of compounds such as those illustrated overleaf.

AAABBBAAABBB ABBABAABABAB

Figure 4.7 Two possible co-polymers.

Each of these compounds contains the same number of A and B monomers, but in a different distribution and it is the sequence of the monomers in the polymer, that determines some of the characteristics of the cured film. This difference in polymer structure, can be detected using the Differential Thermal Analysis (D.T.A.) technique. Where the blocks of the monomers are small and evenly distributed throughout the polymer, then only one glass transition is observed, corresponding to the combined effects of the polymer constituents. Where there are large blocks of monomers polymerised together, then more than one glass transition may be observed, corresponding to the Tg's of the monomer blocks. The presence of two glass transition temperatures was noted by Kumins and Roteman <37> who suggested that the two Tg's observed for VYHH in their experiments, corresponded to the glass transitions of vinyl chloride and vinyl acetate in the polymer. The lower Tg being attributed to the oscillation and movement of the acetate groups and the upper Tg caused by mobility of the main polymer chains. For the vinyl polymers studied in this work, two transitions were observed and therefore it was assumed that the distribution of vinyl chloride and vinyl acetate is such that blocks of each monomer exist in the polymer. No third Tg was observed which could correspond to the maleic acid added to some of the polymers. This was probably due to the small quantities added and to their distribution through the polymer. The Tg observed at 29/30^{o}C, corresponds to the Tg of vinyl acetate, as previously reported <37>. VROH does not contain vinyl aetate and shows no transition at this temperature. However, all the vinyl polymers contain vinyl chloride and

show a second Tg at 64°C (67°C for VYHH). This Tg could, theoretically be either that of vinyl chloride, or of the other constituent compounds. It is known that whilst the Tg of vinyl chloride is generally accepted to be 77°C <37>, the temperature at which the monomer is polymerised can affect the Tg of the polymer <55> and this could account for the Tg of 64-67 C measured for the resins. The Tg of the films was much lower, 55 °C, probably due to the plasticising effect of the retained solvents in the films.

Since the acrylic films exhibit only one glass transition temperature, it is possible to assume a more even and random distribution of the monomers through the polymers. The polymer chains are crosslinked into a network by the crosslinking agent Cymel 301, which may contribute to the random "order" of the groups.

The presence of retained solvent and water in the films, may also be detected using the D.T.A. method, as they appear as temporary depressions on the graph. When the sample is heated to above its Tg, the solvent, which may have been trapped in the resin during its manufacture, or in the film during casting and curing, is released. When a second run is carried out on the same specimen, the depression on the graph is no longer observed, confirming the loss of the solvent. The identity of the retained solvent may be deduced by comparing the boiling point of the released solvent, from the depression on the graph, with those of the polymer solution constituents. Retained solvent can also have a plasticising effect upon polymer films, that is a lowering of their Tg. This effect can also be observed with the D.T.A. technique. The glass transition temperatures calculated from subsequent runs on the same specimen, showed the Tg of the second run to be higher.

From these experiments, it can be observed that there is very little physical evidence to account for the different degrees of corrosion protection conferred by the two polymer types. It is proposed therefore, that the determining factor is the number of defects in a film, with some polymers producing more defective films than others. The variation in the number of defects or pores in the film has been attributed in this work, to the degree of crosslinking of the polymer chains, some areas being less crosslinked than others. Such areas have been termed "D" areas <36>. For non-chemically crosslinked films, areas of defect or weakness cannot be called "D" areas, but such regions could contain a higher proportion of hydrophillic groups than other areas of the film and such regions would allow the easier conduction of water and ions through the film. When a second layer is applied, several of the original defects may be covered, resulting in the formation of a more protective film.

The vinyl polymers posess such an un-crosslinked structure and contain hydrophillic groups, for example acetate, around which water molecules could cluster, thereby attracting further water molecules and ions and thus aiding their entry into the film.

The validity of the theory that it is the number of defects in a film, caused by the polymer structure, was tested using an agar gel. Agar is known to have a very open structure and to absorb water into itself. It was expected therefore, to behave as a very defective coating. This was indeed the case, the film allowed general corrosion to occur over the metal surface, in contrast to the "spot" corrosion pattern observed with the vinyl and acrylic polymers. When the gel was removed, it was noted that the surface of the steel was bluish in

colour, suggesting that the steel was in the Fe^{2+} state. It is probable that the Fe^{2+} to Fe^{3+} conversion, producing the characteristic orange rust, occurs at the metal-agar interface. The presence of absorbed Fe^{3+} compounds in the gel, supported this theory. Build up of the rust compounds in the gel would then account for the increase in the solution resistance observed after some time of immersion. The initial decrease in the solution resistance is caused by the absorption of water and ions into the inherently open structure of the agar. Once these species reached the substrate, the corrosion process began. For agar, this was about thirty-six hours after immersion, as compared with several days or weeks for the vinyl and acrylic polymers. The presence of water in the gel was confirmed by the increase in the capacitance values obtained from the diffusional shaped impedance plots. Although a general corrosion process was occurring on the steel surface, the impedance response reflected only the permeation of the solution into the agar. No part of the impedance plot could be attributed to the corrosion process.

4.5 Artificial Defects in Films.

Diffusional impedance plots observed during the agar experiments are thought to be due to solution transport processes within the pores of the gel. To examine the further effects of large pores, an artificial defect was created in an otherwise intact film. The exposed metal began to corrode, which was reflected in the rapid initial decrease of the rest potential (from -119mV to -540mV S.C.E.) when the defect was created and the potential continued to decrease with time. The capacitance data obtained showed that for this experiment the corrosion process impedance was being monitored since the capacitance was that of

an electrochemical double layer on the metal. Prior to the creation of the pinhole, the capacitance had been that of the film. It is likely that the large size of the pinhole (1mm diameter) allowed the corrosion process impedance to be monitored, rather than that of diffusion as observed with the agar coating. With defective films, only the corrosion process impedance was monitored with time, i.e. the impedance technique records only the low resistive path. The rest potential also reflects only the corrosion process and there is no response from the polymer film.

The occurrence of a natural defect or pore in a film and the passage of solute through the defect to the substrate, may become apparent after a period of immersion. This would be observed as a change in the impedance plot shape and also in the parameters derived from it. This may result in a falsely high estimate of the capacitance. Thus for a combined diffusional process and film effect, this may give rise to data as shown overleaf. (Figs 4·8-4·10)

In the latter two diagrams, the diffusion process of the plot will distort the higher frequency or capacity data and will give rise to an excessively high value for the film capacitance. An increase in the rest potential of the specimen towards more noble values, often occurs simultaneously with this change in apparent diffusion. This effect was observed with VAGH-G after three days immersion, for VAGH-N after one day and for VROH-1 after ten, sixteen and twenty-two days immersion. It is suggested that this type of impedance behaviour appears as pores form and later fill with corrosion product.

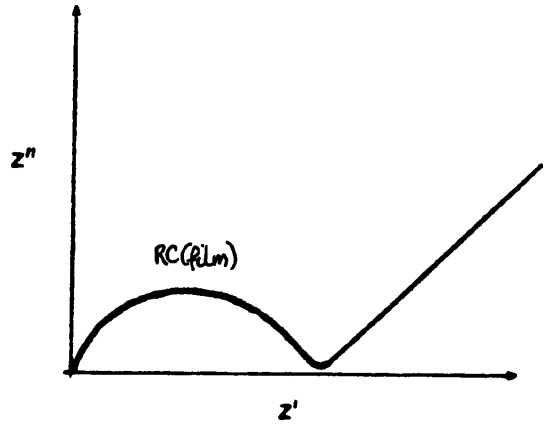

Figure 4.8 No diffusion influence.

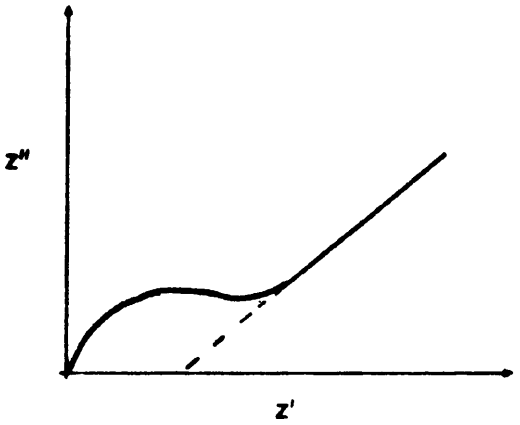

Figure 4.9 Slight diffusion influence.

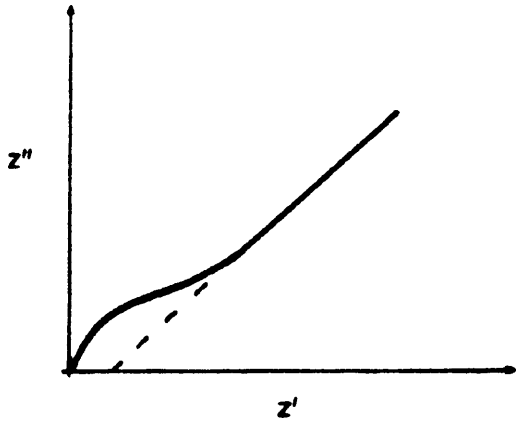

Figure 4.10 Large diffusion influence.

When the anodic sites becomes blocked by the build up of corrosion products, the impedance plot reverts to its original behaviour, that is, for the VAGH specimens, a semicircular plot. Such changes in the plot shape are also shown by VROH-BN. After fifteen minutes in deaerated solution, a pore or some other defect becomes apparent. The solution resistance decreased and the capacitance increased, indicating that a diffusion process was occurring through the film. The subsequent increase in the solution resistance to its original value, implied that the defect had become plugged, probably with corrosion products. It was noted that the small black spots which initiated, did not appear to "grow" at a uniform rate, the periods of growth that occurred followed a decrease in the solution resistance or a decrease in the rest potential. The cyclic nature of the process was indicated by the VROH-BN specimen. The capacitance increased when a diffusional plot was obtained and then decreased back to that of the polymer as the solution resistance decreased. With time, the capacitance showed an increase and therefore an uptake of water into the film. After fifteen days of immersion, the solution resistance decreased and the capacitance again increased, indicating the cyclic nature of the process of solution entry into the polymer.

4.6 Substrate Effects.

4.6.1 Substrate Preparation.

In addition to the effects of the solution and polymer parameters, substrate changes also influence the impedance response and these will now be considered. Firstly, the effect of changing the method of preparation of the substrate, showed that a pickled specimen allowed a

greater amount of underfilm corrosion to occur than did a polished specimen. This is probably due to citrate ions remaining on the metal surface after the pickling process. These ions then act as an underfilm contaminant when the specimen is immersed in solution. The contaminants can presumably exert an osmotic pull on the water molecules, which are drawn through any defects present and this decreases the time for the corrosion sites to initiate on the metal substrate. The result is a fairly uniform distribution of small spots over the surface and these increase in size with time.

In contrast, a polished specimen has relatively little underfilm contamination, apart from dust particles, and substantially fewer corrosion sites were formed after immersion in solution. The sites showed a characteristic "ring pattern", for example the photograph of VYHH-GN on page 91. This suggests that an anodic site initiates below an area of weakness, or at a defect in the film. The defect must be of a reasonable size for the corrosion process to continue, otherwise it becomes blocked by the corrosion products. The cathodic process occurs in a ring area around the anodic site and no anodic processes take place in this area. Further sites initiate some distance away. These may be either further ring patterns or general underfilm spot corrosion with no definite pattern. Only the vinyl polymers showed the ring pattern; the acrylic films generally allowed one or two spot sites to initiate after long periods of immersion. After some months, filiform corrosion was observed on several acrylic specimens, as shown in the photograph on page 136. Filiform corrosion usually initiates only under certain conditions of humidity and temperature and its occurrence under completely immersed conditions has not been previously recorded.

The vinyl polymers exhibited different corrosion behaviour towards the two methods of substrate preparation. Each showed reasonable protection towards a polished specimen, but their responses varied towards a pickled specimen. VMCH showed capacitive type plots and from the visual results, appeared to provide the greatest protection to the pickled substrate. VYHH and VAGH both showed lesser degrees of protection, with a greater variety of impedance plot shapes. VROH exhibited semicircular plots from its immersion and was sufficiently unprotective as to allow the build up of corrosion products to such an extent that the film ruptured.

The choice of the preparation method for the substrate has been shown to have an important effect on the protective abilities of the vinyl polymers. In the case of VROH, it was especially obvious and allowed many more sites to initiate and those spots to increase in size to a much greater extent on the pickled specimen.

4.6.2 Effect of No Substrate.

The effect on the impedance response of removing the substrate, was considered using detached vinyl films. The impedance measurements were made using the new electrode arrangement, with the reference and working electrodes placed in the same arm of the apparatus, the auxilliary electrode in the other arm. The detached VROH film exhibited a lower solution resistance than either VMCH or VYHH and this may be explained as thin areas of film or as defects, such as conductive phases, within the film. Both of these would be "measured" by the impedance technique as being the easiest path through which the perturbing signal could pass and be observed as lower values of the solution resistance.

A thin area of film can be represented in terms of an equivalent circuit, as a "leaky" capacitor; that is a capacitor with a large resistor in parallel to it. The larger the defect in the film, or the thinner the film at that area, the smaller the value of the resistor to be considered and therefore, the more "leaky" the capacitor. This results in the solution resistance decreasing and in the impedance plot changing from a straight capacitance line to a more semicircular shape. These changes in the impedance plot may also be attributed to differences within the polymer itself, assuming it to be of a uniform thickness. Kendig and Leidheiser <25> proposed in figure 1.1, that a polymer contains areas of conductive and dielectric phases. The conductive phases may be represented by resistors and the dielectric phases by capacitors. The impedance response of a film consisting of this type of polymer structure, would be the same as for a film of uneven thickness.

After the creation of a pinhole in the detached films, it was observed that orange compounds (presumably the iron corrosion products) passed from the arm containing the working electrode, into the other, down a concentration gradient. The ease of passage of the solution and ions between the arms, was reflected in the impedance data obtained from these experiments. The solution resistance of the system fell by several orders of magnitude when the pinhole was created. This new, low value of 5 to 40 ohm cm^{-2}, may be considered to be the true solution resistance of the sodium chloride solution, which had previously been masked by the large value of the polymer film resistance. It has been proposed <128> that for an intact film, the following equivalent circuit may be applicable.

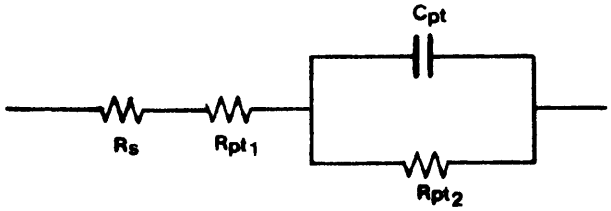

Figure 4.11 Equivalent circuit of an immersed polymer film.

The polymer and solution resistances are considered to be separate entities and can be differentiated when a pinhole is created in a film. Prior to the pinhole, the solution resistance and the polymer film resistance in series, are observed as the "solution resistance". Some function of the polymer film is also observed in parallel with the film capacitance and is taken, in this work, to be the ionic resistance of the film. When the pinhole is created, only the true resistance of the solution is observed, the more resistive path of the polymer being undetectable by the impedance technique and therefore no longer represented on the impedance plot.

The shape of the measured inpedance plot was also different after the creation of a pinhole. Previously, capacitive or semicircular plots had been observed, but on production of the defect a plot usually associated with diffusion processes was obtained. From the capacitance values, it is probable that the impedance technique was measuring the transport of water and ions through the newly created pinhole only and that again, any response of the film itself is no longer measured.

When detached films were exposed to conditions of changing temperature, variations in the rest potential and the film capacitance occurred. The solution resistance remained constant, indicating the continued integrity of the films. Changes in the rest potential occurred at about the upper Tg of the vinyl films (about 55°C). This suggests that there may be some contribution to the rest potential by the film itself and that this contribution changes when the Tg of the film is reached, thus causing a change in the measured rest potential. This may be explained as follows. On reaching the Tg, the polymer chains of the film can move more easily and the increased temperature may also lead to an increase in the free energy of the films. This in turn may allow for greater movement of the polymer chains <37>. The changes in the oscillation, vibration and interchain bonding of the backbones, may be reflected in the value of the rest potential. It is possible that the polymer film may contribute to the overall rest potential of the specimen, as it has been suggested <55> that absorption of acetate groups onto metal, affects the surface potential of the metal. The extent of the effect, depends on the orientation of the dipoles of the molecules, as has been reported elsewhere <7>. It was observed in the experiments reported here, that the capacitance of the films, changed with variations in the rest potential of the specimen and this may be the result of increased water absorption into the film, facillitated by the easier movement of the polymer chains at higher temperatures. Water may form hydrogen bonds with the side groups on the polymer chains, such as acetate or carboxyl, breaking the interchain hydrogen bonds in the process. This would leave "holes" in the polymer network, resulting in the easier and faster movement of the chains. As the number of "holes" and the chain movement increased, so the diffusion of water and ions into the film would be made easier. As the quantity of water in the film

increased, this would cause an increase in the dielectric of the film and so lead to an increase in the measured film capacitance.

An examination of the constituents of VMCH and VROH, suggest that VMCH is possibly less mobile below its Tg than VROH, since the former contains acetate side groups on the backbone, which the latter does not. These acetate groups, together with the carboxyl groups also present in his polymer, may restrict the chain movements by inter-chain hydrogen bonding and the lack of easy movement caused by their physical shape and size. It is possible (as noted earlier) that the acetate groups may have an effect upon the substrate and may assist, in some way, in the bonding of the polymer to the metal. This would therefore, result in a more protective film. VROH, which does not have these groups, did not appear to be as protective as the VMCH polymer, although the lack of bulky sidegroups on the backbone, may allow VROH a greater degree of flexibility in the cured state.

4.7 Summary.

Arising from this discussion are a number of important points. Firstly, that the impedance technique is able to distinguish between a protective and a non-protective film. The ability of the technique to reveal defects within a film, is useful in studying the progressive breakdown of the coating. It was shown that changes in the specimen apperance, the impedance plot shape and its resultant parameters and the specimen rest potential, occurred together in many cases, allowing physical processes to be related to the recorded data. The impedance technique also proved useful in the examination of the capacitance and

resistance of dry films and thereby provided valuable data concerning both the rate and amount of water uptake into polymer films. The electronic conductance of polymer films was also observed using this new technique.

It was unfortunate that the impedance technique was unable to detect corrosion processes occurring underneath an intact film, however, it was noted that the corrosion which did occur, was confined to a few small spots or to filiform type events and was not extensive. When the corrosion sites were active for some time, the film was disturbed and this was reflected in the impedance response.

Secondly, the structure of the polymer appears to affect the protective abilities of the coating. It was proposed that it is the number of defects in the film that determines the time before corrosion sites initiate and also the "pattern" of the corrosion products under the film, together with their rate of growth. The three types of coating examined here, differed in their responses to each of the above, the acrylic films being the most protective, agar the least protective. Differences between the four vinyl polymers were observed when different methods of substrate preparation were used.

The protective ability of the film is governed by the number of inherent defects. These defects can be related to the degree of crosslinking of the polymers. Chemically crosslinked polymers such as the acrylic types contain very few defects and were designed by I.C.I. to give a hard, resistant finish. The vinyl polymers were linked by interchain hydrogen bonding and the structure of the agar molecule is such that it readily absorbs water into itself and is therefore not a

protective coating.

The number of coats applied has also been shown to be important, as it also affects the number of defects within the finished film. Several thin layers afford greater protection than one thick layer, as defects in lower layers are covered by subsequent layers, exposing fewer defects to the environment <53>.

Finally, it was shown that the rest potential of the specimen can provide valuable data concerning its corrosion state. Its value changes with events on the specimen and has been observed to be linked to the shape of the impedance plot. It is however, subject to the same limitations as the impedance technique with respect to intact films, but nevertheless, it can give a quick indication of the corrosion state of a specimen.

Chapter 5. Conclusions and Recommendations.

5.1 Conclusions.

1) The impedance technique is useful in the examination of defects within a film and can differentiate between defective and non-defective films.

2) The impedance technique cannot detect the presence of corrosion which is occurring under an intact film.

3) The number of defects within a film, determines its protective ability. The number of defects is affected by the degree and type of crosslinking of the polymer chains and the number of coats applied.

4) The method of substrate preparation affects the protective ability of the vinyl polymers.

5) In the absence of oxygen, corrosion processes can continue by using hydrogen ion reduction as the cathodic process.

6) The specimen rest potential can be indicative of the corrosion state of the specimen.

7) The impedance technique can be used to provide information concerning the dry capacitance and resistance of a film, using a new experimental method.

8) Information can also be obtained about the electronic conductance of the polymers, which is related to their structures.

5.2 Recommendations for Further Work.

1) Measure the electronic conductance of polymers of different constituents and of various thicknesses.

2) Change the ion concentration of the external solution; e.g. deionised water, concentrated solution, etc.

3) Place solutions of different osmotic pressure in the arms of the detached film apparatus to study water transport.

4) Monitor the effect of deaerated solution on a number of different polymers.

References

1. Gillies,G.L., Aus. Corr. Eng. 19 No.6, 27 (1975).

2. Biddle,C.J., Aus. Corr Eng. 20 No.4 9 (1976).

3. Bell,S.H., J.O.C.C.A. 38 595 (1955).

4. Wranglen,G., Institut fur Metallskydd (1972).

5. Lapasin,R., Longo,V. and Torriano,G., J.O.C.C.A. 58 286 (1975).

6. Caldwell,D. and Furguson,W.D., J.O.C.C.A. 60 93 (1977).

7. Croll,J.S., J. Coatings Tech., 51 No.648 64 (1979).

8. Katz,R. and Munk,B.F., J.O.C.C.A. 52 518 (1969).

9. Berger,D.M., Metal Finishing, April (1978).

10. Bullett,T.R. and Rudram,A.T.S., J.O.C.C.A. 44 787 (1961).

11. Biddle,G.J., Aus. Corr. Eng. 18 No.5 5 (1974).

12. Khullar,M., J.O.C.C.A., 51 (1968).

13. Tomshov,N.P., Mikhailovskii,Y.N., and Leonov,V.V., Corrosion, 20 125 (1964).

14. Mayne,J.E.O., J.O.C.C.A., 32 481 (1949).

15. Cherry,B.W., Aus. Corr. Eng. 18 No.10, 23 (1974).

16. Michaels,A.S., Official Digest, June (1965).

17. Mayne,J.E.O., Br. Corr. J. 5 106 (1970).

18. Bacon,R.C., Smith,J.J. and Rugg, F.M., Ind. and Chem. 40 161 (1948).

19. Anderton,W.A., J.O.C.C.A., 53 181 (1970).

20. Brasher,D.M. and Kingsbury,A.H., J. App. Chem. 4 62 (1954).

21. Toushant,R.E. and Leidheiser,H., Corrosion, 28 435 (1972).

22. Gentles,J.K., J.O.C.C.A., 46 850 (1963).

23. Beckman,A.O., Badger,R.M., Gullekoon,E.E. and Stevenson,D.P., Ind. and Eng. Chem. 33 985 (1941).

24. Craig,B.D. and Olson,D.L., Corrosion, 32 No.8 (1976).

25. Kendig,M.W. and Leidheiser,H., J. Electrochem. Soc. 123 982 (1976).

26. Miller,R.N., Mat. Prot. 7 No.35 (1968).

27. O'Brien,H.C., Ind. and Eng. Chem. 58 45 (1966).

28. Perera,D.Y. and Heertjes,P.M., J.O.C.C.A., 54 395 (1971).

29. Zimm,B.H. and Lundberg,J.L., J. Phys. Chem., 60 425 (1956).

30. Perera,D.Y. and Selier,P., Prog. in org. coatings., 1 57 (1973).

31. Wolock,I. and Harris,B.L., Ind. and Eng. Chem., 42 134 (1950).

32. Haagen,H. and Funke,W., J.O.C.C.A., 58 359 (1975).

33. Guruviah,S., J.O.C.C.A., 8 669 (1970).

34. Kumins,C.A., Roteman,J. and Rolle,C.J., J. Polym. Sci., 57 541 (1963).

35. Perera,D.Y. and Heertjes,P.M., J.O.C.C.A., 54 313 (1971).

36. Kinsella,E. and Mayne,J.E.O., Br. Polym. J., 1 173 (1969).

37. Kumins,C.A. and Roteman,J., J. Polym. Sci., 55 683 (1961).

38. Kumins,C.A.and Roteman,J., J.Polym. Sci., 55 699 (1961).

39. Perera,D.Y. and Heertjes,P.M., J.O.C.C.A., 54 589 (1971).

40. Holtzman,K.A., J. Paint Technol. 43 47 (1971).

41. Funke,W. and Haagen,H., Ind. and Eng. Chem., 17 March (1978).

42. Perera,D.Y. and Heertjes,P.M., J.O.C.C.A., 54 774 (1971).

43. Kittelberger,W.W. and Elm,A.C., Ind. and Eng. Chem., 38 265 (1946).

44. Brasher,D.M. and Nurse,T.J., J. App. Chem., 9 96 (1959).

45. Perera,D.Y. and Heertjes,P.M., J.O.C.C.A., 54 546 (1971).

46. Vittal,R.R and Yaseen,M., Anti-corr. (Pigment + resin Tech.) March (1978).

47. Murray,J.D., J.O.C.C.A., 56 210 (1973).

48. Kittelberger,W.W. and Elm,A.C., Ind. and Eng. Chem., 39 876 (1947).

49. Mayne,J.E.O., J.O.C.C.A., 33 210 (1950).

50. Yasseen,M. and Funke,W., J.O.C.C.A., 61 284 (1978).

51. Kinsella,E., Ph.D. Thesis, Cambridge Univ. (1967).

52. Kinsella,E., Mayne,J.E.O. and Scantlebury,J.D., Br. Polym. J., 3 41 (1971).

53. Mayne,J.E.O. and Mills,D.J., J.O.C.C.A., 58 155 (1975).

54. Mayne,J.E.O. and Scantlebury,J.D., Br. Polym. J., 2 240 (1970).

55. Kumins,C.A., J. Coating Tech. 52 40 (1980)

56. Ulfvarson,U. and Khullar,M., J.O.C.C.A., 54 604 (1971).

57. Cherry,B.W. and Mayne,J.E.O., Official Digest, 37 13 (1965).

58. Maitland,C.C and Mayne,J.E.O., Official Digest, 34 922 (1962).

59. Glass,A.L. and Smith,J., J. Paint Technol., 38 203 (1966).

60. Glass,A.L. and Smith,J., J. Paint Technol., 39 490 (1967).

61. Kittelberger,W.W. and Elm,A.C., Ind. and Eng. Chem., 44 326(1952).

62. Yasuda,H., Lamaze,C.E. and Ikenberry,L.D., Die Makromolekulare Chemie, 118 19 (1968).

63. Murray,J.D., J.O.C.C.A., 56 507 (1973).

64. Drabble,J.R., Aus. Eng. Chem., 18 No.6., 5 (1974).

65. Whitely,P., Rothwell,G.W. and Kennedy,J., J.O.C.C.A., 58 200 (1975).

66. Sato,K., Prog. in Organic Coatings, 8 1 (1980).

67. Johnson,W., Ph.D. thesis, Victoria Universtiy of Manchester (1980).

68. Walker,P., Official Digest., December (1975).

69. Bullett,T.R., J.O.C.C.A., 46 441 (1963).

70. Joint Services Committee on Paints and Varnishes., J.O.C.C.A., 46 273 (1963).

71. Sickfield,J., J.O.C.C.A., 61 292 (1978).

72. Smelt,D., Ph.D. thesis, University of Oxford (1980).

73. Stern,M. and Geary,A., J. Electrochem. Soc., 104 56 (1957).

74. Wolstenholme,J., Corr. Sci., 13 521 (1973).

75. Leidheiser,H., Prog. in Org. Coatings., 7 79 (1979).

76. Scantlebury,J.D. and Ho,K.N., J.O.C.C.A. 62 89 (1979)

77. Devay,J., Janaszik,F., Mezaros,L. and Horkay,F., Acta Chimica Academiae Scientiarum Hungaricae. 74 199 (1972).

78. Yamamoto,T., Amako,H. and Oyabu,Y., Shikizai Kyokaishi 48 352 (1975).

79. Vetere,V., Rosados,E. and Carbonari,R., J.O.C.C.A. 61 419 (1978).

80. Mikhailovskii,Y.N., Leonov,V.V. and Tomashov,N.D., Korr Met e Spanov. N.L.L. Trans. P.291. Metallurgizdat Moscow. (1975).

81. Rozenfel'd,I.L., Oshe,E.K. and Akimov,A.G., Korr Met e Spanov. N.L.L. Trans. P.302.

82. Andrade,C. and Gonzalez,J.A., Werkstoffe and Korrosion. 25 515 (1978).

83. Houston society for coatings technology., J. Paint Tech. 47 57 (1975).

84. Randles,J.E.B., Diss. Faraday Soc. 1 11 (1947).

85. Dawson,J.L., Callow,L.M. and Richardson,J.A., 187th Event of European Fed. of Chem Eng. City University, London. September 1977.

86. Epelboin,I., Keddam,M. and Takenouti,H., J. App. Chem. 2 71 (1972).

87. Warburg,E., Ann Physik. 7 493 (1899).

88. Warburg,E., Ann Physik. 9 125 (1901).

89. Hladky,K., Callow,L.M. and Dawson,J.L., Br. Corr. J. 15 20 (1980).

90. Cole,K.S. and Cole,R.H., J. Chem. Phys. 9 341 (1941).

91. De Levie,R., Electrochimica Acta. 10 395 (1965).

92. Franceschetti,D.R. and Macdonald,J.R., J. Electroanal. Chem. 100 583 (1979).

93. Macdonald,J.R., J.Electroanal. Chem. 47 182 (1973).

94. De Levie,R. and Popisil,L., J. Electroanal. Chem. 22 277 (1969).

95. Dickenson,T. and Whitfield,R., Electrochimica Acta. 22 385 (1977).

96. Callow,L.M., Richardson,J.A. and Dawson,J.L., Br. Corr. J. 11 132 (1976).

97. Sluyters,J.H., Rev. Trav. Chem. 79 1092 (1960).

98. Sluyters,J.H. and Oomen,J.J.C., Rev. Trav. Chem. 79 1011 (1960).

99. Rehbach,M. and Sluyters,J.H., Rev. Trav. Chem. 80 469 (1961).

100. Rehbach,M. and Sluyters,J.H., Rev. Trav. Chem. 81 301 (1962).

101. Sluyter Rehbach,M. and Sluyters,J.H., J. Electroanal. Chem. 4 1 (1969).

102. Epelboin,I., Keddam,M. and Takenouti,H., J. App. Chem. 2 71 (1972).

103. John,D.G. and Dawson,J.L., Korrosionscentralen. No.3. April 1979.

104. Sluyters,J.H., Rev. Trav. Chem. 82 100 (1963).

105. John,D.G., Ph.D Thesis. Victoria University of Manchester. (1980).

106. Bottomley,P.D.W., Victoria University of Manchester. (1981).

107. Hladky,K., Ph.D. thesis, Victoria University of Manchester. (1978).

108. Epelboin,I. and Keddam,M., J. Electrochem. Soc. 117 1052 (1970).

109. Armstrong,R.D., Bell,M.F. and Metcalfe,A.A., J. Electroanal. Chem. 77 287 (1977).

110. Callow,L.M., Richardson,J.A. and Dawson, J.L., Br. Corr. J. 11 123 (1976).

111. Scantlebury,J.D., Ho,K.N. and Eden, D.A., A.S.T.M. Symposium. "Progress in electrochem. testing". San Fransisco. May 1979.

112. Ho,K.N., Ph.D Thesis. Victoria University of Manchester (1978).

113. Mansfeld,F., Kendig,M. and Tsai,S., 8th International Congress on Metallic Corrosion. Mainz. September 1981.

114. Sussex,G.A.M. and Scantlebury,J.D., 8th international Congress on Metallic Corrosion. Mainz. September 1981.

115. Callow,L.M. and Scantlebury,J.D., J.O.C.C.A. 64 83 (1981).

116. Callow,L.M. and Scantlebury,J.D., J.O.C.C.A. 64 119 (1981).

117. Callow,L.M. and Scantlebury,J.D., J.O.C.C.A. 65 43 (1981).

118. Lomas,J.P., Callow,L.M., Scantlebury,J.D. and Sussex,G.A.M., presented at 150th meeting of The Electrochemical Society. Denver, Col. October 1981.

119. B.S. 1449

120. Union Carbide, technical memorandum.

121. Bell,S.H., J.O.C.C.A. 35 373 (1952).

122. Chemical Rubber Co. handbook. 58th edition. (1978). Pub. McGraw-Hill.

123. Uchida,T., I.R. Spectroscopy of resins in paint. Japan Paint Inspecting Assoc. (1975).

124. Monk,C.J.H. and Wright,T.A., J.O.C.C.A. 48 520 (1965).

125. Smothers,W.J. and Chiang,Y., D.T.A. Theory and practise. Chem. Rubber Co. (1958). Pub. McGraw-Hill.

126. Kirk,R.E. and Othmer,D.F. (Eds.), Ency. Chem. Tech. 1 232. Interscience Ency. Inc. New York.

127. Reding,F.P., Walter,E.R. and Welch,F.J., J.Polymer Sci. 56 225 (1962).

128. Lomas,J.P., M.Sc dissertation. Victoria University of Manchester 1979.

129. Bockris,J.O'M. and Srinivasan,S., Fuel cells; their electrochemistry. Pub. McGraw-Hill. 1969. Also Bockris, J.O'M., Drazic, D. and Despic, A.R., Electrochem. Acta 4 325 (1961).

130. Mrha,J., Coll. Czech. Chem. Comm. 32 708 (1967).

131. Mrha,J., Coll. Czech. Chem. Comm. 33 583 (1968).

129B. Bent, W.G., Trans. Electrochem. Soc. 83 253 (1943).

Appendix 1.

D.T.A. traces of the vinylites.

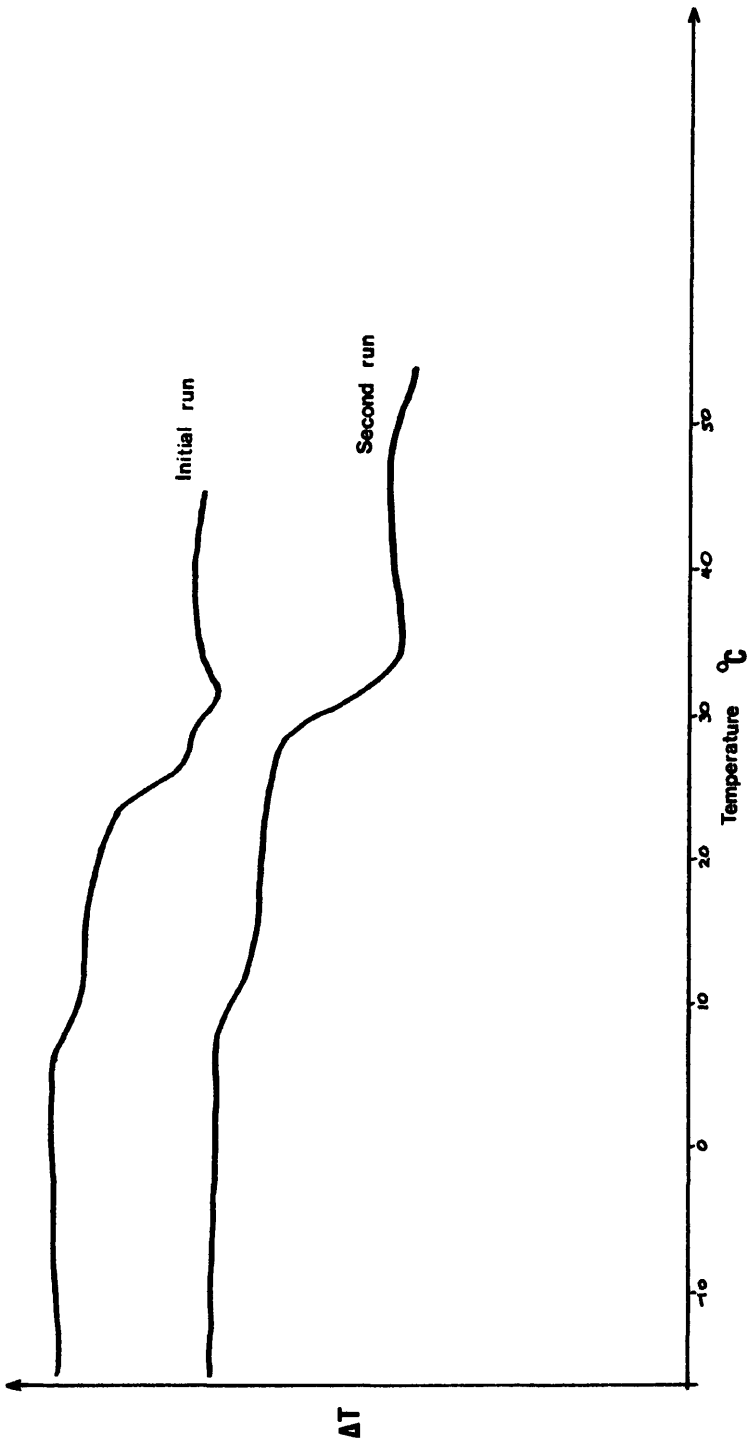

D.T.A trace for VMCH.

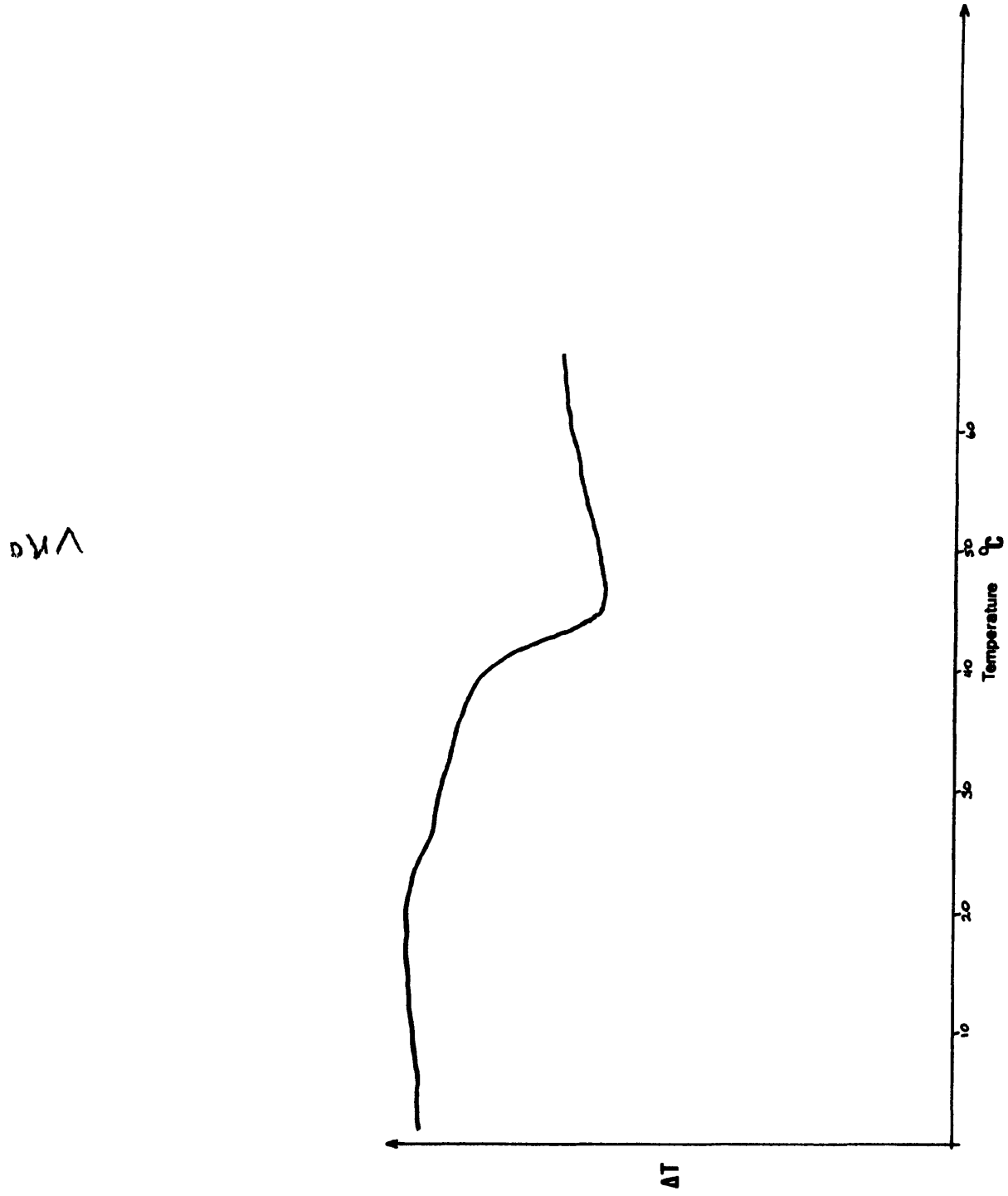

D.T.A trace for VROH.

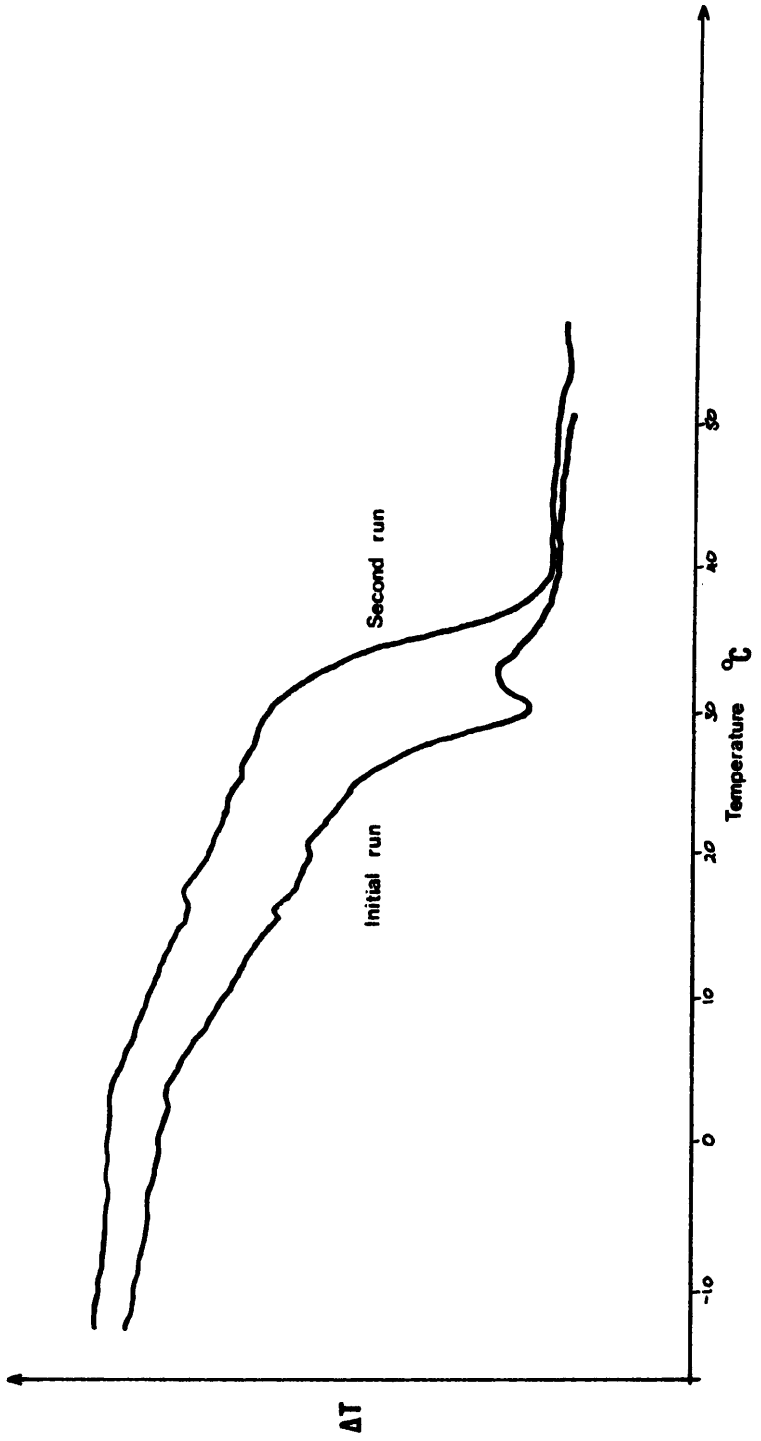

D.T.A trace for VAGH.

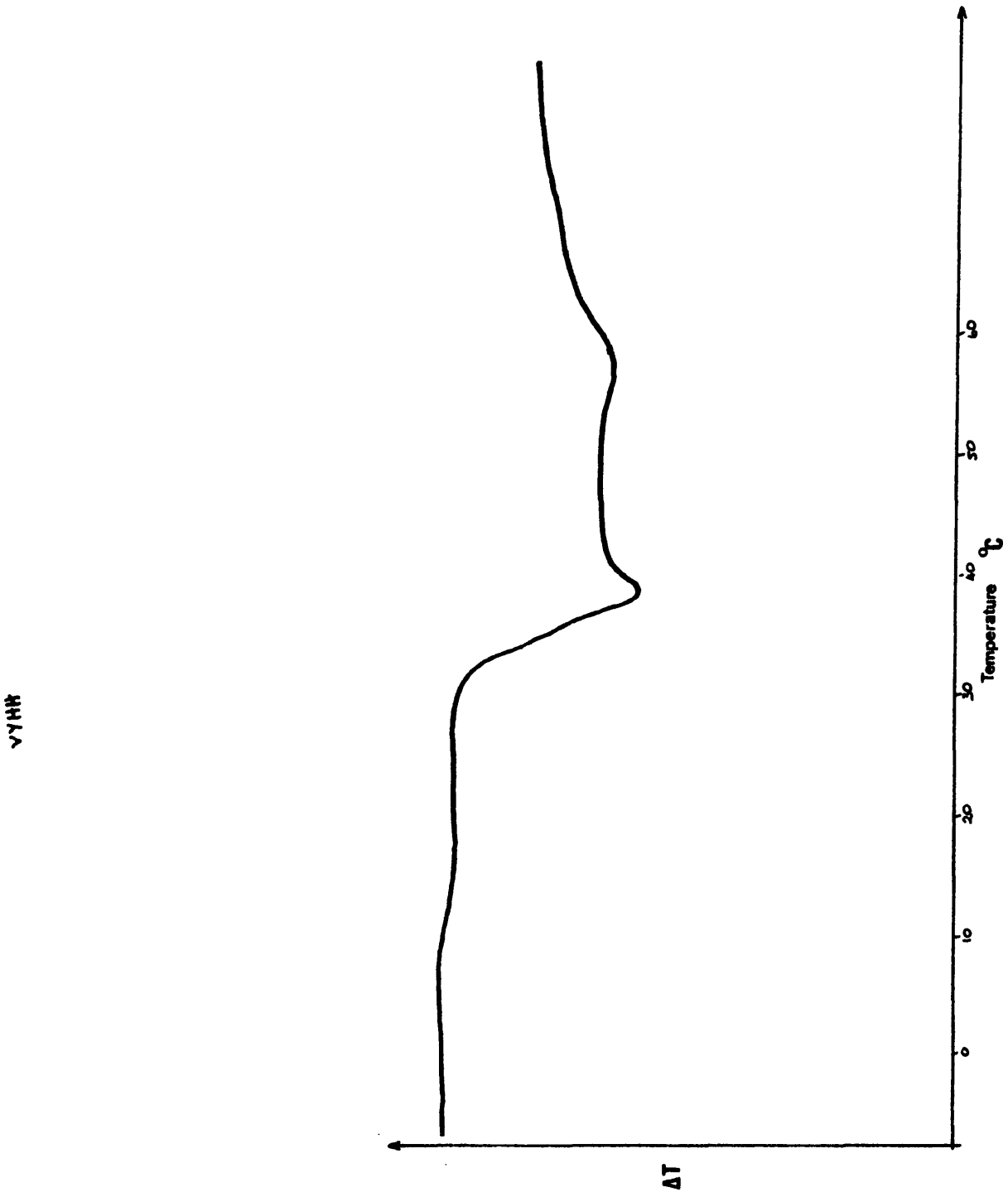

D.T.A trace for VYHH.

Appendix 2.

Impedance Plots.

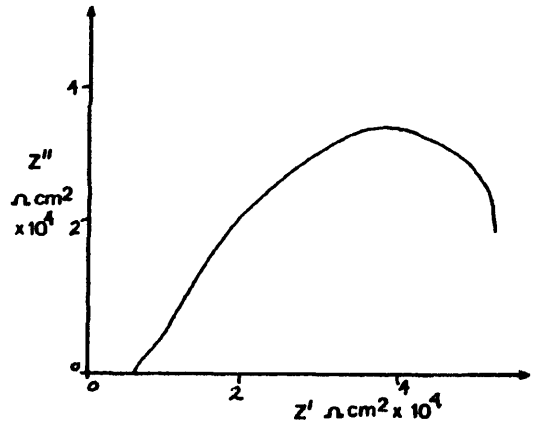

15 minutes after immersion.

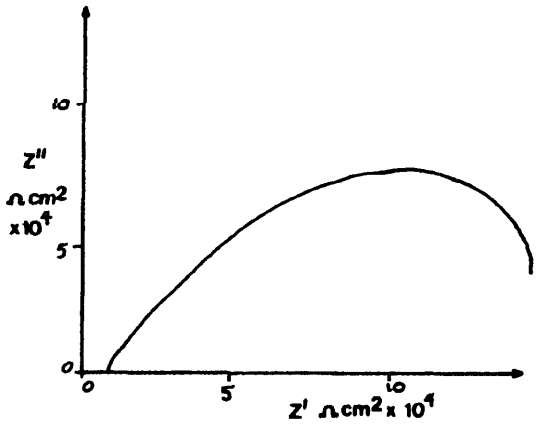

30 minutes after immersion.

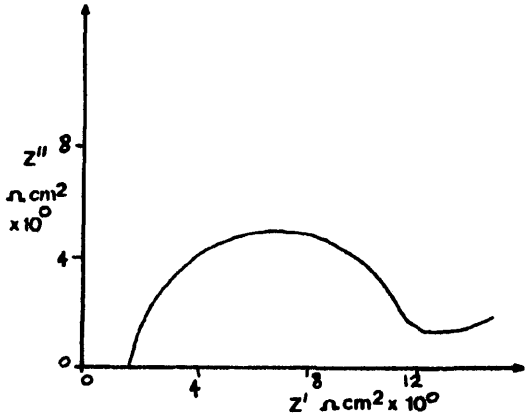

18 days after immersion.

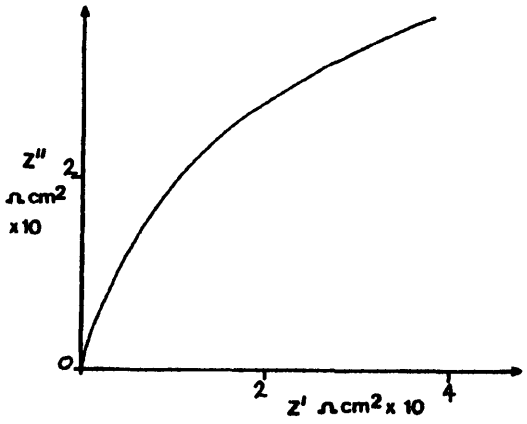

30 to 45 days after immersion.

VYHH - pinholed, detached film.

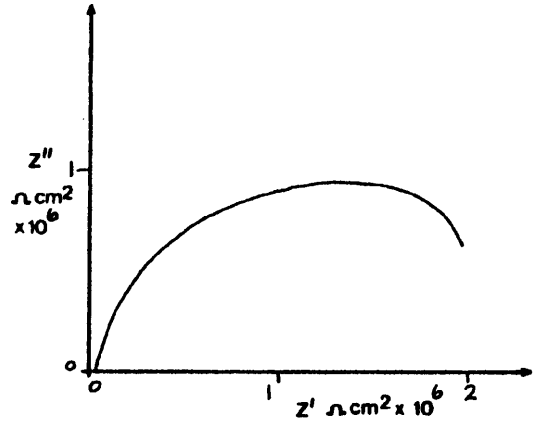

5 to 15 minutes after immersion.

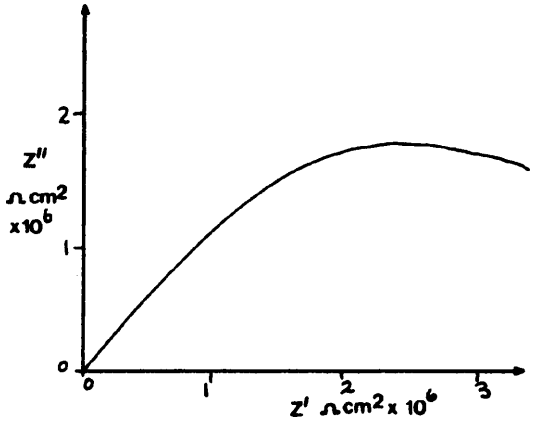

30 minutes after immersion.

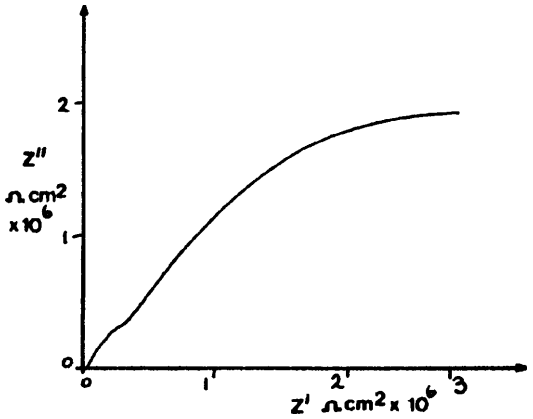

1 hour after immersion.

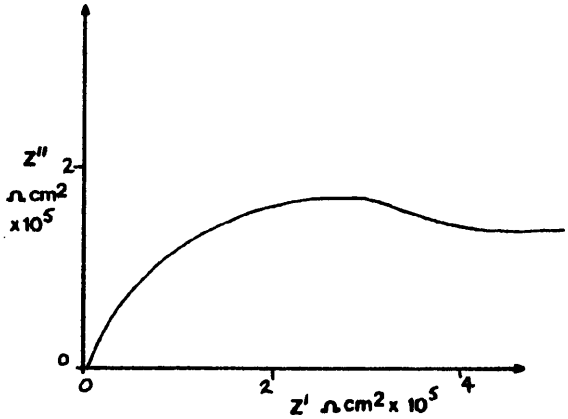

1 day after immersion.

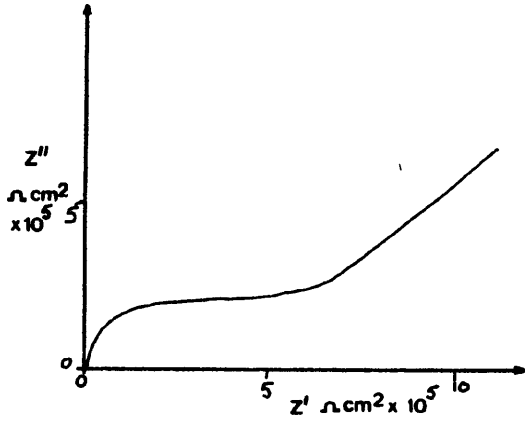

5 days after immersion.

VAGH in aerated solution.

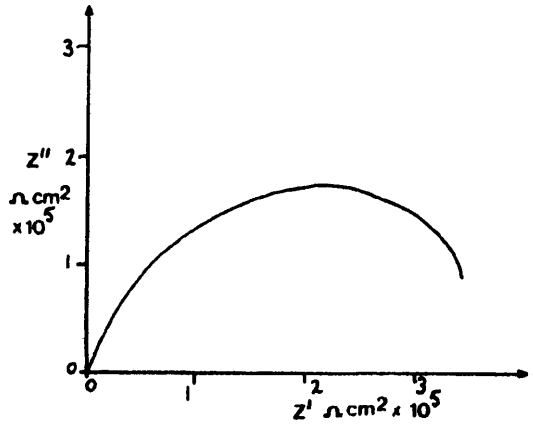

5 minutes after immersion.

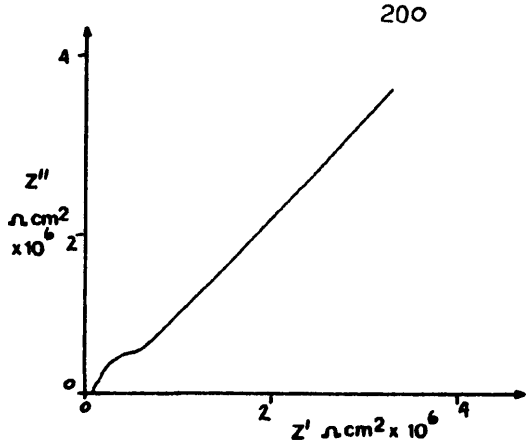

15 minutes after immersion.

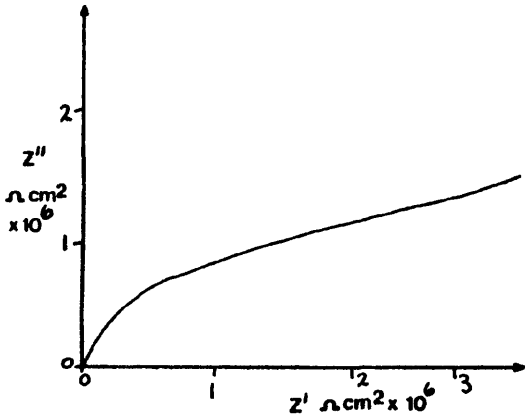

1 hour after immersion.

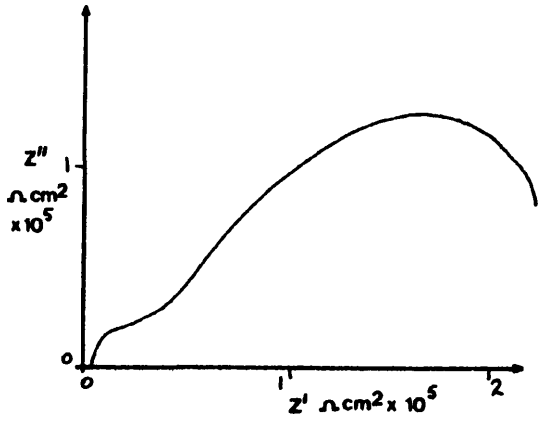

1 day after immersion.

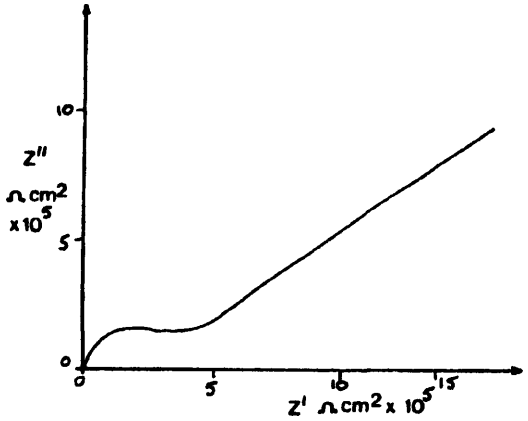

5 days after immersion.

VAGH-N in deaerated solution.

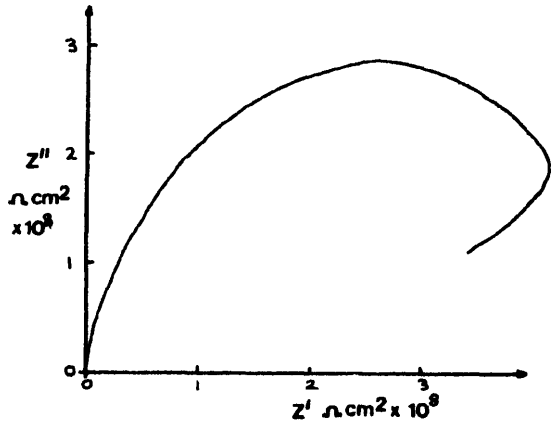

5 minutes after immersion.

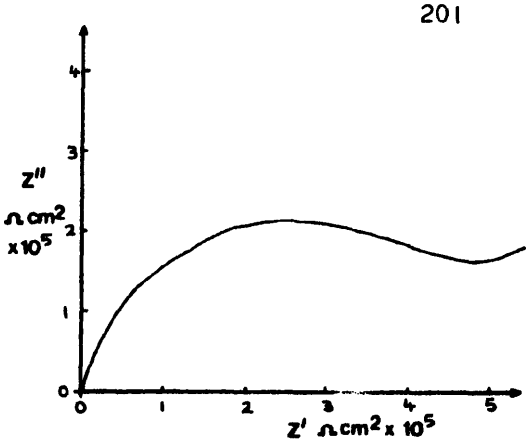

15 minutes after immersion.

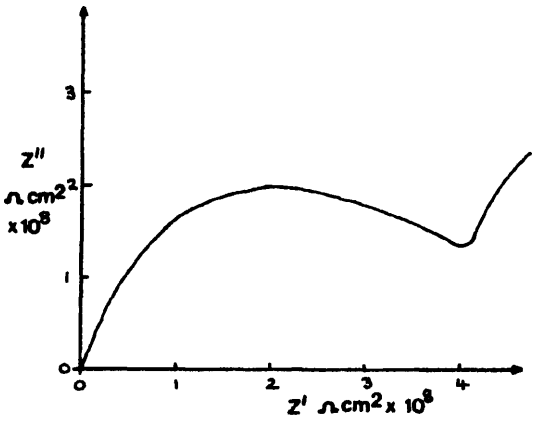

1 hour after immersion.

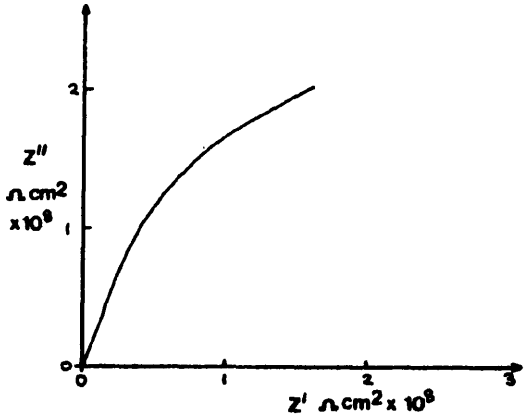

1 to 5 days after immersion.

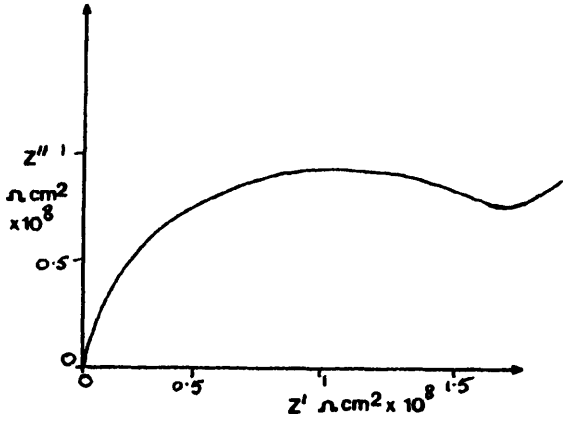

6 days after immersion.

VROH in deaerated solution.

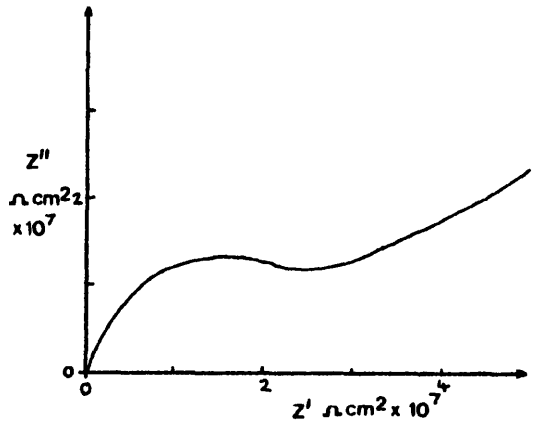

30 to 45 minutes after immersion.

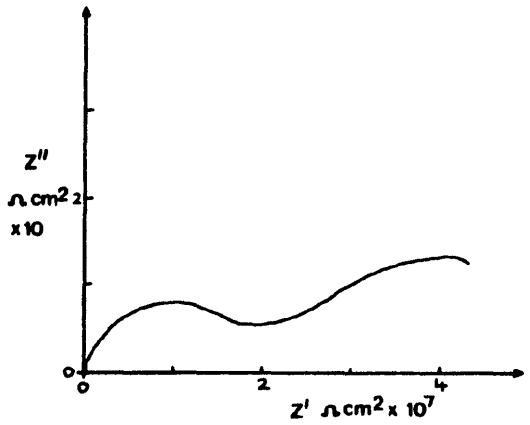

2 days after immersion.

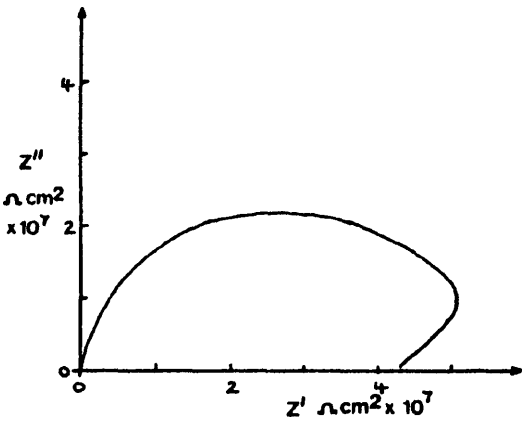

6 days after immersion.

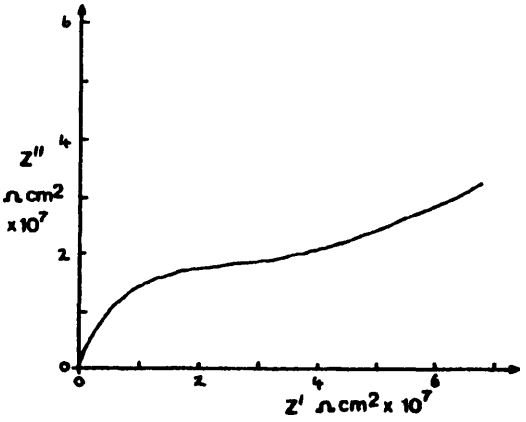

10 to 30 days after immersion.

VROH-Y in deaerated solution.

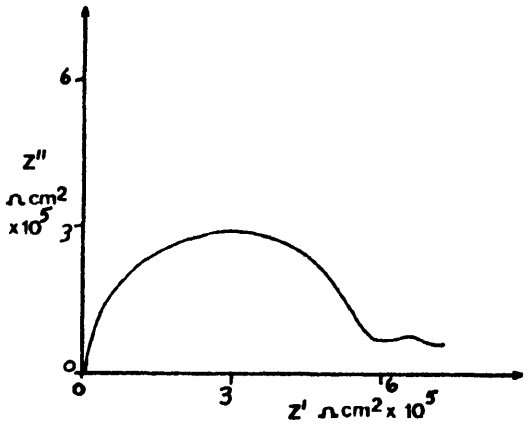

1 day after immersion.

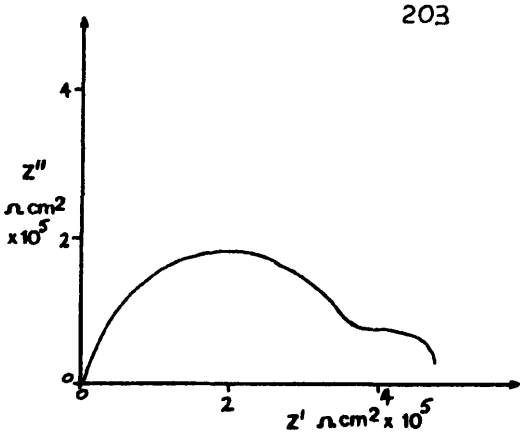

3 days after immersion.

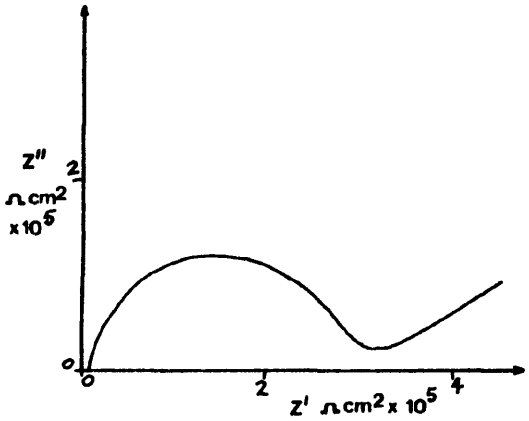

8 days after immersion.

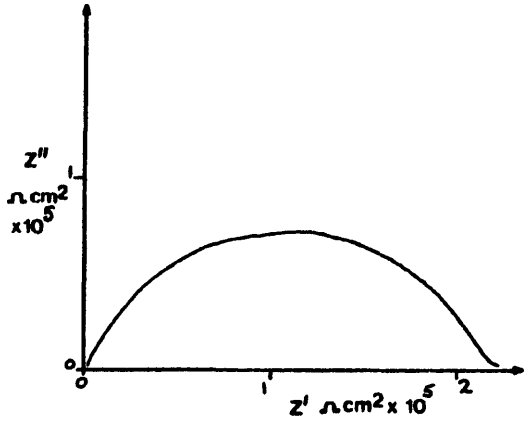

13 days after immersion.

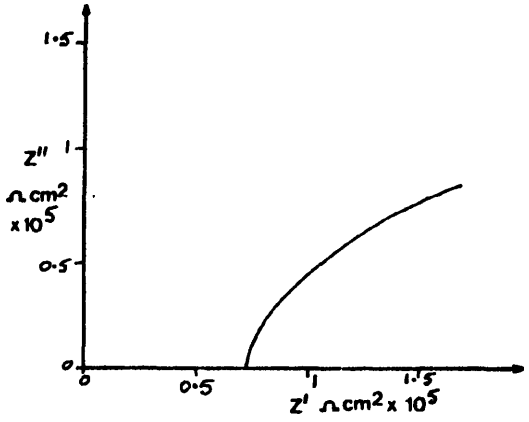

72 days after immersion.

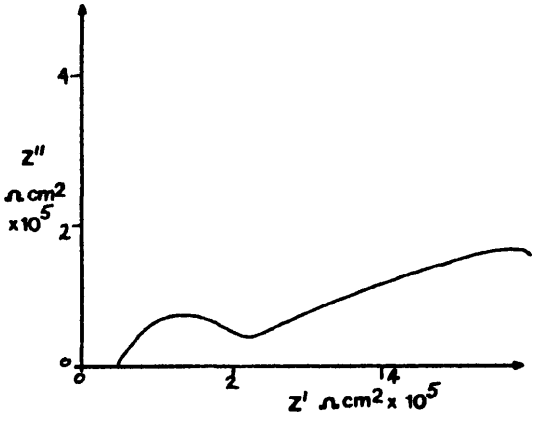

134 days after immersion.

Acrylic B.

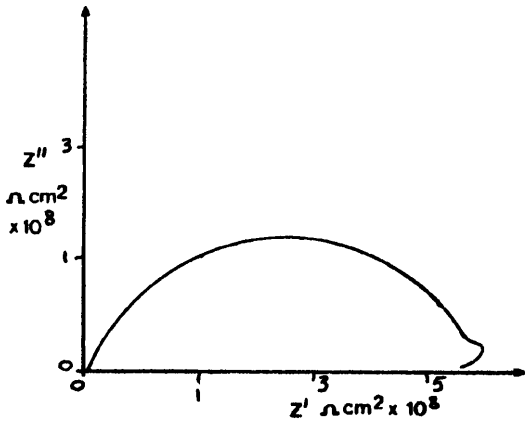

20 days after immersion.

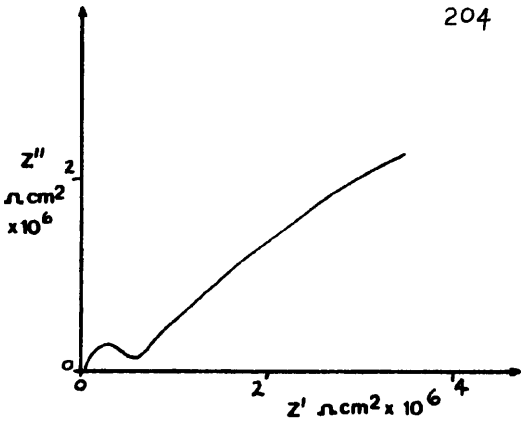

36 days after immersion.

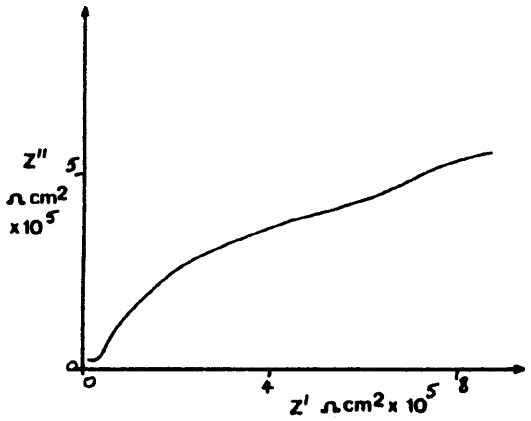

57 days after immersion.

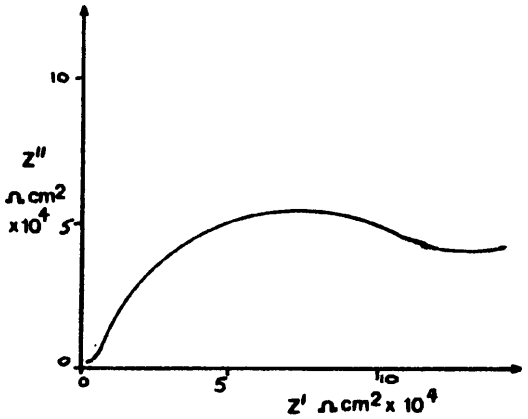

65 days after immersion.

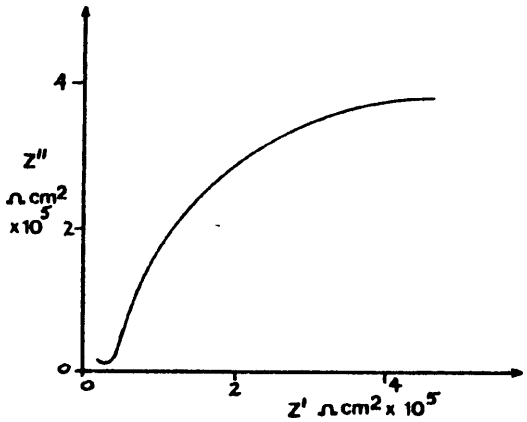

84 days after immersion.

VROH on pickled steel.

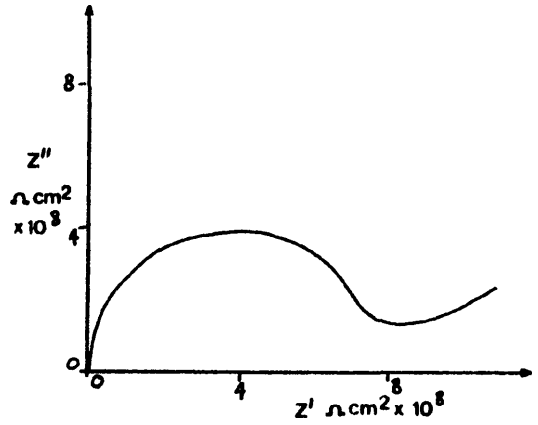

9 days after immersion.

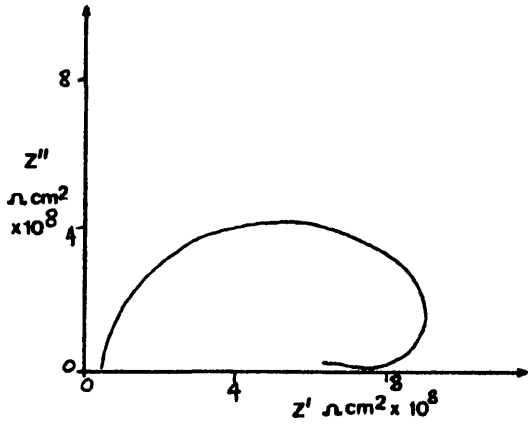

13 to 17 days after immersion.

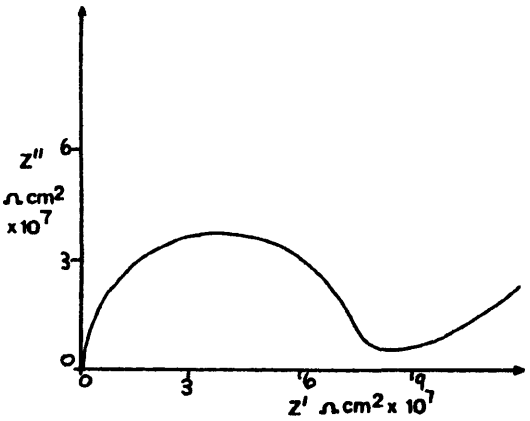

84 days after immersion.

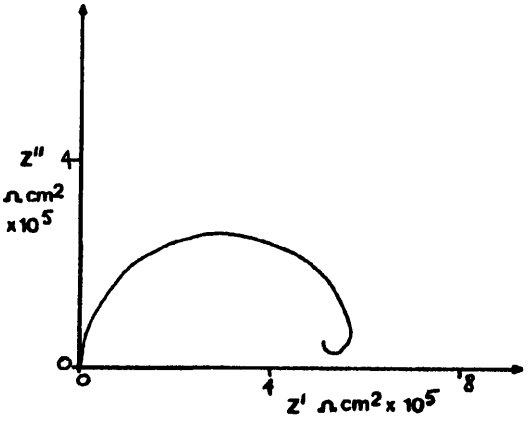

134 days after immersion.

VAGH-1 on pickled steel.